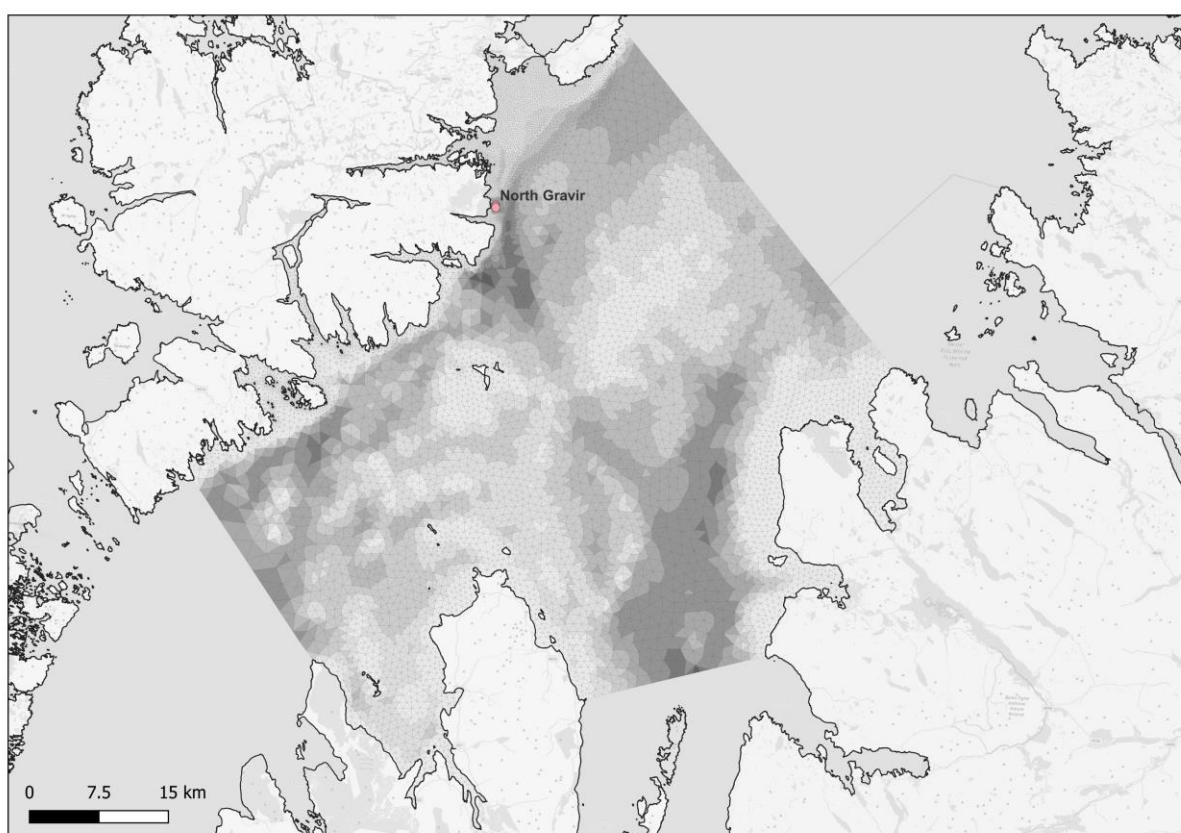


North Gravir Aquaculture Modelling

Hydrodynamic Climatology Model

Model Setup Report



This report has been prepared under the DHI Business Management System certified by Bureau Veritas to comply with ISO 9001 (Quality Management)

ISO 9001
Management System Certification

BUREAU VERITAS
Certification Denmark A/S



North Gravir Aquaculture Modelling

Hydrodynamic Climatology and Hindcast Models

Model Setup Report

Prepared for Bakkafrost Ltd.
 Represented by [REDACTED] (Site Development Manager)



Area of interest and computational mesh of Outer Hebrides North Gravir hydrodynamic model

Project manager	[REDACTED]
Authors	[REDACTED]
Quality supervisor	[REDACTED]
Project number	26802148
Approval date	11 August 2023
Revision	Final 2.0 – 06 September 2023 – Addressing SEPA’s comments on additional plots Final 1.0 – 04 August 2023 Draft 1.0 – 15th July 2023 : Initial draft
Classification	Restricted

CONTENTS

Executive Summary	1
1 Introduction	2
1.1 Background to the study	2
1.2 Aims and objectives	3
1.3 Layout of this report	3
2 Geographic and environmental setting	4
2.1 Geographic setting	4
2.2 Climatic and oceanographic conditions	6
2.3 Aquaculture in Outer Hebrides.....	8
3 Data Basis.....	9
3.1 Bathymetry and coastline.....	9
3.1.1 Coastline	9
3.1.2 Bathymetry	9
3.2 Measurements	13
3.2.1 ADCP campaigns.....	13
4 Model Development	18
4.1 Model selection	18
4.1.1 Three-dimensional model	18
4.1.2 MIKE 3 hydrodynamic model.....	18
4.2 Datums	19
4.3 North Gravir hydrodynamic hindcast and climatology models.....	19
4.3.1 The East Coast Lewis and Harris Climatology Model.....	20
4.3.2 Model domain.....	27
4.3.3 Mesh and bathymetry	27
4.3.4 Initial and boundary conditions	32
4.3.5 Atmospheric forcing	33
4.3.6 Model configuration.....	33
4.4 Model outputs.....	35
4.5 Model files	35
5 Hydrodynamic model calibration.....	36
5.1 Model Calibration	36
5.1.1 Initial calibration and tidal component velocity adjustment.....	38
5.1.2 Water levels	41
5.1.3 Currents	43
6 Hydrodynamic climatology model verification	47
6.1 Model Verification.....	48
6.1.1 Water Levels, depth-averaged currents and current directions	48
6.1.2 3D Currents.....	55
7 Model Results.....	65
7.1 Model outputs.....	65

8	Summary.....	70
9	References.....	71

FIGURES

Figure 2.1	Map showing the geographic position of North Gravir area of interest in relation to the Outer Hebrides main islands (west land boundaries) and the Isle of Skye, north of mainland Scotland (east land boundary). North Gravir site is depicted.	5
Figure 2.2	Map of the general circulation pattern within the North Atlantic and North Sea around Scotland (reproduced from [4]). The white arrows show the circulation of Atlantic water, while green arrows represent costal circulation.	7
Figure 2.3	Annual (all-year) wind rose for Lerwick for the period 1996-2005 (Shetland), with a prevailing southwest wind direction through the year and frequent strong winds from southerly to north-westerly directional sectors (reproduced from [6])	7
Figure 2.4	Map showing the locations of BFS's active production sites for the last 3 years at the Outer Hebrides islands.	8
Figure 3.1	Map showing a selection of bathymetric surveys (spot depths soundings) provided by BFS.	11
Figure 3.2	Map showing areas of high resolution multibeam gridded bathymetric datasets (green-blue patched areas) around Outer Hebrides used to inform model bathymetry herein (source UKHO Marine Data Portal). Note that the baseline EMODnet 2020 bathymetric database (grey scale) incorporates already most of the available datasets from UKHO (even though the multibeam datasets are upscaled significantly at a final grid resolution of 60x117m ² from 4-8m ² . Due to lack of available higher resolution bathymetric surveys, grey areas in the EMODnet composite product are filled in with lower spatial resolution bathymetric surveys/composite datasets from partners; where absent the lower resolution GEBCO 2019 global bathymetric model is used (please see https://emodnet.ec.europa.eu/en/bathymetry for a detailed account of EMODnet bathymetric model).	12
Figure 3.3	Survey periods of ADCP deployments provided by BFS at Outer Hebrides sites of interest for the period 2010-2022 that were considered during the hindcast model calibration and verification development stages.	14
Figure 3.4	Geographic locations of ADCP deployments provided by BFS at sites of interest at the Outer Hebrides for the period 2010-2022 that were considered during the calibration and verification stages of the hindcast and climatological versions of the hydrodynamic database development.	15
Figure 3.5	Harmonic analysis for surface elevation (top panel) and current speeds (bottom panel) for observational station North Gravir (210804) during deployment 04.08.2021-06.10.2021	17
Figure 4.1	Example of an unstructured mesh in MIKE3 with 5 sigma (σ) layers.	19
Figure 4.2	East Coast of Lewis and Harris (ECLH) numerical mesh showing the entire model domain.	22
Figure 4.3	East Coast of Lewis and Harris (ECLH) computational mesh at the North Gravir area of interest. See also Figure 4.8 (right panel) for a comparison in spatial discretisation improvement for the area of interest.	23
Figure 4.4	Time-series and annual statistics of climatologically averaged meteorological conditions for a location within the HD _{NG_hindcast/clima} computational domain at the centre of Little Minch, Outer Hebrides. From top to bottom: wind speed, wind direction, atmospheric pressure, and air temperature	25
Figure 4.5	Annual wind rose for a location within the HD _{NG_hindcast/clima} computational domain at the centre of Little Minch, Outer Hebrides from the climatology atmospheric forcing used as input to the ECLH.	26
Figure 4.6	Computational domain of the regional North Gravir hydrodynamic model (left) and zoomed in perspective of the main areas of interest (right). Mesh resolution is significantly improved around the area of interest versus ECLH, as seen in Figure 4.3 and Figure 4.8, allowing for a better representation of coastal and bathymetric features.	28

Figure 4.7	Mesh resolution [m] across the HD _{NG_hindcast/clima} computational domain of BFS (left panel, North Gravir site as red dot) and defined open sea boundaries (see also Section 4.3.6) (right panel).....	29
Figure 4.8	North Gravir model (left) versus ECLH model mesh (right) at area of interest. There are differences in coastline/islands representation and subsequently flow resolution/representation through narrow straights, but bathymetry is relatively consistent between the two models.	30
Figure 4.9	Vertical mesh geometry at the North Gravir site nearby area of interest (North Gravir site location indicated by blue line)	31
Figure 5.1	North Gravir hydrodynamic hindcast model calibration and climatology verification sites.....	37
Figure 5.2	Scatterplot comparisons of observed versus modelled total water level signal BEFORE adjustment of the tidal forcing solution.....	39
Figure 5.3	Selected locations of observed versus modelled tidal velocities during initial assessment of the tidal forcing solution.....	40
Figure 5.4	Scatterplot comparisons of observed versus modelled water levels at selected calibration sites as in Table 5.1 prior to final adjustment of the tidal forcing solution at the model boundaries (left column) and case with higher tide resolution at the model boundaries (right column) (see also Table 5.2)	42
Figure 5.5	Dual rose plots of current speed and directions of observational records vs model output for selected calibration sites.....	44
Figure 5.6	Scatterplot comparisons of observed versus modelled tidal velocities at the North Gravir deployments prior to final adjustment of the tidal forcing solution at the model boundaries (left column) and following the solution selected at the model boundaries (right column) (see also Table 5.2)	45
Figure 5.7	Timeseries of modelled (blue dots) versus observed (black dots) depth-averaged current direction at the two observational deployments at North Gravir.....	46
Figure 6.1	Timeseries (top panel) and frequency plot (bottom panel) of observed vs modelled water level for deployment station 210804 at North Gravir site. Modelled (climatology) timeseries are shifted to match tidal peaks for same seasonal period as in the observational record.....	50
Figure 6.2	Timeseries (top panel) and frequency plot (bottom panel) of observed versus modelled (climatology) depth-averaged current speed for deployment station 210804 at North Gravir site. Modelled (climatology) timeseries are shifted to match tidal peaks for same seasonal period as in the observational record.....	51
Figure 6.3	Timeseries (top panel-left) and frequency plot (bottom panel-left) and rose plot (right panel) of observed versus modelled (climatology) depth-averaged current directions for deployment station 210804 at North Gravir site. Modelled (climatology) timeseries are shifted to match tidal peaks for same seasonal period as in the observational record.....	52
Figure 6.4	Current rose plots of observed versus HD _{NG_clima} (left column) and ECLH (right) of depth-averaged currents at BFS's ADCP locations, see also Table 5.1. Modelled (climatology) timeseries are shifted to match tidal peaks for same seasonal period as in the observational record.....	54
Figure 6.5	Timeseries plots of current speed and directions at near surface (6m from surface), cage bottom (18m from surface) and near bed (middle of bottom model layer) of observational records versus model output at the North Gravir 210804 verification site as in Table 5.1. Observational record levels are measured from the bottom. Modelled (climatology) timeseries are shifted to match tidal peaks for same seasonal period as in the observational record.	59
Figure 6.6	Dual rose plots of directional distribution of currents near surface (6m from surface), cage bottom (18m from surface) and near bed (middle of bottom model layer) of observed versus modelled currents at the North Gravir 210804 verification site as in Table 5.1. Observational record levels are measured from the bottom. Modelled (climatology) timeseries are shifted to match tidal peaks for same seasonal period as in the observational record.	60

Figure 6.7	As in Figure 6.4 but for North Gravir 211008 verification site as in Table 5.1. Modelled (climatology) timeseries are shifted to match tidal peaks for same seasonal period as in the observational record.	63
Figure 6.8	Dual rose plots of directional distribution of currents at near surface (6m from surface), cage bottom (18m from surface) and near bed (middle of bottom model layer) of observed versus modelled currents at the North Gravir 211008 verification site as in Table 5.1. Observational record levels are measured from the bottom. Modelled (climatology) timeseries are shifted to match tidal peaks for same seasonal period as in the observational record.	64
Figure 7.1	Residual circulation around North Gravir based on the hydrodynamic climatology model (HD _{NG_clima}). PMF area <i>European Spiny Lobster</i> is shown with green rectangle while <i>Burrowed Mud</i> PMF as shaded polygon. North Gravir cages' locations shown as red circles.	66
Figure 7.2	Residual circulation throughout the computational domain of the hydrodynamic climatology model (HD _{NG_clima}).	67
Figure 7.3	Statistical 50 th percentile (based on empirical CDF) of depth-averaged current speed throughout North Gravir computational domain for the hydrodynamic climatology model (HD _{NG_clima}).	68
Figure 7.4	Statistical 90 th percentile (based on empirical CDF) of depth-averaged current speed throughout North Gravir computational domain for the hydrodynamic climatology model (HD _{NG_clima}).	69

TABLES

Table 3.1	Summary of bathymetric databases used to inform HD _{NO} model bathymetry in order of highest to lowest priority.	10
Table 3.2	Observational records database provided by BFS to inform on hydrodynamic conditions at the area of interest and calibration of the HD model.	16
Table 4.1	Summary of HD _{NG_hindcast/clima} model settings.	33
Table 4.2	2D model outputs from HD _{NG_clima}	35
Table 4.3	3D model outputs from HD _{NG_clima}	35
Table 5.1	North Gravr hydrodynamic hindcast/clima models calibration/verification deployment campaigns.	36
Table 5.2	Main setups for second phase of calibration on improving model skill on current speeds.	37
Table 6.1	Observed versus modelled water level and depth-averaged currents statistics. ...	49
Table 6.2	Summary of statistics for near surface, cage bottom and near bed levels for the observational versus modelled stations.	56

APPENDICES

A	Hydrodynamic model database files
B	Definition of model quality indices
C	Digital container of calibration/validation plots

NOMENCLATURE

Abbreviations	
BNG	British National Grid
CD	Chart Datum
CDF	Cumulative Density Function
DTM	Digital Terrain Model
DTU10	Danish Technical University global ocean tide model
ECLH	East Coast of Lewis and Harris
ECMWF	European Centre for Medium-Range Weather Forecasts
EMODnet	European Marine Observation and Data Network
FM	Flexible Mesh
FVCOM	Finite-Volume Community Ocean Model
HD	Hydrodynamic
HWS	High water shoreline
IOS	Institute of Oceanographic Sciences
LAT	Lowest Astronomical Tide
MPFF	Marine Pen Fish Farm
MSL	Mean-Sea-Level
OGL	Open Government License
OS	Ordnance Survey
PSU	Practical Salinity Unit
RANS	Reynolds Averaged Navier-Stokes
SEPA	Scottish Environment Protection Agency
SSF	Scottish Sea Farms
SSM	Scottish Shelf Model
TKE	Turbulent Kinetic Energy
TPX08	TPX0 v08 global atlas of tidal solution
TS	Temperature and Salinity
UKHO	United Kingdom Hydrographic Office
UTM	Universal Transverse Mercator
WGS	World Geodetic System
2D	Two-dimensional
3D	Three-dimensional

Definitions	
Time	Times are relative to UTC
Level	Levels are relative to MSL, CD, or LAT as specified
Co-ordinate system	Horizontal datum is established using Ordnance Datum of Great Britain 1936 (OSGB36) - EPSG code: 27700
Direction	Wind: °N coming from and positive clockwise
	Currents: °N going to and positive clockwise

Abbreviations – Quality Indices	
N	Number of data (synchronized)
MEAN	Mean (average) values
STD	Standard deviation
BIAS	Mean difference
AME	Absolute mean error
RMSE	Root mean square error
SI	Scatter index (unbiased)
EV	Explained variance
CC	Correlation coefficient
QQ	Quantile-Quantile (line slope and intercept)
PR	Peak ratio (of Number of peak highest events)

Tidal Levels	
HAT	Highest Astronomical Tide
LAT	Lowest Astronomical Tide
MHWS	Mean High Water Spring
MHWN	Mean High Water Neap
MLWN	Mean Low Water Neap
MLWS	Mean Low Water Spring
Z ₀	Mean Water Level

ACKNOWLEDGEMENT

We wish to acknowledge the generous assistance provided by the Marine Scotland Science Oceanography group for providing access to the Scottish Shelf Climatology Model and respective meteorological forcing.

Executive Summary

Bakkafrost UK Ltd. (BFS) is a leading producer of farmed Atlantic salmon throughout the Scottish Mainland and Outer Hebrides. To support ongoing operations, site developments and regulatory applications, BFS requires a detailed numerical hydrodynamic database covering the part of the Outer Hebrides complex with a particular focus on North Gravir area which contains aquaculture activity of immediate interest.

This report describes the development of a 3-dimensional (3D) hydrodynamic climatology model HD_{NG_clima} database for the North Gravir. The climatology model offers a simple technique for predicting the mean status of the atmospheric and oceanographic conditions over an annual period¹. A hindcast (or else reanalysis) version would provide an approximation to “actual” hydrodynamic conditions covering a similar period.

The hydrodynamic model is produced using the MIKE 3 FM modelling suite (ver.2023) developed by DHI. This numerical engine simulates the water level variations and flows in response to a variety of forcing conditions. The HD model of North Gravir is based on a variable resolution unstructured horizontal mesh with a resolution of <200m along the coastline of the Outer Hebrides islands complex and identified areas of interest. The climatological model is forced by offshore boundaries and climatologically averaged meteorological conditions from the East Coast Lewis Harris (ECLH) hydrodynamic database and is verified against the ECLH at offshore locations and observational records at the site of interest. It uses the DTU10 Ocean Tide model [1] with the TPXO8 [2] 2min global tidal solution for the tidal component. There is a significant refinement of the mesh discretisation inshore to the islands complex, with a spatial resolution of around 26-40 m in the area around existing and planned marine pen fish farms.

A climatology is a representation of the ‘mean’ status of the hydrodynamics over several years. This must be accounted for during any validation/verification of a climatology forced model against an observational measurement campaign to determine model skill based on commonly used metrics.

A two-dimensional (2D) hindcast version $HD_{NG_hindcast}$ was thus constructed to inform on parameterisation of model settings and verification of model solution against the available observational records in terms of propagation of the tidal signal across the domain.

The hydrodynamic climatology model database and the hindcast version validation are provided alongside this report.

¹ The North Gravir climatology model aims to effectively downscale the East coast Lewis Harris (ECLH) climatology (developed for and maintained by Marine Scotland Science) while verifying the hydrodynamic range against the observational record available.

1 Introduction

This report has been prepared for **Bakkafrost UK Ltd.** (BFS) by DHI in relation to the hydrodynamic modelling services for the aquaculture sites at North Gravir, Outer Hebrides. The project will establish a dedicated climatology three-dimensional (3D) hydrodynamic numerical model inclusive of the waters around Outer Hebrides for a one-year period.

This document and its accompanying appendices constitute the **hydrodynamic database climatology model** report.

1.1 Background to the study

The Outer Hebrides, also known as the Western Isles, is an archipelago located off the west coast of mainland Scotland. It consists of a chain of islands, the largest of which are Lewis and Harris, North Uist, South Uist, and Barra.

Aquaculture activities play a significant role in the Outer Hebrides' economy and food production. The region's coastal waters offer ideal conditions for aquaculture due to their clean, nutrient-rich environment. Salmon farming is one of the primary aquaculture activities in the area, with several farms located around the islands. These farms rear Atlantic salmon, providing a sustainable source of high-quality fish.

Aquaculture activities in the Outer Hebrides adhere to strict regulations and sustainability practices to protect the natural environment and maintain the long-term viability of the industry. The industry provides employment opportunities for local communities and contributes to the region's economy while promoting the production of healthy and sustainable seafood. With a focus on increasing production, it is understood that the companies are seeking opportunities for new prospect sites and/or the re-opening of inactive sites.

Operational fish farms have the potential to affect the marine environment in several ways via the release of waste materials in the form of dissolved nutrients, medicines, and particulate organic matter. The management of the risks related to salmon lice are also of fundamental importance to producers. Consequently, the aquaculture sector is highly regulated by the Scottish Government. There is a requirement for fish farm operators to use modelling tools to demonstrate compliance with the environmental standards relating to the spatial extent and the intensity of impacts, both in the local area around fish pens and in the wider environment.

Increasingly, operators are required to use marine hydrodynamic modelling approaches to support license applications. Hydrodynamic modelling refers to a class of numerical models that simulate the flow of water within a specified geographic area in a realistic way. This includes flow due to a range of forcing conditions including tidal variations, density gradients, and meteorological factors (air pressure and wind). Hydrodynamic models provide the physical basis for many other types of numerical environmental modelling such as the transport, dispersion, and decay of dissolved or suspended substances.

1.2 Aims and objectives

The overall aim of the project is to develop a 3-dimensional hydrodynamic database to inform a risk-based approach to management and development of aquaculture sites in the waters around Outer Hebrides with specific focus to North Gravir developments and activities.

To achieve this aim, the objectives of this hydrodynamic modelling report are to:

- develop a 2-dimensional hydrodynamic model that will serve as a test 'platform' for parameterizations focusing on optimizing tidal signals propagation across the computational domain, forcing adjustments, bed friction and boundary placement.
- develop a 3-dimensional hydrodynamic climatology model database that sufficiently represents the hydrodynamics as expressed by marine currents and water exchange around the Minch with a specific focus on North Gravir site. This area is of particular interest to BFS.

The model will provide a database for future modelling to support regulatory applications such as: assessing connectivity between fish farms sites within the Minch area; site selection and site screening; dispersion modelling of waste solids, sea lice and bath treatment medicines.

Climatology Model

The fundamental principle of a climatology model is the assumption that the conditions for a particular day (or month) and at a particular location do not change significantly from one year to the next; hence, the long-term average conditions on a certain day (or month) should be a good approximation to the expected conditions for that day (or month). This offers a simple technique for predicting the *mean status* of the atmospheric and oceanographic conditions within a region (i.e., to understand the seasonal variability, but not to the interannual variability).

The hydrodynamic climatology model thus provides a useful reference for how the expected flow patterns, tidal and/or baroclinically driven, temperature, and salinity vary over seasonal cycles and the wind climate. However, the climatology model output does not reflect episodic weather events as for example winter storms which occur at relatively high frequency at these latitudes.

1.3 Layout of this report

The remaining sections of this report are organised as follows:

- Section 2 summarises information on the geographic and environmental setting of the Minch and Outer Hebrides.
- Section 3 provides an overview of the data basis for the modelling study, including coastline, bathymetry, boundary conditions, and meteorological forcing.
- Section 4 describes the setup of the 3D hydrodynamic model of North Gravir (HD_{NG_clima}). This includes the mesh and bathymetry development, initial and boundary conditions, model settings, and outputs.
- Section 5 presents the calibration/validation of the 2D hindcast version (HD_{NG_hindcast}).
- Section 6 presents the verification of the hydrodynamic climatology version.
- Section 7 provides a summary of the hydrodynamic model climatology database.

2 Geographic and environmental setting

2.1 Geographic setting

The Outer Hebrides, an archipelago located off the west coast of mainland Scotland, consists of a chain of islands, the largest of which are Lewis and Harris, North Uist, South Uist, and Barra (Figure 2.1). The scattered islands of the Inner Hebrides and the archipelago of the Outer Hebrides create a network of channels, sounds and headlands, leading to enhanced currents and turbulence, eddy generation, and flow separation in the region [3].

Geographically, the Outer Hebrides are situated in the North Atlantic Ocean and are influenced by the North Atlantic Current (NAC), see also Figure 2.2, a powerful western boundary warm tropical water current within the Atlantic Ocean that extends the Gulf Stream north-eastward. That results in a maritime climate to the area with milder temperatures, 8°C (winter) to 14°C (summer), for these latitudes. The NAC also influences the transport of nutrients and marine organisms in the waters surrounding the islands providing favourable conditions and supporting a diverse range of marine species. The islands are known for their diverse natural environments, including pristine beaches, moorland, mountains, lochs, and peat bogs. The area is home to a wide range of flora and fauna, including various bird species and marine life.

The circulation around Outer Hebrides is strongly affected by the Atlantic Ocean conditions and ocean circulation. A steep continental slope, acting as a barrier between the open ocean and shelf sea systems leads to complex mixing processes between oceanic and shelf waters in the area with significant impact on marine primary production [4].

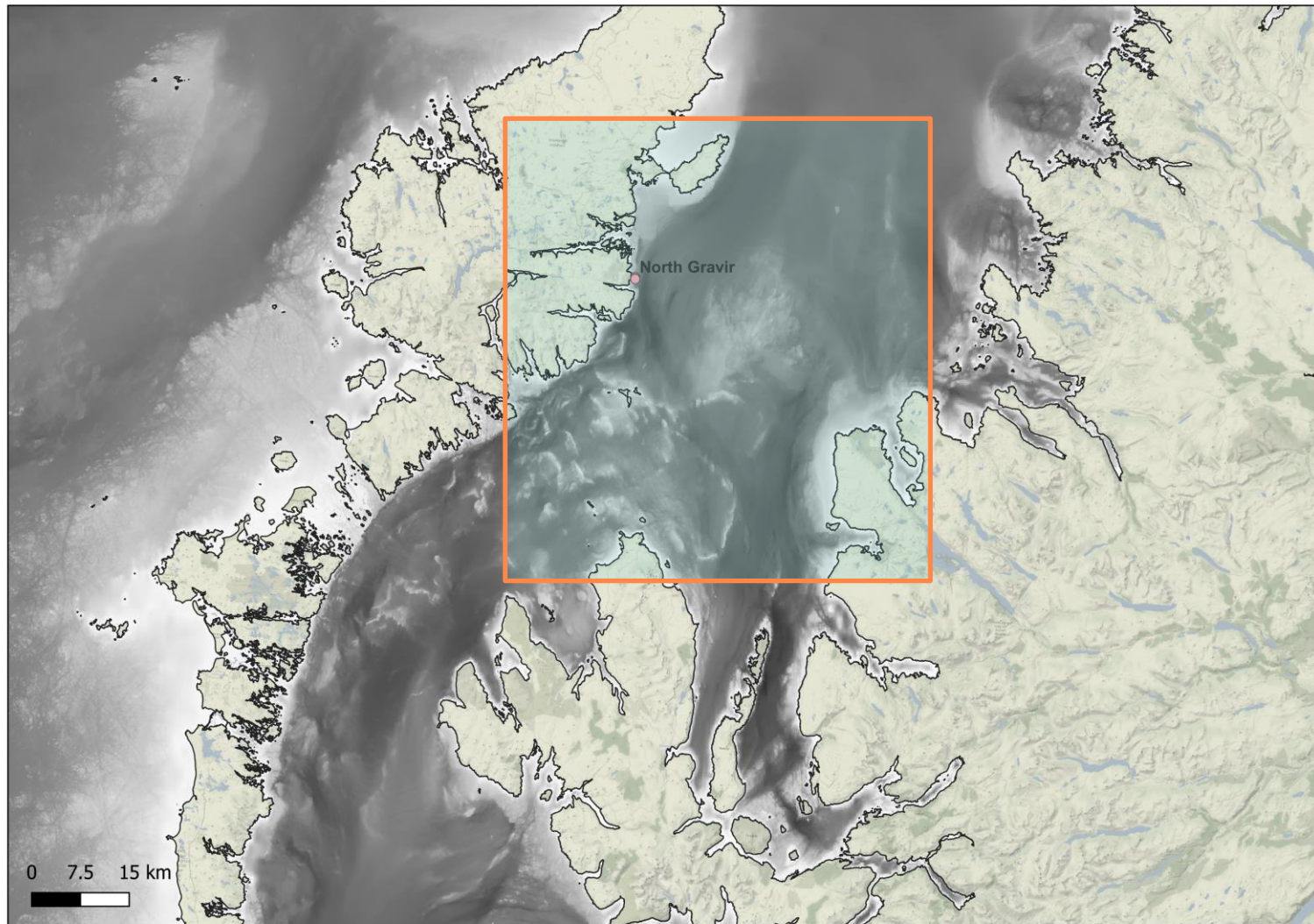


Figure 2.1 Map showing the geographic position of North Gravr area of interest in relation to the Outer Hebrides main islands (west land boundaries) and the Isle of Skye, north of mainland Scotland (east land boundary). North Gravr site is depicted.

2.2 Climatic and oceanographic conditions

Currents

Considering its position at around 57°N of the equator, the climate of the Outer Hebrides is very mild compared to other parts of the world at a comparable latitude. This is explained by the role of the North Atlantic Current, a feature that is partly wind driven and partly driven by the density gradients between the warmer sub-tropical water (to the south) and the cooler sub-polar waters (to the north) [4]. The prevailing south-westerly winds pick up heat from the North Atlantic current, resulting in the relatively mild and wet maritime climate that characterises Scotland, and relatively stable sea temperatures typically ranging from approximately 8°C in March to a peak of 13°C in August [5]. In addition to the North Atlantic Current, a jet-like feature known as the Slope Current (Figure 2.2), flows along the edge of the continental slope from south-to-north roughly at the 400-500m depth contour (see Figure 2.2). The waters in the Slope Current originate from southern Europe (Iberia) and include North Atlantic Water that reaches the Bay of Biscay [4].

Winds

Although the prevailing wind direction is from the south-west, the passage of various low-pressure systems across the North Atlantic accounts for variability in the wind direction around northern and western parts of Scotland. This exposure to the North Atlantic means that Outer Hebrides is among the windiest parts of the United Kingdom, and the frequency and depth of these depressions is greatest in the winter months (December through to February). As Atlantic depressions pass the UK the wind typically starts to blow from the south-west, with prevailing directions shifting to from the west or north-west as the depressions move northwards [6]. The range of directions between south and north-west accounts for most occasions and the strongest winds nearly always blow from these directions (see Figure 2.3).

Tides

The tides all around Scotland are semi-diurnal characterised by a high and low water every ~12.5 hours. At Stornoway, the spring and neap tidal range are 3.88 m and 1.68 m, respectively (see Table 1 of [3]). This is set by the tides in the North Atlantic Ocean which propagate up the west coast of Scotland. This dominant semi-diurnal tide in the region, in essence an along the shelf northward propagating Kelvin wave, leads to a tidal range of around 5 m at spring tides just to the north of Skye [7]. Northward of Skye, the tidal range diminishes slightly with tidal currents typically of the order of only a few cm/s. Outer Hebrides acts as a natural blockage to the northwards sweep of the Atlantic tide, and the tidal wave swings eastwards to the north of the Islands and into the northern North Sea. The result is a difference in the timing of high and low water between the east and west coast, which sets up strong tidal currents where the flow is constrained around the headlands and in narrow channels that connect the North Atlantic and North Sea [3]. However, in the enclosed and deep water voes, tidal currents are generally weak, and the circulation is strongly influenced by wind and the density-driven currents.

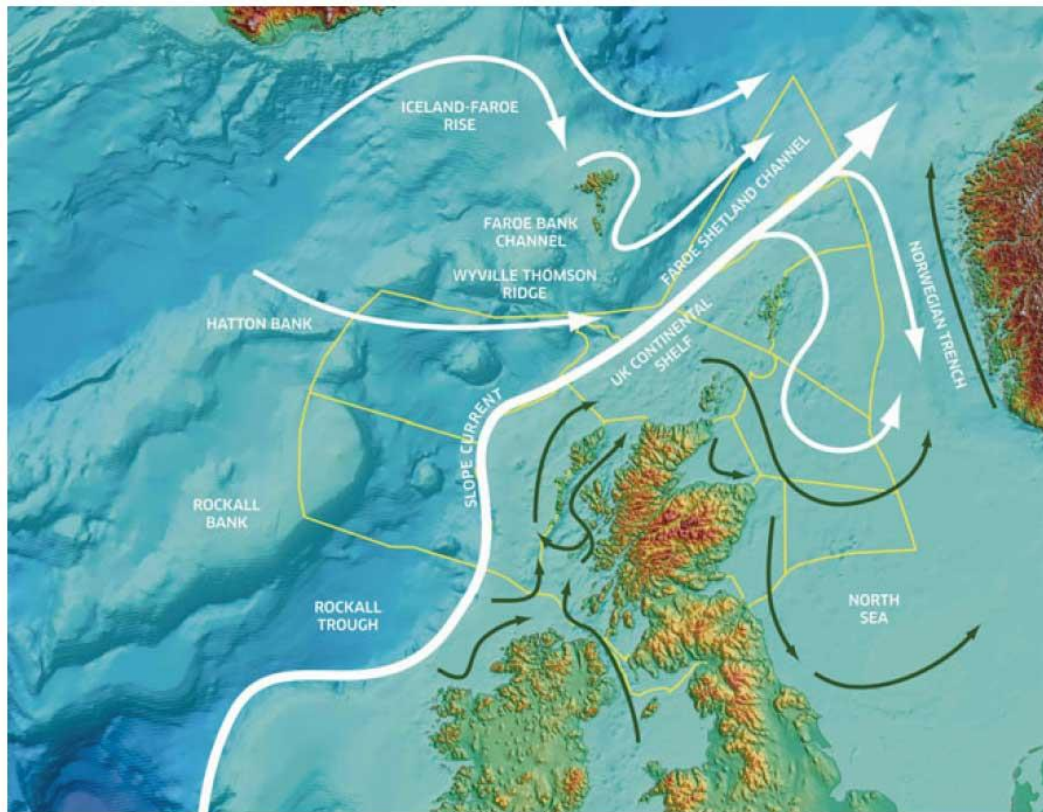


Figure 2.2 Map of the general circulation pattern within the North Atlantic and North Sea around Scotland (reproduced from [4]). The white arrows show the circulation of Atlantic water, while green arrows represent coastal circulation.

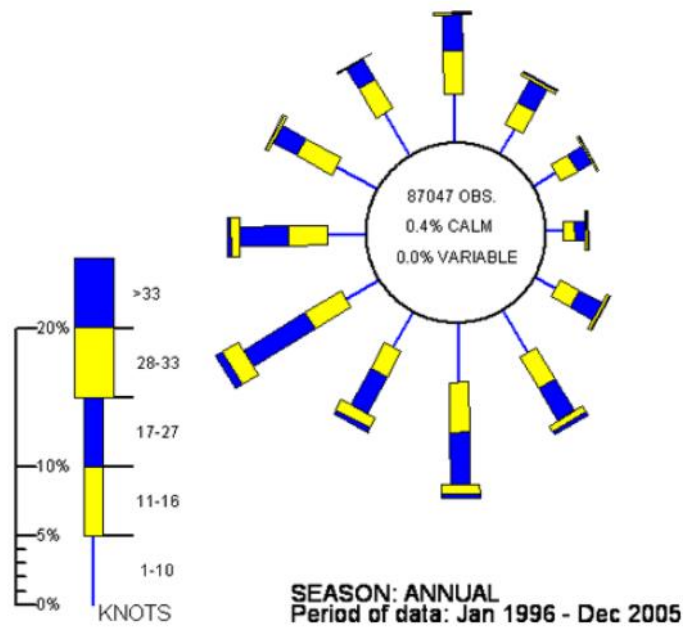


Figure 2.3 Annual (all-year) wind rose for Lerwick for the period 1996-2005 (Shetland), with a prevailing southwest wind direction through the year and frequent strong winds from southerly to north-westerly directional sectors (reproduced from [6])

2.3 Aquaculture in Outer Hebrides

Outer Hebrides has a great dependence on aquaculture, accounting for 10% of Scottish fin fish and 90% of shellfish production [8]. Production takes place within the voes and sounds around the coastline, with the highest concentration of sites on the west coast (see Figure 2.4).

Fin fish production is dominated by Atlantic salmon (*Salmo salar*). In the decade 2011-2020, the annual Salmon production in the waters around Outer Hebrides averaged around 34,000 Tonnes, representing a value of around £175 million. The sector directly employs about 350 full time staff [8], plus supports the wider economy of the islands via fish processing, marine engineering, and transportation.

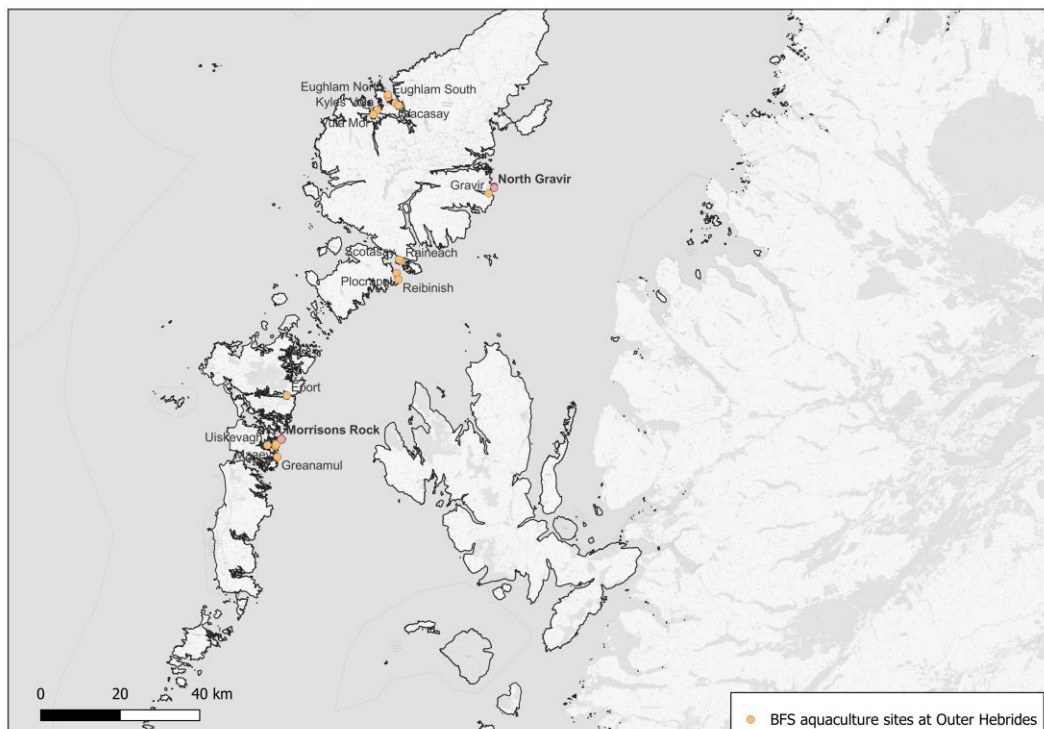


Figure 2.4 Map showing the locations of BFS's active production sites for the last 3 years at the Outer Hebrides islands.

3 Data Basis

In this section, the data sets that are used as input to the modelling study are described. This includes the coastline and bathymetry information (Section 0), the model boundary information for the hindcast and climatology versions (Section 4.3.4), and the meteorological forcing (Section 4.3.5).

3.1 Bathymetry and coastline

3.1.1 Coastline

Ordnance Survey highwater shoreline data (OS HWS) was applied as the governing indicator of the separation between land and water. These data were obtained via OS OpenData² licensed under Open Government License³.

3.1.2 Bathymetry

The North Gravr hydrodynamic model bathymetry was informed by a composite bathymetric database from open-source datasets⁴ and proprietary surveys provided by BFS. These are summarised in Table 3.1 and briefly described below. The vertical reference datum of the baseline bathymetric dataset (EMODnet DTM) was Lowest Astronomical Tide⁵ (LAT). All data were converted to a common reference vertical datum of mean-sea-level (MSL), see also section 4.1.1.

Local site bathymetry data

BFS provided no specific bathymetric sounding dataset at the main area of interest (see Figure 3.1) as part of the current data delivery to inform the development of the North Gravr hydrodynamic database. The soundings derived bathymetric data are typically recorded using depth sounders installed on board fish farm vessels. Bathymetry information are provided relative to a vertical datum of CD, adjusted by the data provider for the depth of sounder below the surface and the predicted local tidal height. These spot depths were mainly used to cross-validate model bathymetry and inform of appropriateness of respective available sources. No high-resolution bathymetric datasets were provided by BFS.

UKHO Admiralty Data

High-resolution bathymetry data for the waters in the Outer Hebrides were obtained from the United Kingdom Hydrographic Office (UKHO) Marine Data Portal⁶. The service provides access to the extensive UK bathymetry holdings held within the MEDIN accredited National Data Archive, allowing users to download bathymetry data under an Open

² [OpenData - Free GIS Data Download - Geospatial Data Sources for Mapping \(ordnancesurvey.co.uk\)](https://www.ordnancesurvey.co.uk/open-data)

³ Contains OS data © Crown copyright [and database right] (2021)

⁴ While high-resolution bathymetry comprises a high percentage coverage of the Minch, there are a few spatial areas (north of the North Gravr site) still poorly covered. Especially straights and shallows that could have a distinct impact of modelled hydrodynamics are currently informed by the GEBCO 2019 DTM (EMODnet DTM incorporates local surveys where available and GEBCO everywhere else). The GEBCO global model is less accurate and detailed in coastal areas and should be used with caution when alternative datasets are not available. In those areas C-MAP data to a buffer zone of 2km from the coastline has been utilised but these were also restricted to the 50m isobath with very low density of points.

⁵ EMODnet uses a global tide surge model (GTSM, Deltares) for LAT to MSL vertical datum references, <https://portal.emodnet-bathymetry.eu/>

⁶ [Admiralty Marine Data Solution, Marine Data Portal \(UKHO\)](https://www.ukho.gov.uk/marine-data-portal) accessed Feb 2022

Government Licence (OGL). The data are offered at a gridded resolution of <10m vertically referenced to CD. Figure 3.2 shows the high-resolution datasets in and around areas of interest in the Outer Hebrides.

EMODnet Digital Terrain Model (DTM)

For offshore areas that are not covered by the multibeam bathymetric datasets, bathymetric data from the Digital Terrain Model (DTM) data products have been adopted from the EMODnet Bathymetry portal (version 2020) (see Figure 3.2). This portal was initiated by the European Commission as part of developing the European Marine Observation and Data Network (EMODnet). The EMODnet digital terrain model has been produced from bathymetric survey data and aggregated bathymetry data sets collated from public and private organisations. The data are provided processed, and quality controlled at a grid resolution of 1/16 x 1/16 arc minutes (approximately 57m, zonal x 115m, meridional). Vertical datum is referenced to LAT derived from the Global Tide and Surge Model (GTSM) developed by Deltares⁷.

C-MAP

An alternative source of bathymetric data was obtained from the Global Electronic Sea Chart Database CM-93 provided by C-MAP. This provides digitised bathymetric chart data vertically referenced to CD. C-MAP data was used in the coastal areas and inlets where high-resolution bathymetric data or local soundings are not available.

Table 3.1 Summary of bathymetric databases used to inform HD_{NO} model bathymetry in order of highest to lowest priority.

Source	Resolution	Vertical Reference [in meters]	Date
UKHO Admiralty Data	2 m to 8 m	Chart Datum [mCD]	Various
EMODnet DTM	57 m x 115 m grid resolution	Lowest Astronomical Tide [mLAT]	2020 version
C-MAP	Isobaths/spot depths	Lowest Astronomical Tide [mLAT]	Variable
Local soundings at fish farm sites	Spot depth soundings	Mean Sea Level [mMSL]	2010 – 2020

⁷ Which information layers? - Data products - EMODnet Bathymetry (emodnet-bathymetry.eu)

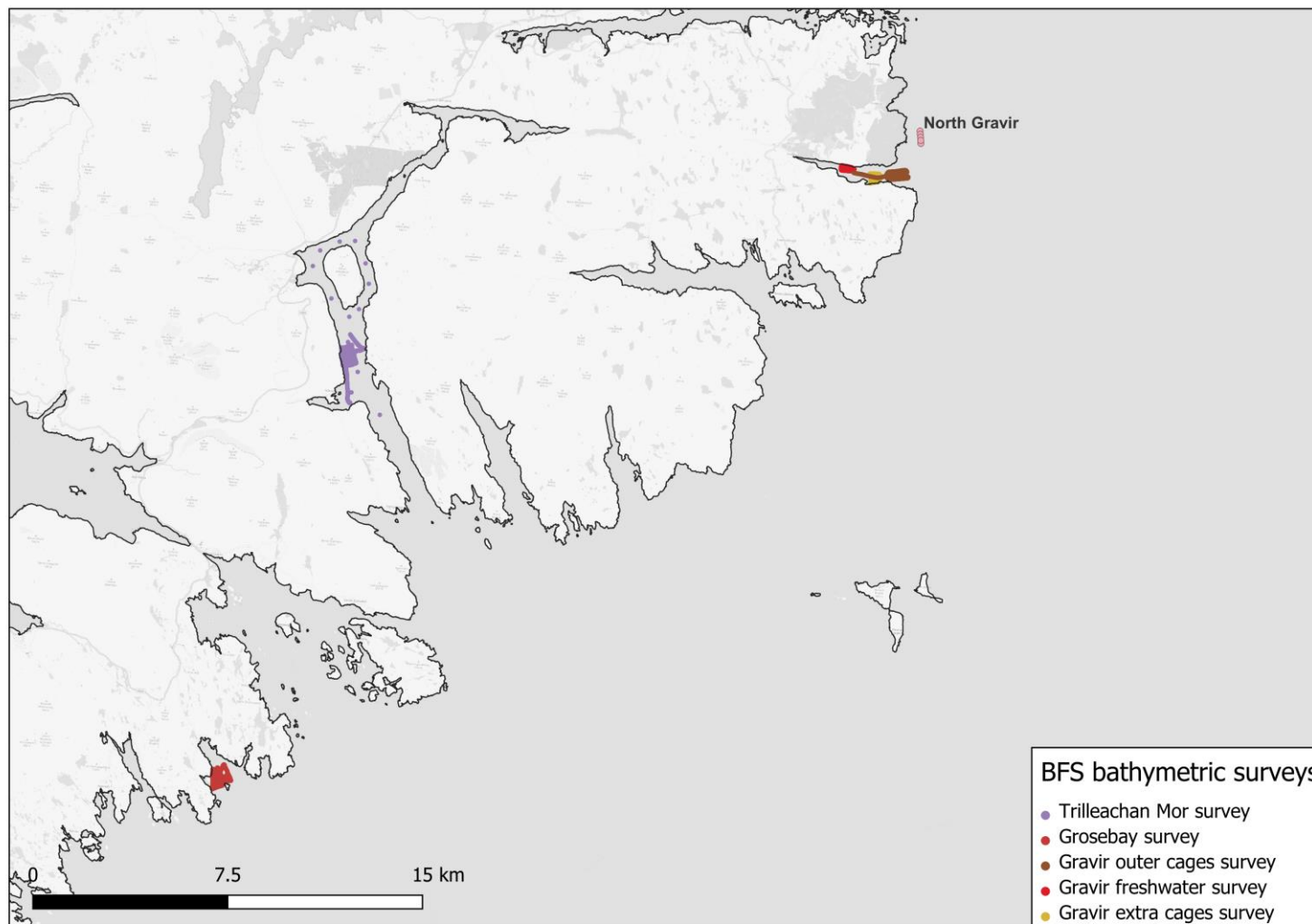


Figure 3.1 Map showing a selection of bathymetric surveys (spot depths soundings) provided by BFS.

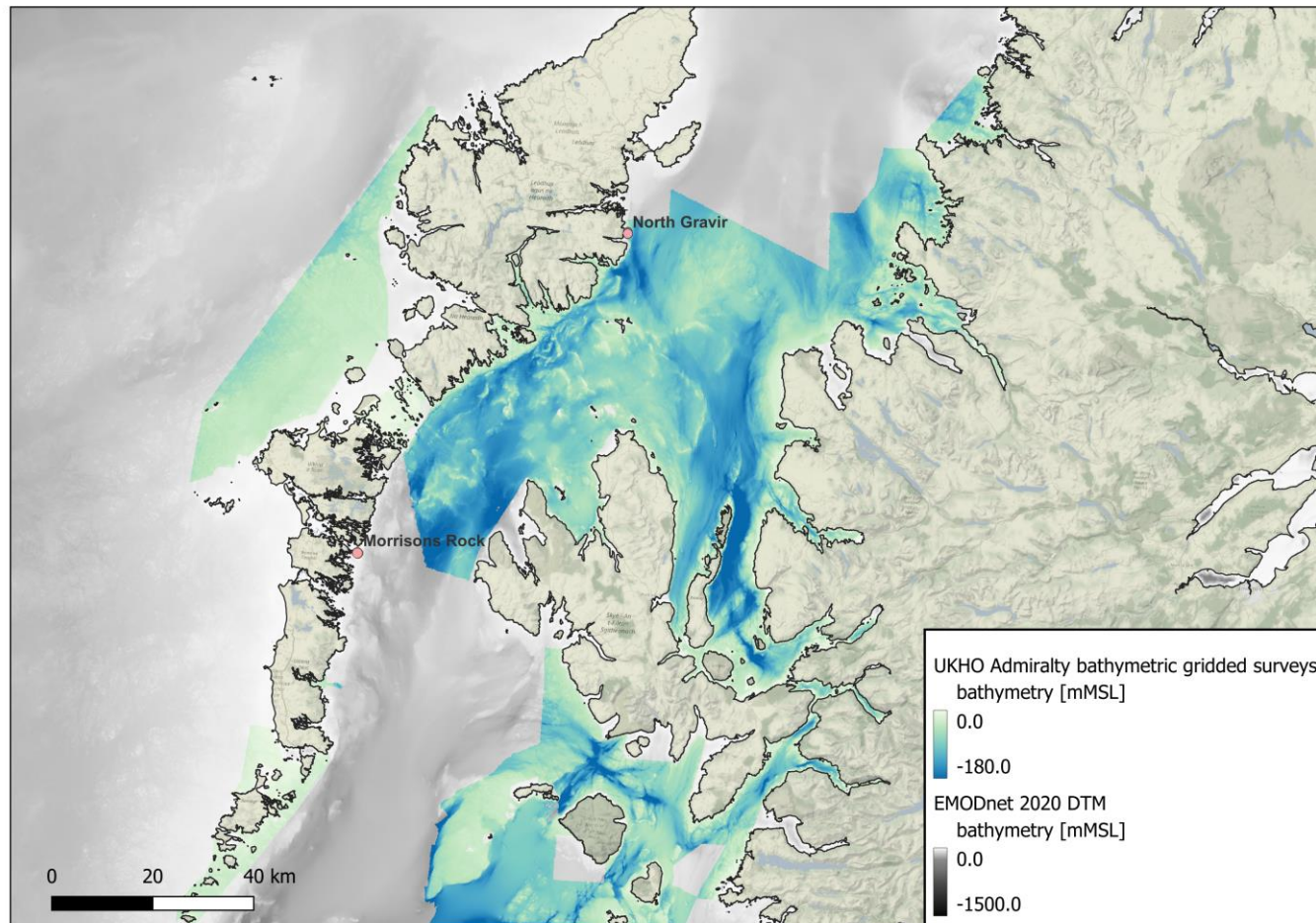


Figure 3.2 Map showing areas of high resolution multibeam gridded bathymetric datasets (green-blue patched areas) around Outer Hebrides used to inform model bathymetry herein (source UKHO Marine Data Portal). Note that the baseline EMODnet 2020 bathymetric database (grey scale) incorporates already most of the available datasets from UKHO (even though the multibeam datasets are upscaled significantly at a final grid resolution of 60x117m² from 4-8m²). Due to lack of available higher resolution bathymetric surveys/composite datasets from partners; where absent the lower resolution GEBCO 2019 global bathymetric model is used (please see <https://emodnet.ec.europa.eu/en/bathymetry> for a detailed account of EMODnet bathymetric model).

3.2 Measurements

3.2.1 ADCP campaigns

Information on current speed/direction, water levels and sea water temperature were provided by BFS during a series of Acoustic Doppler Current Profiler (ADCP) campaigns between 2010 and 2022, see also Table 3.2. Survey periods for each observational deployment provided by BFS are shown in Figure 3.3 and their respective geographic location in Figure 3.4.

The ADCP instruments were frame mounted on the seabed and use acoustic signals to record the current velocity vectors at various depths (bins) through the water column. The derived timeseries were examined to ensure that any anomalous or erroneous data were removed. This included data from the water surface, which are often contaminated by reflections from the surface (so-called side-lobe interference). Observed current speed and direction was depth-averaged (velocity components averaging) through the water column to be comparable to the depth-averaged modelled currents. Current vectors comparisons throughout the water column were performed at respective, matching, vertical levels between the observational records and the modelled 3D currents (i.e., for each mid-depth of a sigma layer the closest matching observational bin depth and/or an average of observational bins within the respective sigma layer thickness).

The measured records included total water depth derived from the pressure sensor. Surface elevation for each site was determined by adding the frame height of the ADCP (sensor distance to seabed – included in the information shared by BFS) to the sensor depth record and then subtracting the MSL value for the ADCP deployment location from the data record.

The surface elevation and velocity vectors timeseries were further processed under the unified tidal analysis and prediction framework U-tide [9] in order to derive the tidal and residual components for records with sufficient duration (>30 days), see also Figure 3.5.

A temperature sensor affixed to the ADCP was also provided for certain deployments.

For most of the available datasets, the calibration and verification periods of the hindcast and climatology model versions, respectively, coincide, see also Figure 3.3:

- Calibration Period (light green) was used to define model parameterisations optimising metrics on tidal signal propagation throughout the domain. On achieving satisfying model skill, these parameterisations are further assessed on the 3D climatological setup and verified (light blue) vs the available observational records at the sites of interest.

Calibration runs were chosen on the basis to provide an overall good spatial coverage of the central model domain, see also Figure 3.4 with whatever available deployments in the respective periods. The verification period was chosen to coincide with an extensive deployment record in the annual period covered while still closely related to the ongoing and prospect aquaculture activities of BFS.

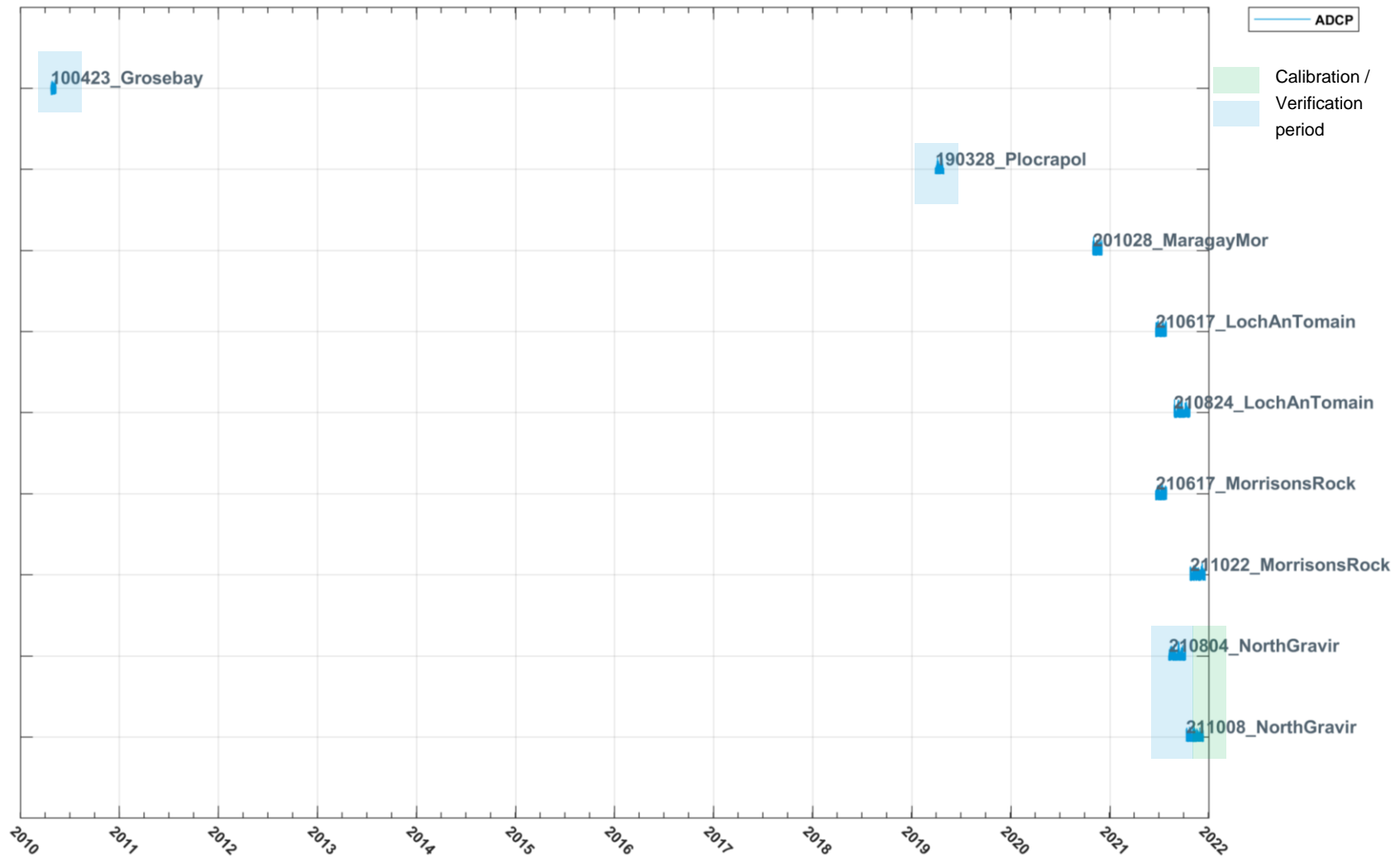


Figure 3.3 Survey periods of ADCP deployments provided by BFS at Outer Hebrides sites of interest for the period 2010-2022 that were considered during the hindcast model calibration and verification development stages.



Figure 3.4 Geographic locations of ADCP deployments provided by BFS at sites of interest at the Outer Hebrides for the period 2010-2022 that were considered during the calibration and verification stages of the hindcast and climatological versions of the hydrodynamic database development.

Table 3.2 Observational records database provided by BFS⁸ to inform on hydrodynamic conditions at the area of interest and calibration of the HD model.

Site	ID	Instrument	SurveyStart GMT	SurveyEnd GMT	Easting BNG [m]	Northing BNG [m]	Deployment depth [m]	Declination (degrees)	Recording Interval [mins]
Grosebay	100423_Grosebay		23/04/2010	12/05/2010	115977E	891332N	24.69		20.0
Plocrapol	190328_Plocrapol		28/03/2019	30/04/2019	118431E	894291N	26.16		20.0
Maragay Mor	201028_MaragayMor		28/10/2020	02/12/2020	88217E	851179N	38.52		20.0
Loch An Tomain	210617_LochAnTomain		17/06/2021	27/07/2021	92436E	859395N			20.0
Loch An Tomain	210824_LochAnTomain		24/08/2021	22/10/2021	92445E	859395N	46.74		20.0
Morrisons Rock	210617_MorrisonsRock	Seaguard II Platform	17/06/2021	28/07/2021	89445E	852913N	40.89	-3.325	20.0
Morrisons Rock	211022_MorrisonsRock	Seaguard II Platform	22/10/2021	17/12/2021	89416E	852894N	40.09	-3.243	
North Gravir	210804_NorthGravir		04/08/2021	06/10/2021	143051E	916012N	59.15	-3.052	20.0
North Gravir	211008_NorthGravir		08/10/2021	10/12/2021	143021E	915986N	56.09	-3.009	20.0

⁸ Following DHI's quality assessment and BFS's commentary on sensor errors and/or instrument drift during survey campaigns

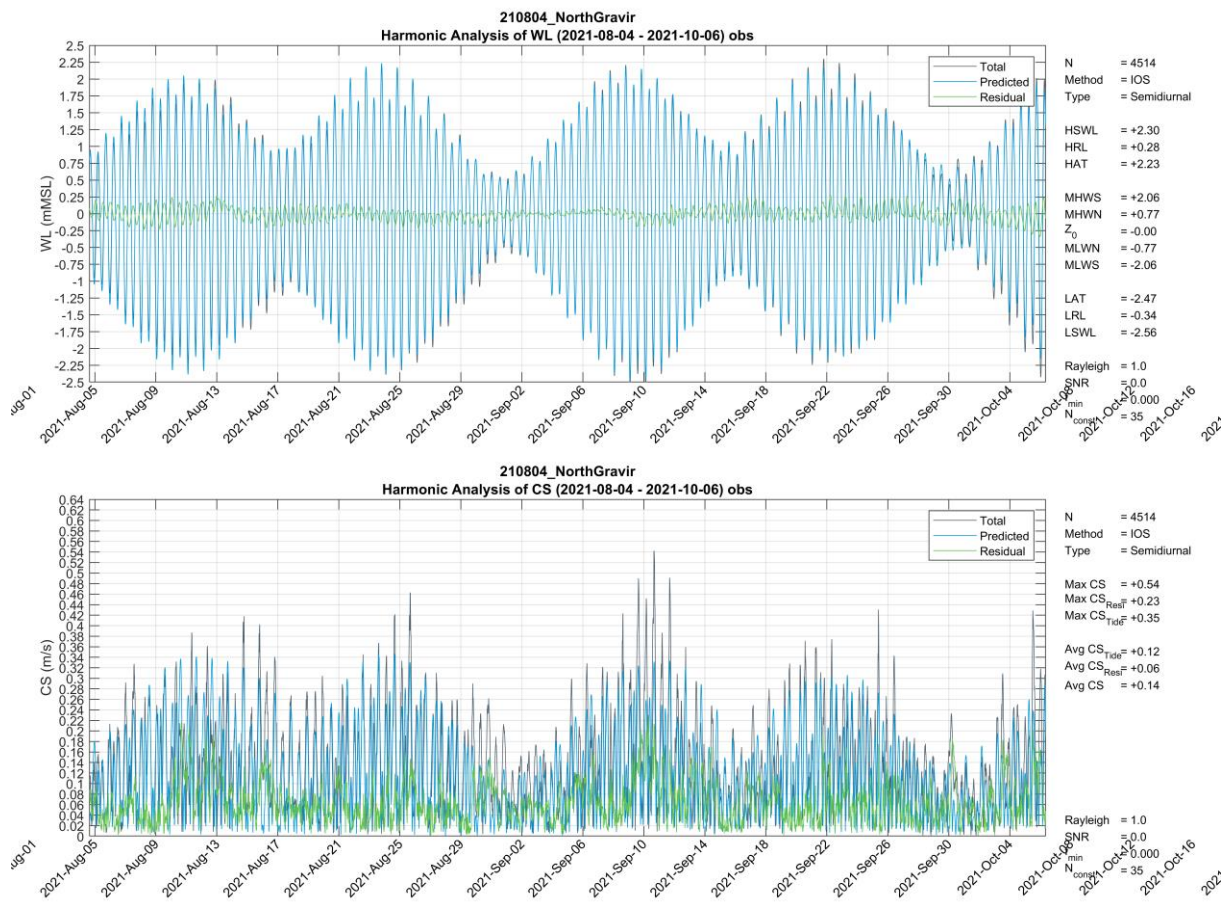


Figure 3.5 Harmonic analysis for surface elevation (top panel) and current speeds (bottom panel) for observational station North Gravir (210804) during deployment 04.08.2021-06.10.2021

4 Model Development

This section describes the development of the three-dimensional North Gravir climatological hydrodynamic model (HD_{NG_clima}) and two-dimensional hindcast version (HD_{NG_hindcast}) within the scope of the project.

4.1 Model selection

4.1.1 Three-dimensional model

Many of the aquaculture sites in the waters around Outer Hebrides are located within complex coastlines close to steep bathymetric gradients (Figure 3.2). These areas have the potential to exhibit both vertical stratification and density driven circulation due to density gradients (as a result to differences in water temperature and salinity), which may have important implications for vertical mixing and flow velocities. In such environments, a three-dimensional (3D) model may be necessary to capture the important processes [10]. Temperature and salinity are also important factors in biological modelling (e.g., for sea-lice development). Finally, wind forcing will also play an important role in driving local flow patterns, which is important for surface dispersion (e.g., for modelling bath-treatment) so this must also be included in the model setup.

As such, the MIKE 3 FM modelling system was chosen, as it can reproduce such hydrodynamic conditions throughout the water column in the area of interest for the North Gravir site (see Section 0).

4.1.2 MIKE 3 hydrodynamic model

The North Gravir hydrodynamic modelling has been performed using the MIKE 3 modelling package developed by DHI. MIKE 3 includes the simulation tools to model 3D free surface flows and associated sediment or water quality processes. The following modules available within MIKE 3 were used during this study:

- **HD – Hydrodynamics:** This module simulates the water level variations and flows in response to a variety of forcing functions. It includes a wide range of hydraulic phenomena in the simulations, and it can be used for any 3D free surface flow. The Flexible Mesh version, which uses a depth and surface adaptive vertical grid, is particularly suitable in areas with a high tidal range.

The MIKE 3 Model used for the present study was version 2023 [11].

The Hydrodynamic Module is the basic computational component of the entire MIKE 3 Flow Model FM, and has been developed for applications within oceanographic, coastal, and estuarine environments [12]. The hydrodynamic module provides the basis for the other modules such as sand transport, mud transport, particle tracking, and ECO Lab.

The computational mesh is based on the unstructured grid in the horizontal direction, an approach which gives maximum degree of flexibility when handling problems in complex domains (such as in voes and narrow straits). In the vertical direction a sigma (σ) discretisation is used meaning that model elements are represented as 3-sided prisms (Figure 4.1)

The MIKE3 modelling system is based on the numerical solution of the three-dimensional incompressible Reynolds Averaged Navier-Stokes (RANS) equations, invoking the assumptions of Boussinesq, and of hydrostatic pressure. Thus, the MIKE 3 flow model

consists of continuity, momentum, temperature, salinity, and density equations and a turbulence closure scheme. In the horizontal domain both Cartesian and spherical coordinates can be used. The free surface is considered using a sigma-coordinate transformation approach.

The spatial discretisation of the primitive equations is performed using a cell-centred finite volume method. The spatial domain is discretised by subdivision of the continuum into non-overlapping element/cells. In the horizontal plane an unstructured grid is used while in the vertical domain a structured discretisation is used. The elements can be prisms or bricks whose horizontal faces are triangles and quadrilateral elements, respectively. An approximative Riemann solver is used for computation of the convective fluxes, which makes it possible to handle discontinuous solutions.

For the time integration a semi-implicit approach is used where the horizontal terms are treated explicitly, and the vertical terms are treated implicitly.

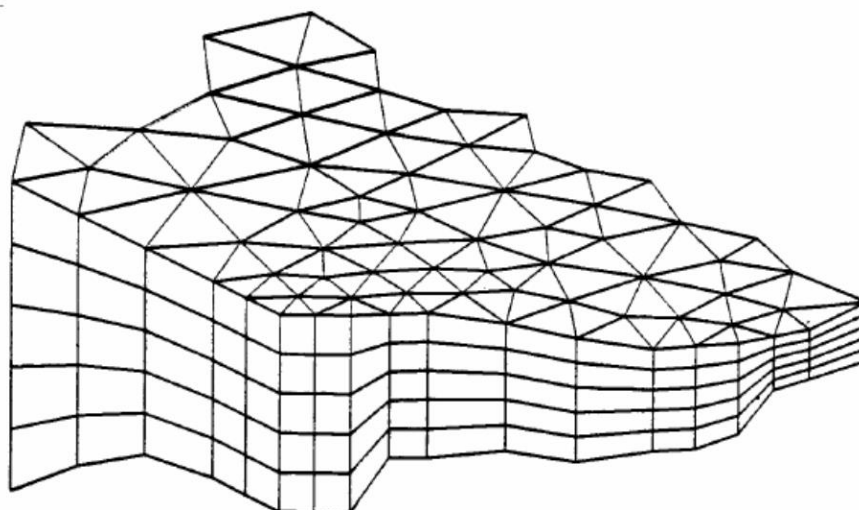


Figure 4.1 Example of an unstructured mesh in MIKE3 with 5 sigma (σ) layers.

4.2 Datums

Unless explicitly stated otherwise, the following reference datums were adopted for the models developed during this project.

- Horizontal datum is established using the Ordnance Survey of Great Britain 1936 (OSGB36) datum, also referenced as EPSG 27700 – OSGB36 British National Grid
- Vertical datum is referenced to mean-sea-level (MSL). Conversion from LAT to MSL is performed using EMODnet LAT to MSL gridded product⁹.

4.3 North Gravr hydrodynamic hindcast and climatology models

The regional 3D hydrodynamic model of North Gravr was established as a climatology (HD_{NG_clima}) version. The HD_{NG_clima} model is a dynamically downscaled version of the ECLH

⁹ EMODnet uses a global tide surge model (GTSM, Deltares) for LAT to MSL vertical datum references, <https://portal.emodnet-bathymetry.eu/>

(see Section 4.3.1). Thus, HD_{NG_clima} is a high-resolution local model that dynamically extrapolates the effects of the large-scale processes of the ECLH to local scales of interest around the waters of the North Gravir site.

A climatology is constructed as a representation of the ‘mean’ status of hydrodynamics over a period of years. On that basis, it is difficult to justify a calibration/validation of a climatology forced model with an observational record as a measure of model skill. Therefore, a 2D hindcast version HD_{NG_hindcast} was constructed which was calibrated and then validated against the available observational record¹⁰ through the measurement campaigns provided by BFS, see also section 3.2. Thus, parameterisations and calibration settings were considered applicable for the climatology version of the model. The climatological version was then verified versus the observational record in terms of magnitude and directional distribution of the velocity field throughout the water column at the observational locations.

The following sections describe the establishment of the 2D HD_{NG_hindcast} and subsequently 3D HD_{NG_clima} model, including the model mesh and bathymetry, the specification, and model outputs.

4.3.1 The East Coast Lewis and Harris Climatology Model

The East Coast of Lewis and Harris (ECLH) model is hydrodynamic numerical solution of the Outer Hebrides, Skye and the Small Isles, as well as the north-west coast of Scotland, developed for and maintained by Marine Scotland Science, to describe the circulation of the Outer Hebrides continental shelf waters [13], [14]. The ECLH has been designed to support a varied range of marine science and policy applications, including for rapidly developing marine renewable energy and aquaculture sectors.

The wider domain ECLH encompasses all the Outer Hebrides’s waters and most of the north-west Scotland (Figure 4.2). The horizontal resolution varies from approximately 3 km in the outer domain to around 500 m around the Scottish Coast to less than 200 m around the Outer Hebrides coastline (Figure 4.3). For the vertical discretization a σ coordinate system (terrain following coordinates) based on 10 uniform layers is used (each representing 10% of the water column).

The ECLH is effectively nested within the wider Scottish Shelf Model (SSM) [15, 16]. A brief description of the ECLH setup is provided below. The version used herein is the ECLH 1.02 [14].

The ECLH is a one-year climatology model that represents average conditions with a 1993 tidal component - that is the same 1993 tidal component (Lerwick) applied to the wider SSM. The model was implemented using an unstructured grid coastal ocean model, FVCOM (Finite-Volume Community Ocean Model) [17]. The model forcing includes:

- Offshore boundary conditions (temperature, salinity, currents, and sea-surface elevation) from monthly mean over the 25-year period (1990-2014) provided by the SSM
- Climatology atmospheric forcing is also included based on monthly 1990–2014 data set derived from ERA-Interim data [18] (further discussed in Section 0)
- Freshwater inputs (i.e., Rivers) from climatological runoff discharges were obtained from the Centre for Ecology and Hydrology (CEH) Grid-to-Grid (G2G) model [19, 20], covering the period from 1962 to 2011 and including 577 rivers in Scottish Waters.

¹⁰ Only with respect to the tidal signal propagation throughout the computational domain

As the conditions of the ECLH encompass an averaging period of 25-years (1990-2014), the climatology seeks to smooth the natural variability of the climate and achieve an approximately stationary characterisation that averages out the interannual variability.

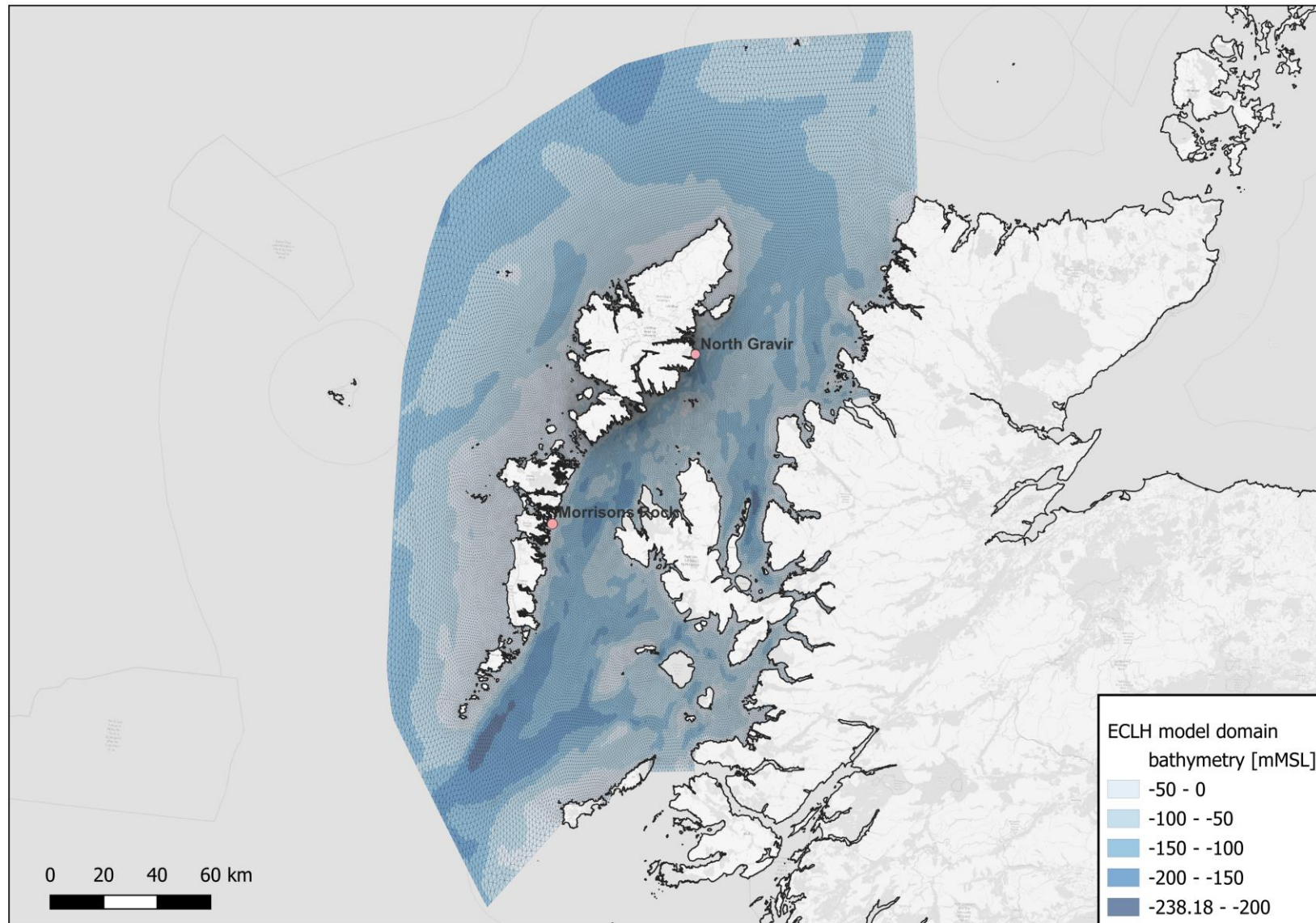


Figure 4.2 East Coast of Lewis and Harris (ECLH) numerical mesh showing the entire model domain.

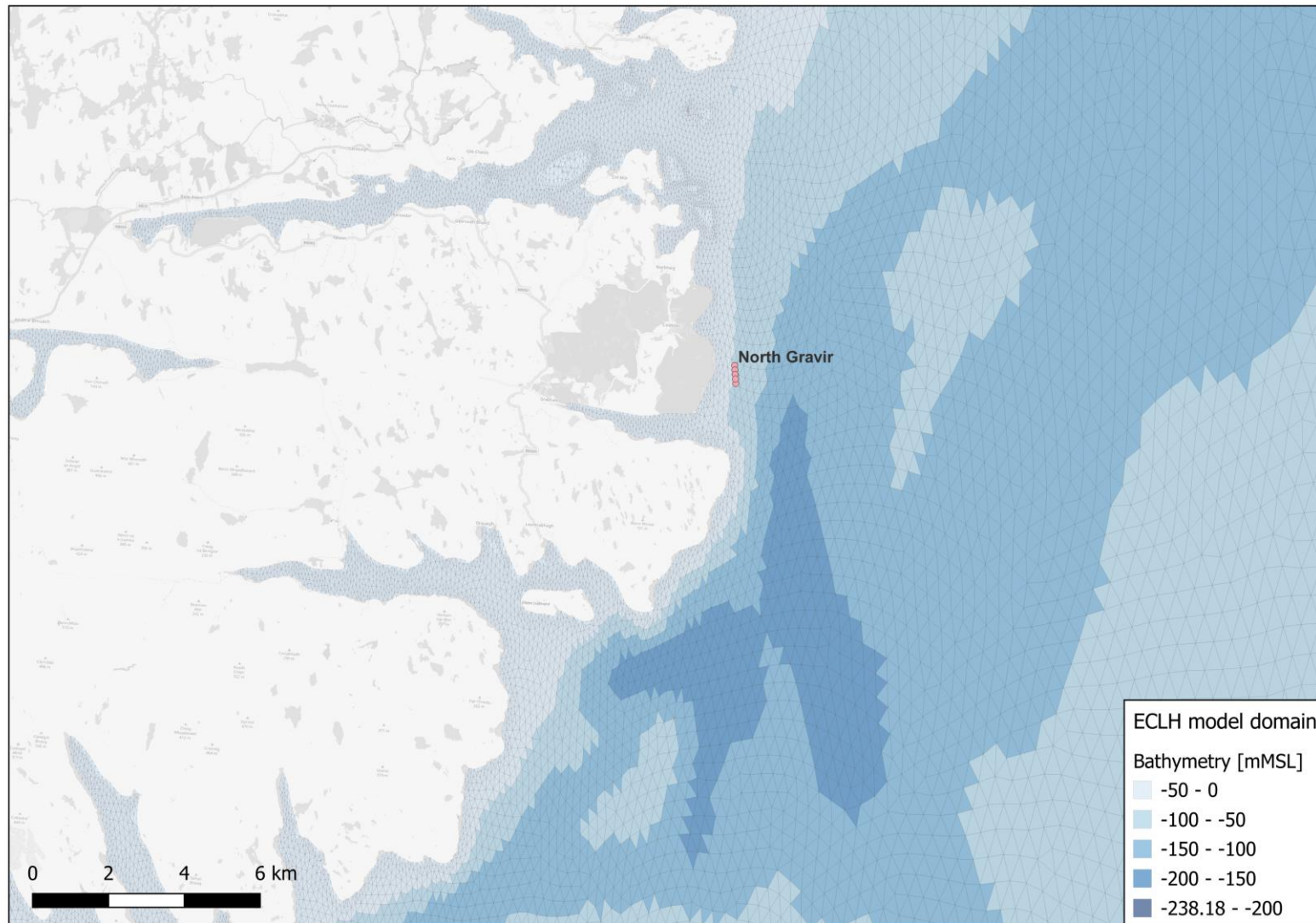


Figure 4.3 East Coast of Lewis and Harris (ECLH) computational mesh at the North Gravir area of interest. See also Figure 4.8 (right panel) for a comparison in spatial discretisation improvement for the area of interest.

4.3.1.1 Meteorological conditions

Climatologically averaged meteorological conditions used to force the ECLH are derived from the ERA-Interim re-analysis (1990-214) products produced by the European Centre for Medium-Range Weather Forecasts (ECMWF) [18]. A monthly mean wind climatology was derived from these data. The met forcing was derived as monthly means, which were then linearly interpolated to 6-hourly smoothed forcing data for each grid-point, i.e. mean February data were applied at the middle of February; then mean March data were applied mid-March etc., with time-interpolation between (see Section 5.3 of [15]).

The atmospheric conditions include wind conditions (wind speed and direction), atmospheric pressure, surface heat flux, precipitation, evaporation, relative humidity, air temperature, thermal/solar radiation. For wind, the 6-hourly data were used to construct a monthly mean wind stress, which was then converted back into an equivalent wind field [16]. It should be noted that the AMM7 model, that was used to derive the offshore boundary conditions for the ECLH climatology, were also forced by ERA-Interim reanalysis; hence, providing some consistency in the boundary forcing of the ECLH.

Figure 4.4 shows a time-series plot of the climatologically averaged meteorology for selected parameters for a location at the centre of the Little Minch within the `HDMR_hindcast/clima` computation domain. As expected for a climatology model there is a low temporal variability at shorter temporal scales (hours and days), but the seasonal pattern is quite clear. For example, the largest wind speeds occur during the winter months (December to February) with lowest wind speeds in the summer (June to August). Conversely, air temperatures are lowest in the winter and highest during the summer.

The time-series of wind direction (second panel in Figure 4.4) shows minor variations throughout the year. This can also be observed in Figure 4.5, which shows a rose plot of the distribution of wind speed and wind direction (coming from) extracted from the climatologically averaged meteorology at the same offshore location. The wind direction is dominated by south-westerly conditions; directional sectors from 210°N to 240°N accounting for approximately 80% of the total. This is consistent with the prevailing wind direction for the Northern Isles. However, this does not reflect the full range of wind directions that may occur on these latitudes during the passage of low-pressure systems (as mentioned in Section 2.2), which are averaged out in the model climatology.

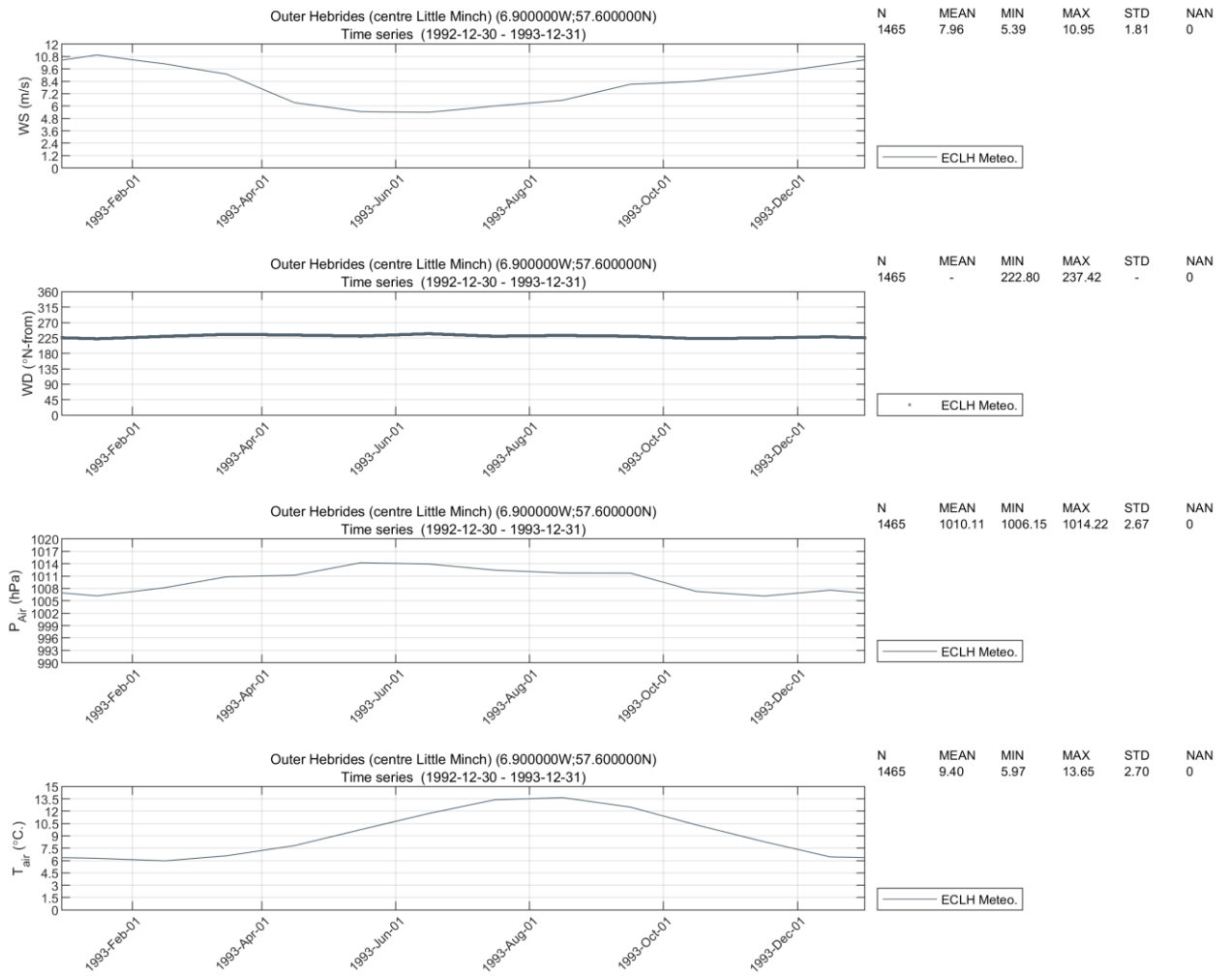


Figure 4.4 Time-series and annual statistics of climatologically averaged meteorological conditions for a location within the HD_{NG_hindcast/clima} computational domain at the centre of Little Minch, Outer Hebrides. From top to bottom: wind speed, wind direction, atmospheric pressure, and air temperature

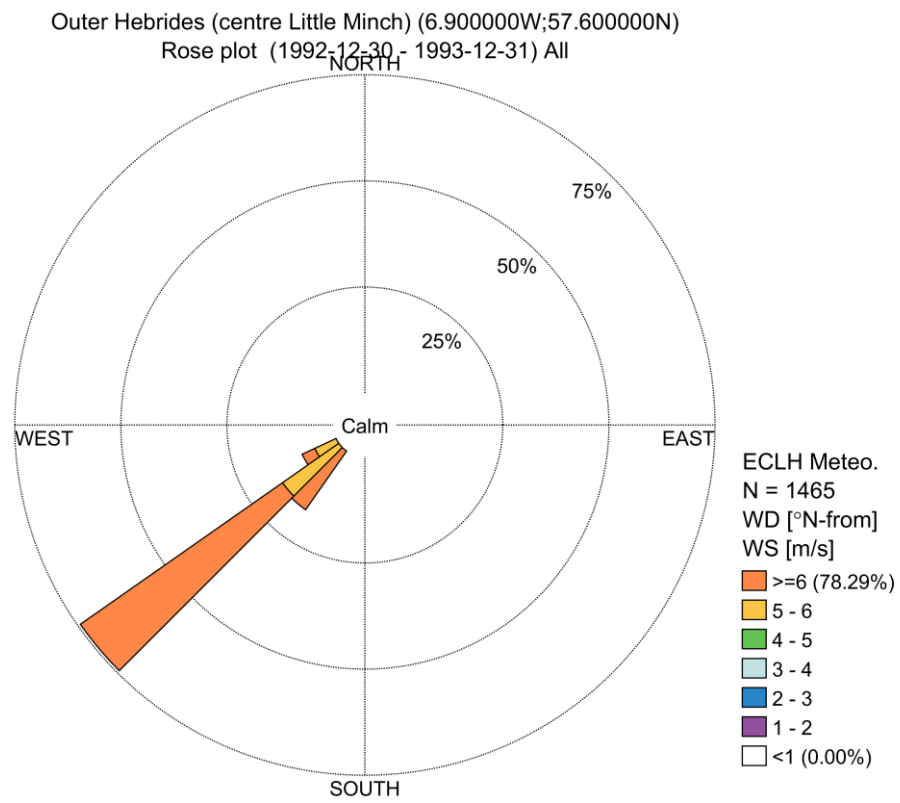


Figure 4.5 Annual wind rose for a location within the HD_{NG_hindcast/clima} computational domain at the centre of Little Minch, Outer Hebrides from the climatology atmospheric forcing used as input to the ECLH.

4.3.2 Model domain

The computational domain of the regional model encompasses most of the Inner Seas of the West coast of Scotland (south of the Minch) within the area east of the Lewis and Harris islands and the west coast of north mainland Scotland and north coastline of Skye island, see Figure 4.6 and Figure 4.7. The model has three open (sea) boundaries to the Minch, the Little Minch and between Skye island and mainland Scotland. Land boundaries are defined according to OS HWS (see Section 3.1.1). In total the model domain covers an area of approximately 3,223 km².

4.3.3 Mesh and bathymetry

The computational mesh is based on a variable resolution unstructured grid in the horizontal direction. The mesh resolution was chosen to capture the important hydrodynamic processes within the scope of this hydrodynamic database construction, while maintaining practical computational run times. This was also informed by similar regional scale models (such as the ECLH sub-domain for the East coast of Lewis and Harris model) and following discussions with BFS on model scoping.

The computational mesh of the hydrodynamic model is shown in Figure 4.6. In the outer domain, close to the model boundaries, the horizontal mesh element length is set at around 1.2 km, 2.5 km and 800 m respectively for boundaries 22, 33 and 44 (see Figure 4.7). The mesh element length gradually reduces to between 400m and 150m in the coastal areas within the Outer Hebrides archipelago (right panel, Figure 4.6 and left panel, Figure 4.7). The highest resolution is specified in the focus areas of North Gravir (element side length ~36m) and subsequently near the shoreline, designated PMF areas, narrow straits between islands and within inlets. In these areas, the mesh element length is <150m. In total the horizontal mesh consists of 13,902 nodes defining 24,026 mesh elements. In the vertical dimension the discretisation is based on ten (10) non-equidistant sigma (terrain following) layers, see Figure 4.9, with increasing resolution (decreasing layer thickness) towards the surface (see also 4.3.6).

Thus, the down-scaled regional climatology model HD_{NG_clima} offers significant improvement in the resolution around the coastline and includes detailed features (e.g., smaller islands and inlets) that are not represented in the shelf-sea scale ECLH model, see Figure 4.8.

The bathymetry datasets described in Section 3.1.2 were interpolated to the computational mesh. Careful attention was given to smoothing of bathymetry to alleviate large bathymetric gradients between adjacent computational cells.

The model has three (3) open boundaries one (1) to the north and two (2) to the south south-east as seen in Figure 4.7.

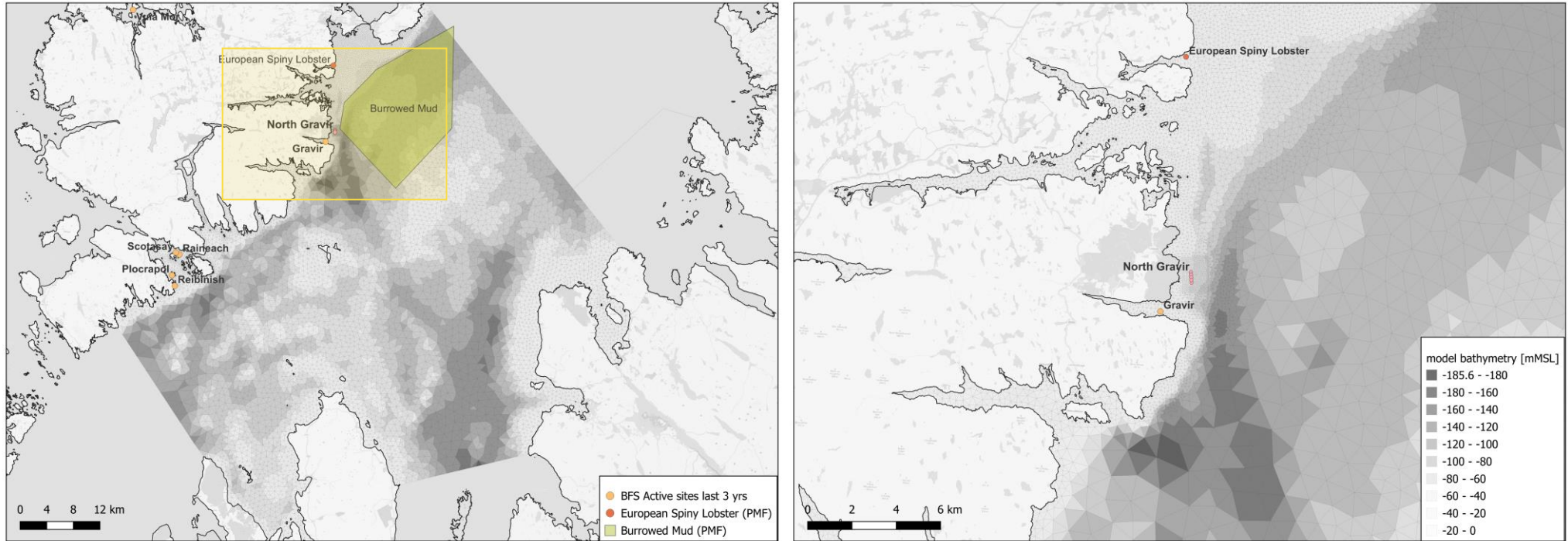


Figure 4.6 Computational domain of the regional North Gravir hydrodynamic model (left) and zoomed in perspective of the main areas of interest (right). Mesh resolution is significantly improved around the area of interest versus ECLH, as seen in Figure 4.3 and Figure 4.8, allowing for a better representation of coastal and bathymetric features.

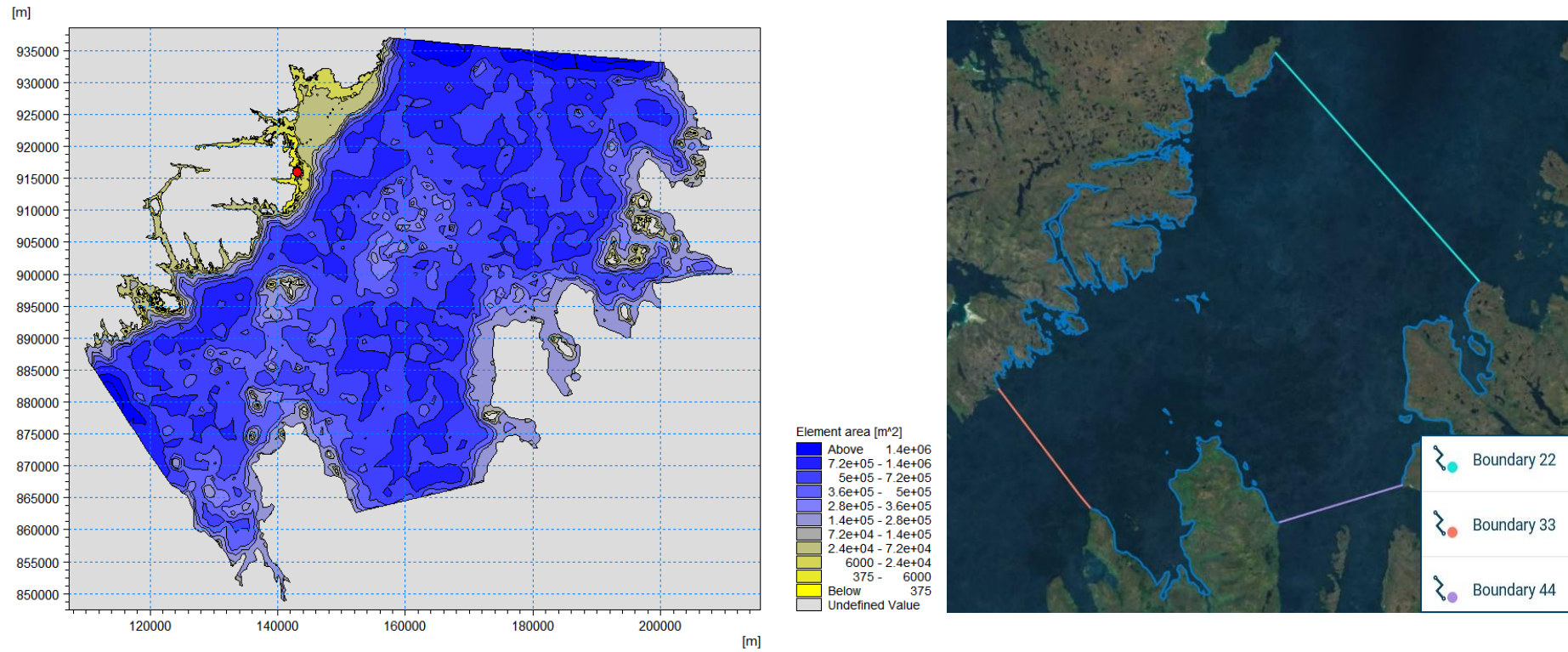


Figure 4.7 Mesh resolution [m] across the HD_{NG_hindcast/clima} computational domain of BFS (left panel, North Gravr site as red dot) and defined open sea boundaries (see also Section 4.3.6) (right panel)

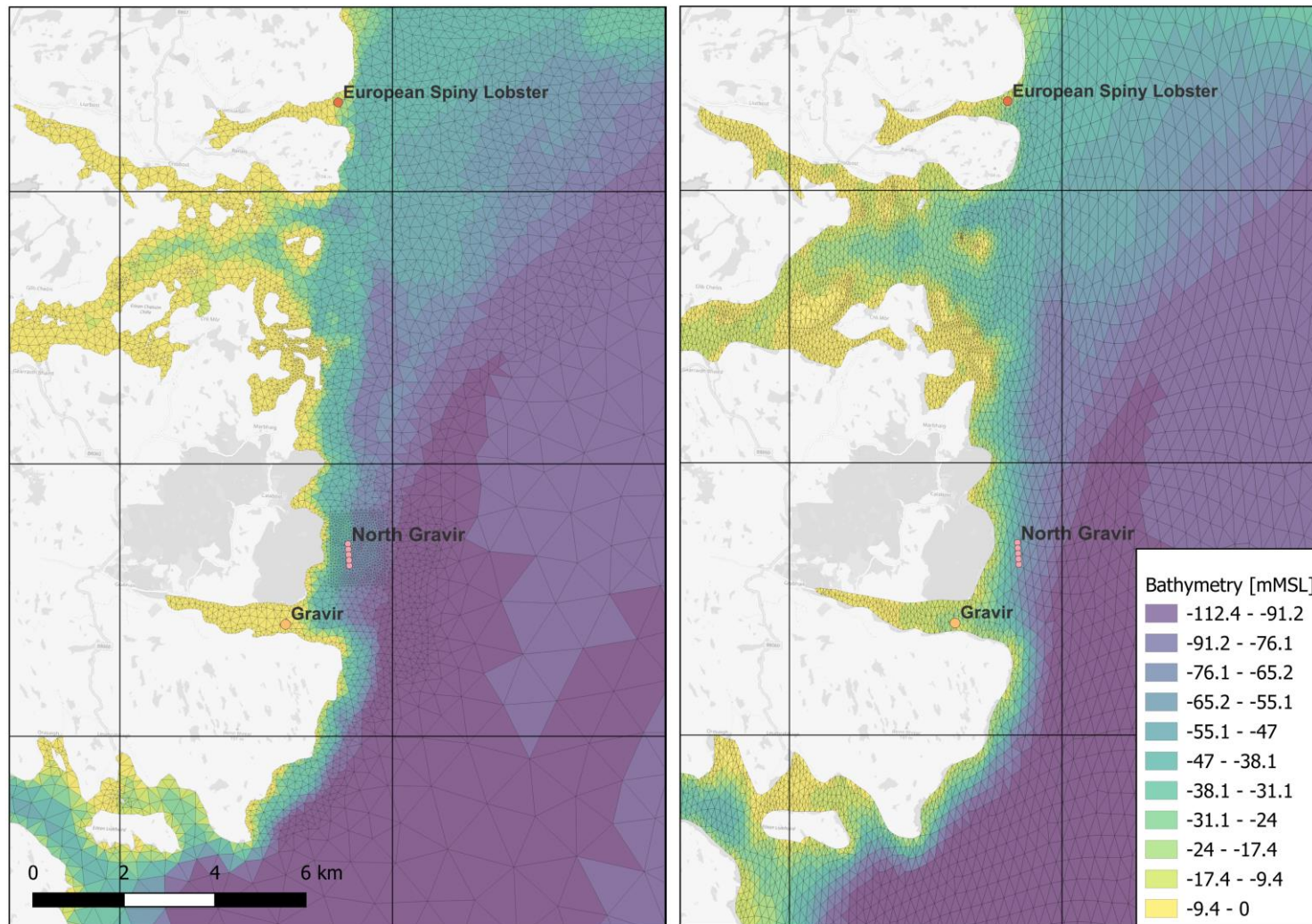


Figure 4.8 North Gravir model (left) versus ECLH model mesh (right) at area of interest. There are differences in coastline/islands representation and subsequently flow resolution/representation through narrow straits, but bathymetry is relatively consistent between the two models.

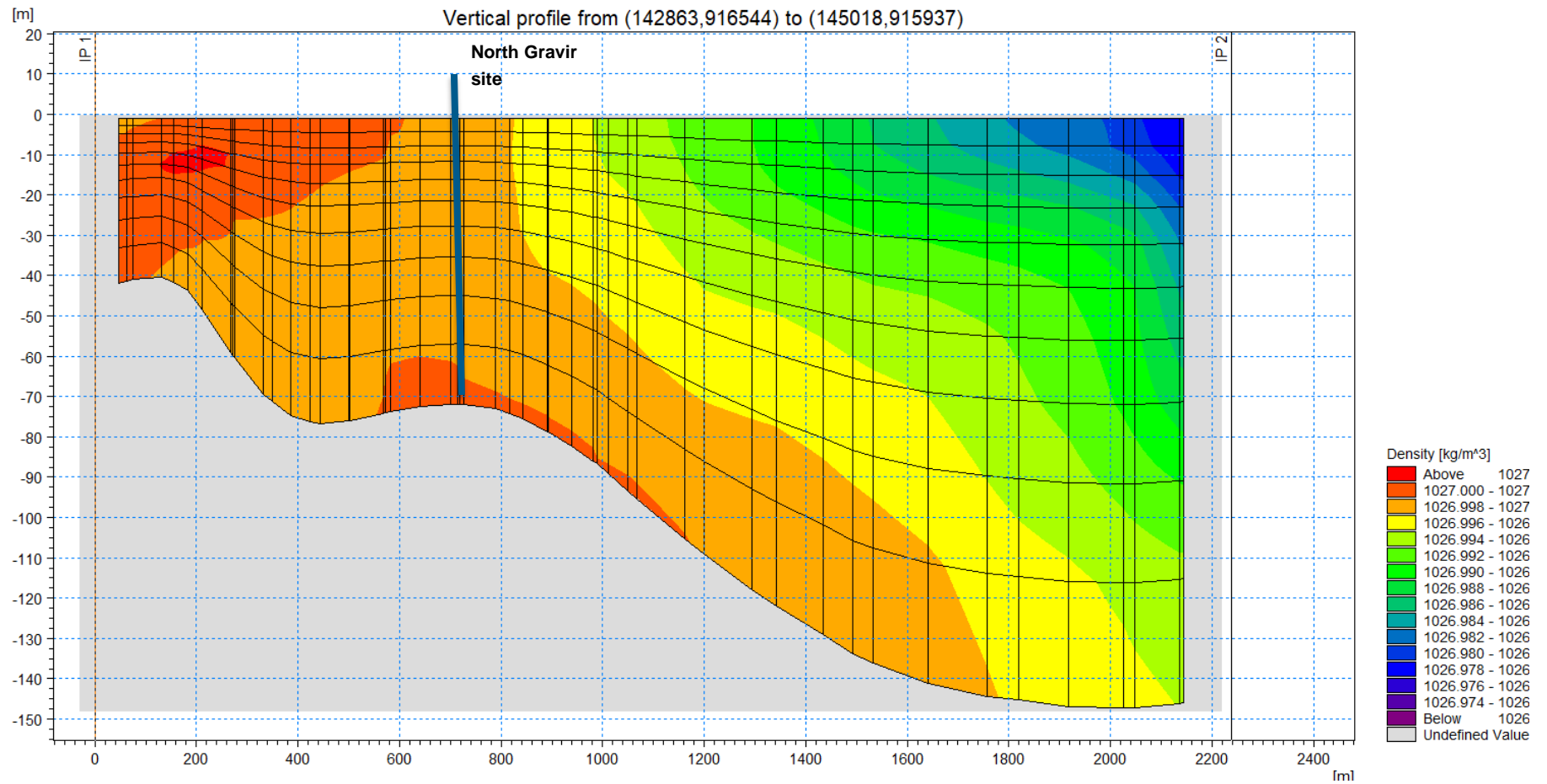


Figure 4.9 Vertical mesh geometry at the North Gravir site nearby area of interest (North Gravir site location indicated by blue line)

4.3.4 Initial and boundary conditions

4.3.4.1 2D Hindcast

The barotropic component comes from a global tidal model produced by *Denmark's Technical University* at DTU Space in 2010 (DTU10)¹¹ using a response method of residual analysis of multi mission altimeter data. The model has a resolution of 2 min and includes the 12 major tidal constituents. The model is an empirical ocean tide model which means that it does not include tidal currents [21].

Hydrodynamic boundaries (water levels and depth averaged current velocities) were specified as Flather boundary conditions [22]. This is an efficient open boundary condition method for downscaling coarse model simulations to local areas.

4.3.4.2 3D Climatology

Similarly, to the hindcast version, the barotropic component comes from the 2 min global tidal model produced by *Denmark's Technical University* at DTU Space in 2010 (DTU10). The 1992-1993 tidal solution is selected to coincide with the nominal period in the ECLH climatology.

The baroclinic component of current velocities (3D) and the temperature and salinity physical parameters were derived from the ECLH one-year climatology (see Section 4.3.1).

The baroclinic velocity component is combined with the barotropic tidal signal to generate the boundary forcing of current velocities throughout the water column.

Hydrodynamic boundaries (water levels and current velocities) were specified as Flather boundary conditions [22]. This is an efficient open boundary condition method for downscaling coarse model simulations to local areas especially when also imposing stratified density at water level boundaries as it can generally help to avoid model instabilities.

Initial conditions were set for the spatially varying distribution of water levels (2D) and temperature and salinity (3D) throughout the computational domain at the beginning of the simulation. These were derived from the DTU10 plus the mean dynamic topography signal from the ECLH initial conditions (interpolated onto the HD_{NG_clima} computational mesh).

Similarly, boundary forcing conditions are based on the combined DTU10 and ECLH one-year climatology for both surface elevation (1D, horizontal) and current velocities (2D, vertical), temperature and salinities (2D, vertical).

Temperature and salinity physical parameters from the ECLH climatology are also gradually nudged to the solution (3D, volume) at 24 hr intervals working in essence as internal boundaries for the HD_{NG_clima}. The HD_{NG_clima} thus is, in that aspect, constrained to the ECLH solution and matches closely the ECLH climatology sea water temperature, salinity and by extent density. The use of the ECLH temperature and salinity fields as internal boundaries for the HD_{NG_clima} allows us to oversee atmospheric forcing in terms of heat exchange to inform modulation of surface waters and subsequent effect on density driven currents.

¹¹ https://www.space.dtu.dk/English/Research/Scientific_data_and_models/Global_Ocean_Tide_Model.aspx

4.3.5 Atmospheric forcing

4.3.5.1 Hindcast

No atmospheric forcing is applied in HD_{NG_hindcast} model as it used to examine the tidal signal propagation in isolation throughout the computational domain.

4.3.5.2 Climatology

Atmospheric forcing applied in HD_{NG_clima} model include the wind speed and wind direction at 10mMSL and atmospheric pressure at mean-sea-level. This forcing adopts climatologically averaged meteorological conditions derived from the ERA-Interim re-analysis product (see Section 0). This is the same meteorological forcing as used in the wider domain ECLH model; hence, achieving consistency with the model boundary forcing 4.3.4.2.

Other meteorological inputs specified in HD_{NG_clima} include items related to heat exchange between the sea and the atmosphere. The temperature variations are used in the MIKE3 temperature/salinity (TS) module which sets up additional transport equations in the model. The calculated temperature and salinity are fed-back to the hydrodynamic equations through buoyancy forcing induced by density gradients. The inputs to the heat exchange include air temperature, short-wave radiation, and long-wave radiation. Once again, these data were adopted climatologically averaged meteorological conditions used in the ECLH (see Section 0).

4.3.6 Model configuration

The configuration of the HD_{NG_hindcast/clima} model is summarised in Table 4.1. For more information on the scientific background of the model settings or the governing equations of the model, please refer to [11, 23].

Table 4.1 Summary of HD_{NG_hindcast/clima} model settings.

Setting	Description/Value
Basic equations	Shallow water equations
Numerical scheme	Higher order scheme (time integration and space discretisation)
Horizontal mesh	Variable resolution unstructured grid (see Section 4.3.3)
Vertical resolution	Climatology: Non equidistant variable thickness sigma layers
Simulation period	Hindcast: A one-year hindcast run representing actual conditions in the period covered by the observational record (see Section 3.2.1) Climatology: A one-year climatological run, which represents average conditions for the period 1990-2014 with a 1993 tidal component.
Model time step (adaptive)	0.01 to 30 seconds
Flooding and drying	Drying depth 0.005m, wetting depth 0.1m
Density	Hindcast: NA Climatology: Function of temperature and salinity
Horizontal Eddy viscosity	Smagorinsky formulation with constant = 0.28

Setting	Description/Value
Vertical Eddy viscosity	Hindcast: NA Climatology: K-epsilon formulation with eddy viscosity values min:1.8e-06/max:0.4 [m ² /s]
Bed resistance	Spatially varying roughness height ranging from 0.045 (deep bathymetric zones) to 0.08 (for coastal zones)
Coriolis Forcing	Varying in domain
Wind forcing	Hindcast: NA Climatology: Varying in time and domain climatologically averaged meteorological conditions derived from the ERA-Interim re-analysis products used in the ECLH climatology forcing
Wind friction	Varying with wind speed (Linear variation Speed): • 7 [m/s] Friction: 0.001255 • 25 [m/s], Friction: 0.002425
Tidal potential	Not included
Precipitation/Evaporation	Hindcast: Not included Climatology: Not included but instead T/S3D fields from ECLH climatology are assimilated (nudged) to prevent model drift and constrain sea water density modulation to the ECLH solution, see Section 4.3.4.2
Initial conditions	Hindcast: Spatially varying surface elevation (2D) derived from the 2 min DTU10 global tide model Climatology: Spatially varying surface elevation (2D) derived from the 2min DTU10 combined with ECLH mean dynamic topography and temperature and salinity (3D) from the ECLH climatology (interpolated to the HD _{NG_clima} mesh)
Boundary conditions	Hindcast: Flather boundary conditions, temporally and spatially water levels derived from 2 min DTU10 global tide model (1D, horizontal) and currents from DTU10 Climatology: Flather boundary conditions, temporally and spatially water levels and 3D current velocities from combined 2 min DTU10 and ECLH climatology
Temperature and salinity module	Hindcast: NA Climatology: Temporally and spatially boundaries from the ECLH plus nudging of the temperature and salinity fields (internal boundaries) at 24 hours intervals ¹²

¹² As the ECLH temperature (T) and salinity (S) parameters are used as internal boundaries (nudged) for the HD_{NG_clima} will fully replicate those fields. Thus, T and S verification plots are not provided within this report (please see [26] for ECLH assessment on seasonal temperature and salinity)

4.4 Model outputs

The outputs from the hydrodynamic hindcast and climatology models are summarised in Table 4.2 and Table 4.3. All parameters were saved in all model mesh elements (grid cells) at 0.5-hourly time intervals.

Table 4.2 2D model outputs from HD_{NG_clima}.

Parameter	Unit	Description
Surface elevation	m	Still water level relative to MSL
Total water depth	m	Total water depth
u-velocity component	ms ⁻¹	Depth-averaged velocity speed in the west-to-east direction
v-velocity component	ms ⁻¹	Depth-averaged velocity in the south-to-north direction
P Flux	m ³ s ⁻¹ m ⁻¹	Flow flux per metre in west-to-east direction
Q Flux	m ³ s ⁻¹ m ⁻¹	Flow flux per metre in south-to-north direction

Table 4.3 3D model outputs from HD_{NG_clima}

Parameter	Unit	Description
u-velocity component	ms ⁻¹	Current velocity in the west-to-east direction
v-velocity component	ms ⁻¹	Current velocity in the south-to-north direction
w-velocity component	ms ⁻¹	Current velocity in the vertical direction
Density	kgm ⁻³	-
Temperature	°C	-
Salinity	PSU	Practical Salinity Unit
TKE	m ² s ⁻²	Turbulent Kinetic Energy
ϵ	m ² s ⁻³	Dissipation of turbulent kinetic energy

Still water depth and element size of the computational mesh (common for both model realisations) are provided as a separate time-invariant output.

4.5 Model files

The hydrodynamic climatology model is supplied to BFS as part of the project deliverables. The data are provided in DHI MIKE format and can be used to generate boundary conditions for local climatology/hindcast modelling or as input for scenario modelling.

[Appendix A](#) includes a description of the model files that are provided alongside this report.

5 Hydrodynamic model calibration

In this section, the calibration of the 2D hydrodynamic hindcast model is presented.

In general, all stations examined had a good representation of the water level signal and thus the model was well replicating the tidal signal propagation. On the contrary, the modelled depth averaged tidal velocity field was not replicating magnitudes as depicted by the observational record. This discrepancy guided final calibration efforts towards adjusting the velocity field that was being used as boundary forcing. The adjustment was based on the bias of the tidal current speed signal used as forcing versus the inferred one following tidal analysis of the observational records at the stations in question.

5.1 Model Calibration

The North Gravir hydrodynamic hindcast model was calibrated against observed hydrographic data (water levels and currents) provided by BFS as part of their measurement campaigns in respective sites of interest at the North Gravir general area, see also section 3.2.

The model calibration/validation periods were selected based on the temporal and spatial coverage of the available data as described in section 3.2. These are detailed in Table 5.1 (see also Table 3.2 for specific deployment details) and shown in Figure 5.1.

Table 5.1 North Gravir hydrodynamic hindcast/clima models calibration/verification deployment campaigns.

Site	ID	Survey Start (yyyymmdd)	Survey End (yyyymmdd)	Deployment depth (m)	Easting (BNG) [m]	Northing (BNG) [m]
Calibration stations (HD_{NG_hindcast} - 2D)						
North Gravir	210804_NorthGravir	04/08/2021	06/10/2021	59.2	143051E	916012N
North Gravir	211008_NorthGravir	08/10/2021	10/12/2021	56.1	143021E	915986N
Verification stations (HD_{NG_clima} - 3D)						
North Gravir	210804_NorthGravir	04/08/2021	06/10/2021	59.2	143051E	916012N
North Gravir	211008_NorthGravir	08/10/2021	10/12/2021	56.1	143021E	915986N
Grosebay	100423_Grosebay	23/04/2010	12/05/2010	24.7	115977E	891332N
Plocrapol	190328_Plocrapol	28/03/2019	30/04/2019	26.2	118431E	894291N

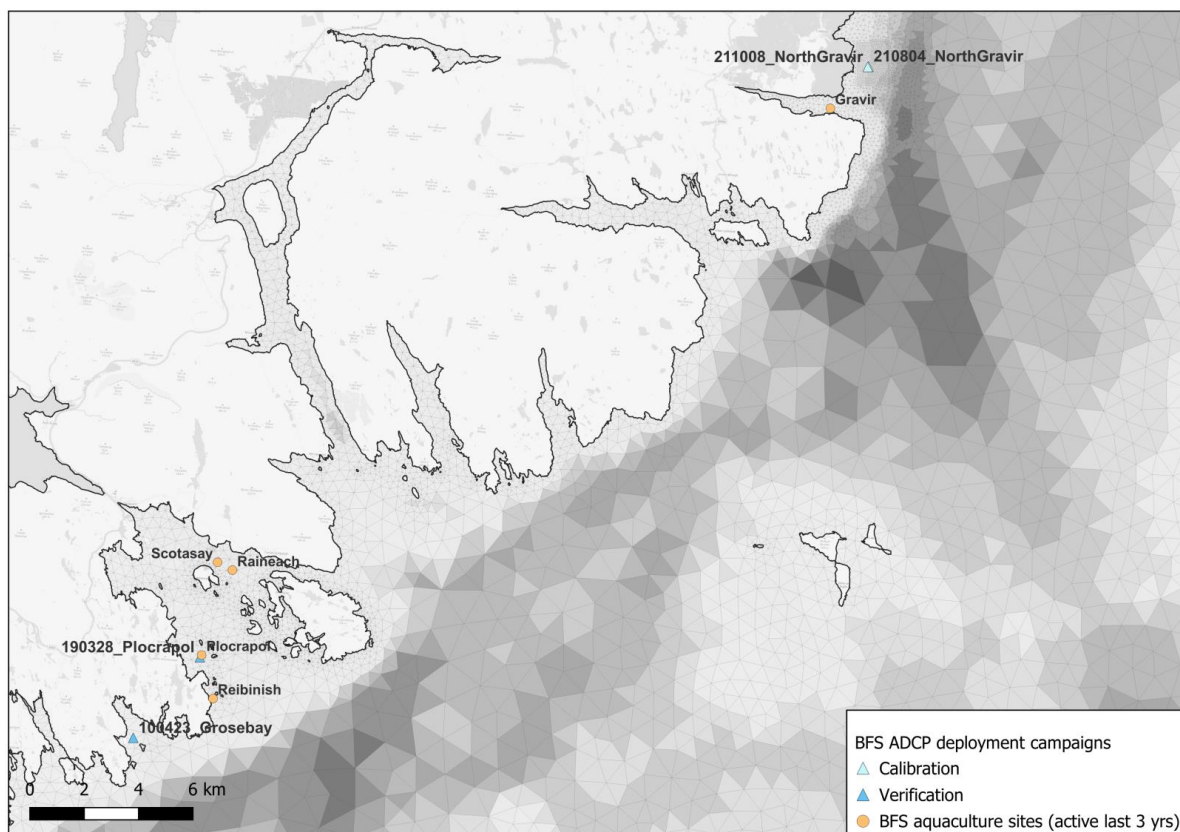


Figure 5.1 North Gravar hydrodynamic hindcast model calibration and climatology verification sites

Section 6 details the results from these calibration periods and sites. A brief mention at each calibration site is detailed below. The full set of calibration plots for water level, current speed and direction for the BFS sites are detailed in Appendix C.

Several iterations in the context of sensitivity runs, involving parameter adjustments (for example spatial varying bed friction and bathymetric adjustments), were initially assessed to define calibration limits. The choice of the final setup was based on achieving good model skill (in terms of performance metrics against the observational record with special focus on the velocity field – current speeds and directions) collectively in the whole computational domain and optimal performance measured against the North Gravar measurement campaigns. Section 5.1.1 provides a brief account of the second phase¹³ of calibration aiming to improve model skill on observational record current speed representation.

Table 5.2 Main setups for second phase of calibration on improving model skill on current speeds.

Calibration setup name	period	Forcing		
		Tidal (boundaries)	Baroclinic (boundaries)	Wind (domain)
NG_MSL_onlyDTU10_2021_final_v2_DAModule	2021	DTU10 0.25deg	NA	See Table 4.1
NG_MSL_onlyDTU10_2min_2021_final_v2_DAModule	2021	DTU10 2min	NA	See Table 4.1

¹³ The first phase, not presented herein, was focused on assessment of propagation of tidal signals across the computational domain and relevant parameterisations, i.e., bed friction, bathymetry, etc.

5.1.1 Initial calibration and tidal component velocity adjustment

Surface elevation (water level), both total and tidal components (not shown here), was well represented at most of the calibration sites, Figure 5.2. Thus, the tidal water level signal was correctly propagated throughout the computational domain. However, current speeds were underestimated significantly in comparison to the observational records at the respective locations, Figure 5.3. It was therefore decided to use a higher resolution tidal solution (2min versus 0.25deg spatial resolution) at the boundaries. This tidal forcing adjustment improved representation of the velocity field at the North Gravr calibration stations while maintaining skill in representation of the tidal water signal. At section 5.1.2, an account on water level model performance of the barotropic component at both North Gravr measurement stations is provided prior to the velocity field adjustment and after.

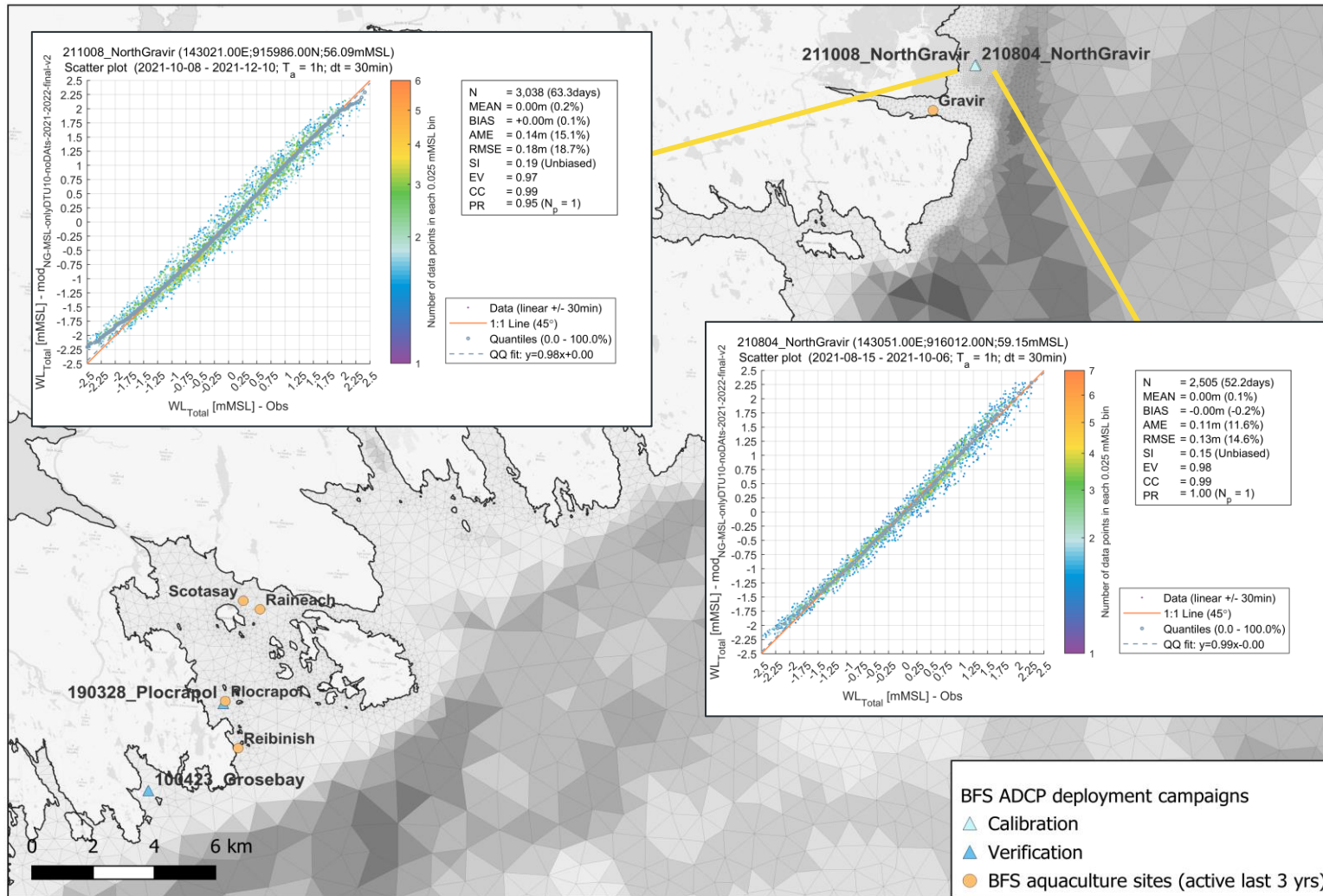


Figure 5.2 Scatterplot comparisons of observed versus modelled total water level signal BEFORE adjustment of the tidal forcing solution.

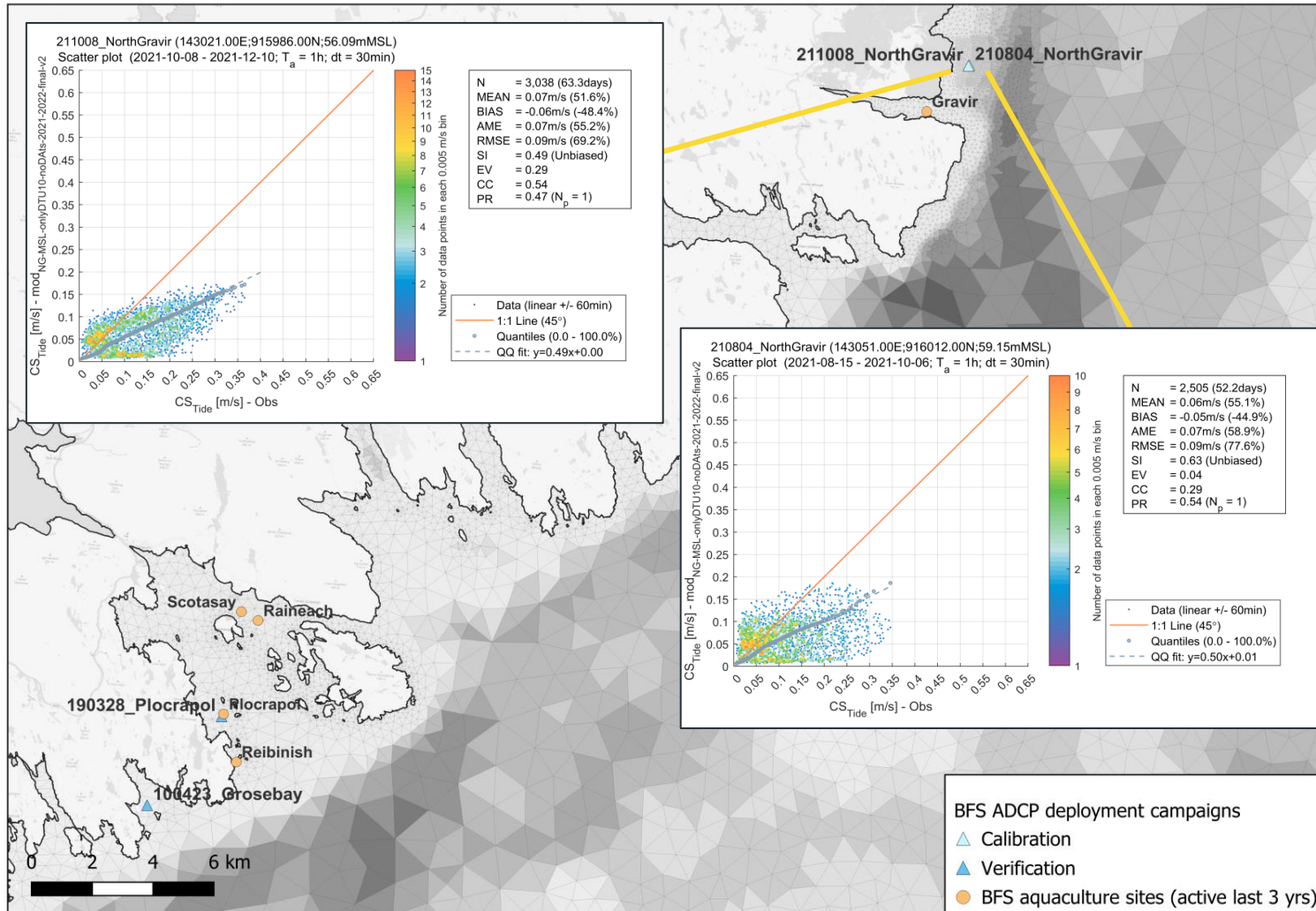


Figure 5.3 Selected locations of observed versus modelled tidal velocities during initial assessment of the tidal forcing solution.

5.1.2 Water levels

Scatterplots comparisons of observed versus modelled water levels for selected calibration sites prior to the velocity field adjustment are presented in Figure 5.4 (left column). Inspection of the calibration plots show that for total (and tidal) water level - not shown herein - there is a good overall fit between the observations and the model output especially with respect to the timing of high and low water. Discrepancies could be attributed to the observational record itself and/or misrepresentation of local bathymetric features rather than episodic events not within the variability resolution capacity of the modelled hydrodynamics.

Also, in Figure 5.4 are shown comparisons of observed (left column) versus modelled (right column) water levels following the revision of the tidal forcing solution at the model boundaries. The selected tidal solution results in a better representation of water level at the calibration stations examined (a marginal improvement can be seen); the overall Q-Q fit and scatter index (SI) improve, approximately to 1:1 and reduced by up to 3 units respectively.

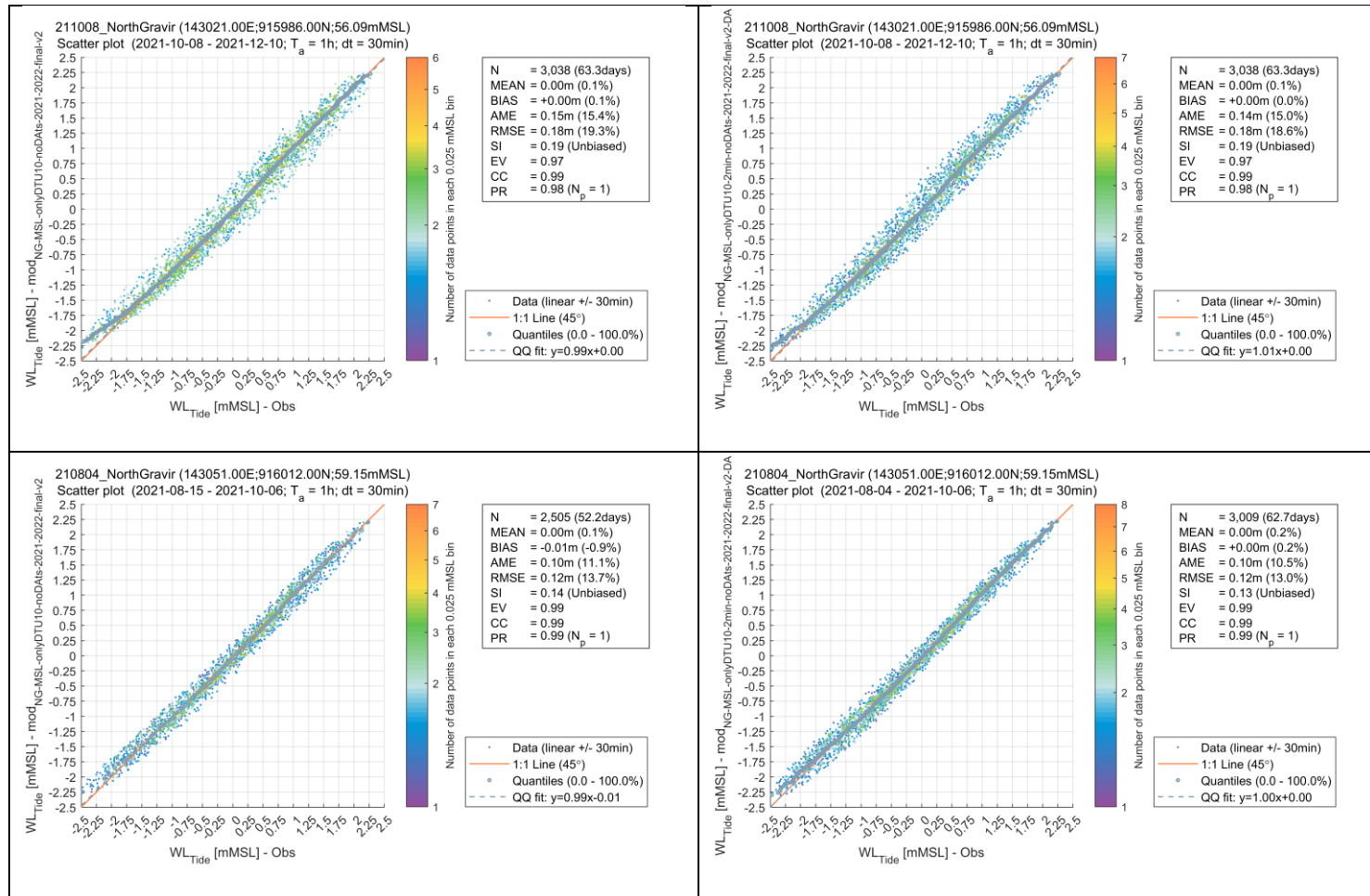


Figure 5.4 Scatterplot comparisons of observed versus modelled water levels at selected calibration sites as in Table 5.1 prior to final adjustment of the tidal forcing solution at the model boundaries (left column) and case with higher tide resolution at the model boundaries (right column) (see also Table 5.2)

5.1.3 Currents

The model skill on mean current speed and directions at the calibration stations at North Gravir is considered good on basic qualitative judgement, see Figure 5.5. The model is consistent in the current speed directional distribution between the two nearby deployments. At station 210804 there seems to be an overestimation of the northward current versus the observational record (by about 15%). The two deployments while covering different periods there are apart by a mere 40 m. Additionally, differences cannot be attributed to erroneous bathymetry as the model bathymetry (see also Section 3.1.2) agrees with the pressure sensor recording at the respective location. In general, tidal current speeds satisfy criteria as set out in [10] for 74 and 76% of the time respectively at 211008 and 210804 stations. Mean directions are better represented in general but with low conformity to criteria as in [10].

In Figure 5.6, tidal current speeds are depicted for the two North Gravir deployments. At both locations there is measurable improvement in current speed representation versus initial assessment. Still, the tidal component magnitude, even with the use of the high-resolution tidal forcing solution at the boundaries (see Section 4.3.6), is underestimated. On the contrary, the water level signal (see Section 5.1.2) and directions are depicted more precisely.

Current directions (Figure 5.7 and Figure 5.5) when averaged over the whole water column are consistent with the observational record at both deployments at the North Gravir location. The observational record shows more variability in the directional distribution of velocities while the model has a clear north-south alignment of 2D currents at both locations.

The discrepancies could potentially be associated to the baroclinic component contribution. Though, it is more possible that it is the result of underrepresentation of the tidal component rather than for example inaccurate bathymetry (given that mesh bathymetry at the most of the model domain and at North Gravir area is based on high resolution gridded bathymetric datasets from Admiralty UK, see also Section 3.1.2).

To alleviate the tidal velocity discrepancy discussed above, a hybrid solution was applied at the velocity boundary of the 3D model. The tidal velocity component from the DTU10 2min solution was combined with the total 3D velocity field from ECLH. The water level tidal signal was maintained unadjusted (from DTU10 2min). The assumption is that applying a Flather conditions scheme at the boundaries the solution will radiate out deviations from exterior values since the scheme is less sensitive to errors in prescribed values [24], [22]. When examining the 3D velocity representations on the following section during verification of the HD_{NG_clima}, we see that velocity range is well replicated at both North Gravir locations.

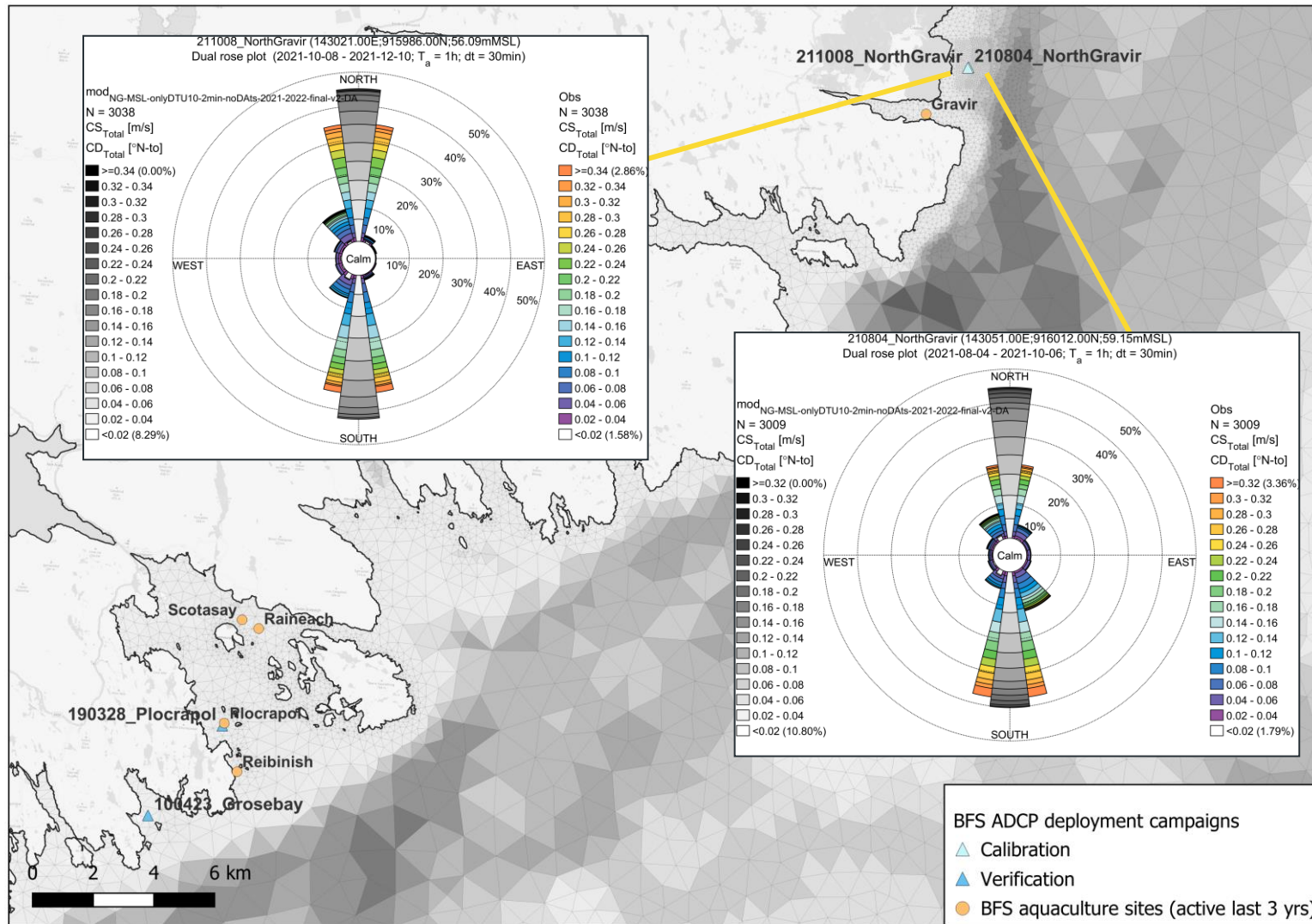


Figure 5.5 Dual rose plots of current speed and directions of observational records vs model output for selected calibration sites.

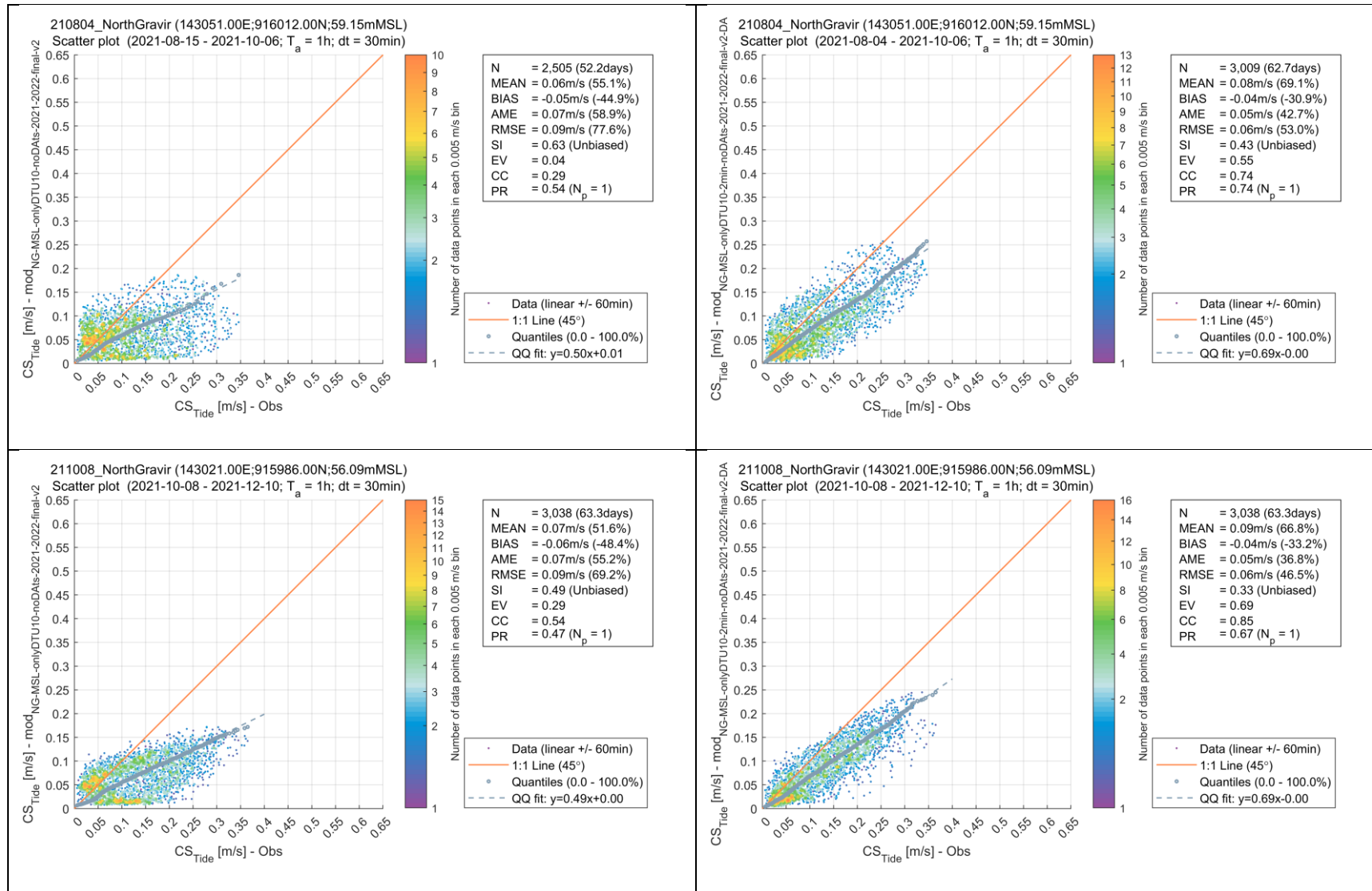


Figure 5.6 Scatterplot comparisons of observed versus modelled tidal velocities at the North Gravir deployments prior to final adjustment of the tidal forcing solution at the model boundaries (left column) and following the solution selected at the model boundaries (right column) (see also Table 5.2)

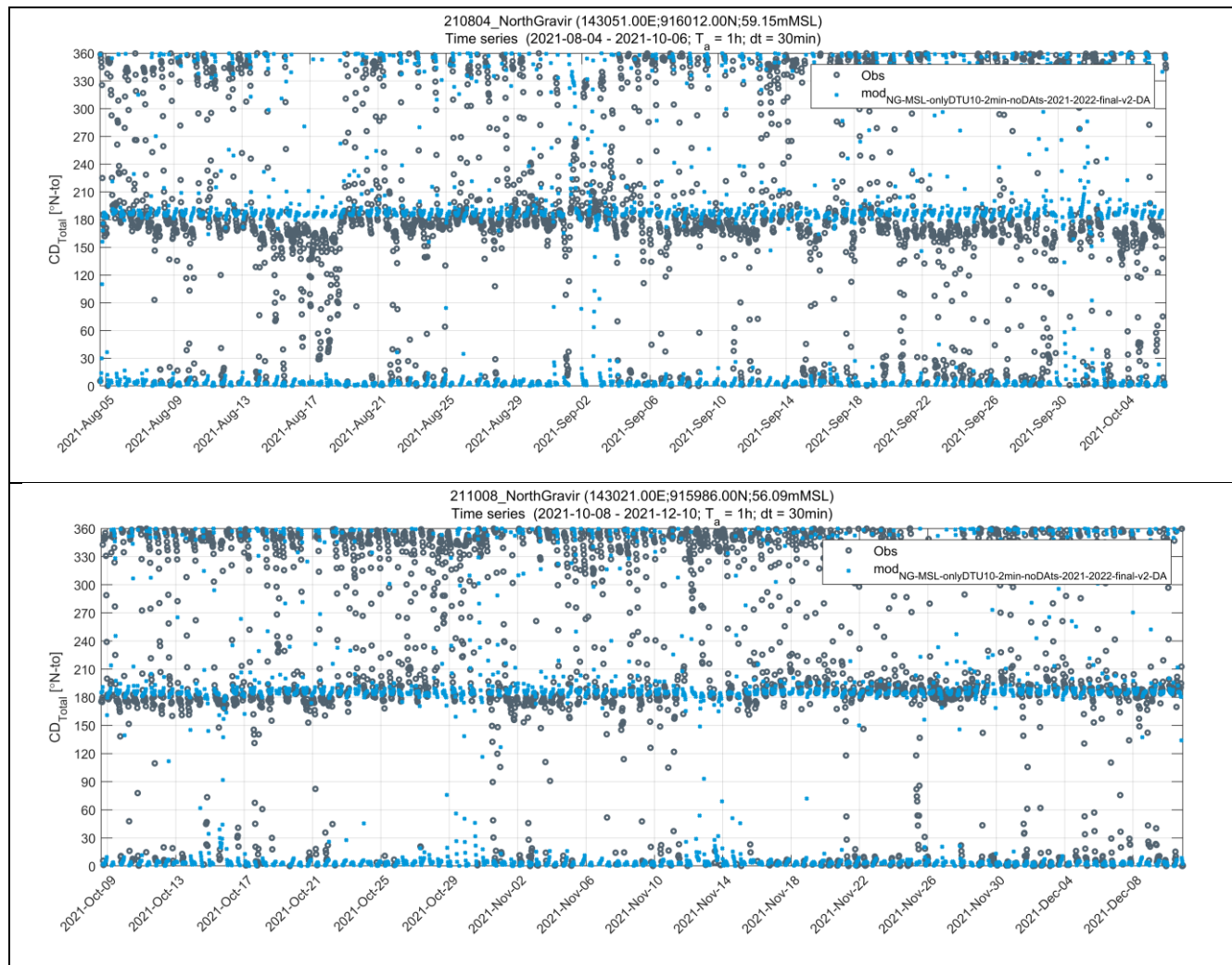


Figure 5.7 Timeseries of modelled (blue dots) versus observed (black dots) depth-averaged current direction at the two observational deployments at North Gravir.

6 Hydrodynamic climatology model verification

As mentioned previously, a climatology model is a representation of the mean status or clima of the hydrodynamic conditions over a specified period of years (e.g., herein 1990-2014). Long-term (multi-year) records of currents or water properties to assess model performance are usually not available. Thus, it is inconsistent to compare model predictions against short-term measurement data, which reflect a specific set of conditions during which the measurements were made. Herein we provide a qualitative assessment of model skill versus the observational record on a seasonal basis, assuming a degree of consistency between the climatology and actual conditions on average. An assessment of the regional North Gravr hydrodynamic climatology is performed in the following way:

- Deriving the velocity field from the regional climatological model (HD_{NG_clima}) and conducting a qualitative comparison against those derived from the observational campaigns by BFS. Having previously demonstrated the performance of the barotropic component in the hindcast version versus the observational record we now look at the combined signal both as a depth-averaged expression as also at selected vertical levels. The comparison is provided among both the ECLH and HD_{NG_clima} versus the respective observational record.

The regional North Gravr hydrodynamic climatology model is a down-scaled version of the ECLH shelf-wide domain model; it is forced by ECLH derived boundary conditions (combined with DTU10 plus TPX00.8 tidal component) with consistent meteorological inputs, but with higher spatial resolution in and around North Gravr, better representation of coastlines and small islands/inlets and more accurate bathymetry were available. For a nearshore assessment of HD_{NG_clima}, the deployment locations of the measurement campaigns delineate the effect of downscaling of ECLH.

6.1 Model Verification

The North Gravir hydrodynamic climatology model was verified against observed hydrographic data (water levels and 3D currents) from four (4) measurement campaigns in North Gravir (2), Procrapol (1) and Grosebay (1). BFS has a specific interest in North Gravir where prospect developments are scheduled as denoted in the initial scope requirements of the North Gravir hydrodynamic database.

The model verification periods were selected based primarily on the spatial relevance of the available data at the main area of interest. These are detailed in Table 5.1 and Figure 5.1.

Section 6 details the results from these sites for the verification period. All comparison plots are included as a digital appendix to this report (Appendix C). Plots for North Gravir are shown in the following section.

6.1.1 Water Levels, depth-averaged currents and current directions

Below an account on model performance at each of the observational records at the North Gravir site is provided. Assessment is based on a qualitative verification¹⁴ of the HD_{NG_clima} versus the range of conditions as seen from the respective observational record.

Table 6.1 summarises statistics of water level and the current field at all observational records within the HD_{NG_clima} computational domain.

Timeseries comparisons¹⁵ of observed and modelled water levels and depth-averaged currents and directions at North Gravir 210804 station are presented in Figure 6.1, Figure 6.2 and Figure 6.3 respectively. Figure 6.4 shows dual rose plots, more representative of mean hydrodynamic conditions, of depth-averaged currents for observed versus HD_{NG_clima} (left) and ECLH (right). Displayed period is selected for a similar seasonal calendar period to the observational record.

Reviewing statistics for both the observational records and model database (Table 6.1) North Gravir stations are consistency replicated in the depth averaged expression of the hydrodynamics. At both other stations, Procrapol and Grosebay, mean current speed is underpredicted by about 0.1m/s. Model captures directional distribution at Procrapol still not replicating range of velocities at the site. In comparison to the ECLH, HD_{NG_clima} is collectively in better agreement to the observational record (see Figure 6.4). ECLH has more increased velocities at Grosebay (still underestimating range and directions) and Procrapol (missing main directional alignment and higher percentages at lower speeds vs the observational record).

When examining the directional distribution of depth averaged currents (see Figure 6.4) the HD_{NG_clima} replicates better the observational record in comparison to the ECLH at North Gravir. Still, it does not fully capture the same pattern at **North Gravir** site, overestimating both the northward and southward components at station 210804. At station 211008 the rose plot shows a better fit to the measurement directional distribution of currents. At **Procrapol**, the model replicates main direction of currents but fails to match current

¹⁴ In essence we verify a mean status representation of the hydrodynamics in the area versus the instantaneous record.

¹⁵ Modelled (climatology) timeseries are shifted to match tidal peaks within same seasonal period as in the observational record in order to be able to provide these quantitative comparisons.

magnitude. At **Grosebay** site the model has too slow currents (<0.05 m/s) in comparison to the observational record and is considered not well represented.

As mentioned in Section 4.3.3, model bathymetry at most of the domain is based on high resolution UKHO gridded datasets. That includes all BFS sites mentioned herein. At North Gravrir site there are no bathymetric discrepancies between model bathymetry and the derived one from the observational record. At the Procrapol and Grosebay ones the bathymetric discrepancy between the model bathymetry and the recorded water depth by the respective observational station is 5 m (20%) and 3 m (8%) respectively (the model being shallower). In contrast, the ECLH bathymetry is 10 m and about 20 m shallower at Procrapol and Grosebay respectively versus the ADCP deployment depth. Thus, regardless the improved bathymetric representation and coastline in HD_{NG_clima} the current field is misrepresented at those two sites¹⁶.

Table 6.1 Observed versus modelled water level and depth-averaged currents statistics.

Verification												
Observational station	Water Level - Observed						Water Level - Modelled					
	N	Ndays	Mean	Min	Max	STD	N	Ndays	Mean	Min	Max	STD
210804_NorthGravir	3011	42	0.0	-2.5	2.3	1.1	3025	42	0.0	-2.4	2.3	1.1
211008_NorthGravir	3039	42	0.0	-2.6	2.4	1.1	3025	42	0.0	-2.3	2.3	1.0
100423_Grosebay	916	13	0.0	-2.3	2.3	1.1	913	13	0.0	-2.4	2.2	1.2
190328_Plocrapol	1537	21	0.0	-2.6	2.3	1.1	1489	21	0.0	-2.6	2.4	1.1

Verification												
Observational station	Depth-Averaged current speed - Observed						Depth-Averaged current speed – Modelled					
	N	Ndays	Mean	Min	Max	STD	N	Ndays	Mean	Min	Max	STD
210804_NorthGravir	3011	42	0.14	0.01	0.54	0.09	3025	42	0.17	0.00	0.50	0.10
211008_NorthGravir	3039	42	0.15	0.01	0.56	0.09	3025	42	0.16	0.00	0.44	0.10
100423_Grosebay	916	13	0.09	0.01	0.19	0.04	913	12	0.02	0.00	0.04	0.01
190328_Plocrapol	1537	21	0.09	0.00	0.32	0.06	1489	21	0.05	0.00	0.11	0.02

Verification												
Observational station	Depth-Averaged current direction - Observed						Depth-Averaged current direction- Modelled					
	N	Ndays	Mean	Min	Max	STD	N	Ndays	Mean	Min	Max	STD
210804_NorthGravir	3011	42	194	0	360	103	3025	42	207	0	360	118
211008_NorthGravir	3039	42	222	0	360	113	3025	42	220	0	360	116
100423_Grosebay	916	13	189	0	360	84	913	13	219	0	360	109
190328_Plocrapol	1537	21	213	1	360	89	1489	21	210	1	360	88

¹⁶ BFS has revised a few of the provided ADCP measurements due to erroneous surface bins in the original record. These involved the station at Procrapol. The derived bathymetry from the total revised cell bin count is more consistent with the model bathymetry herein.

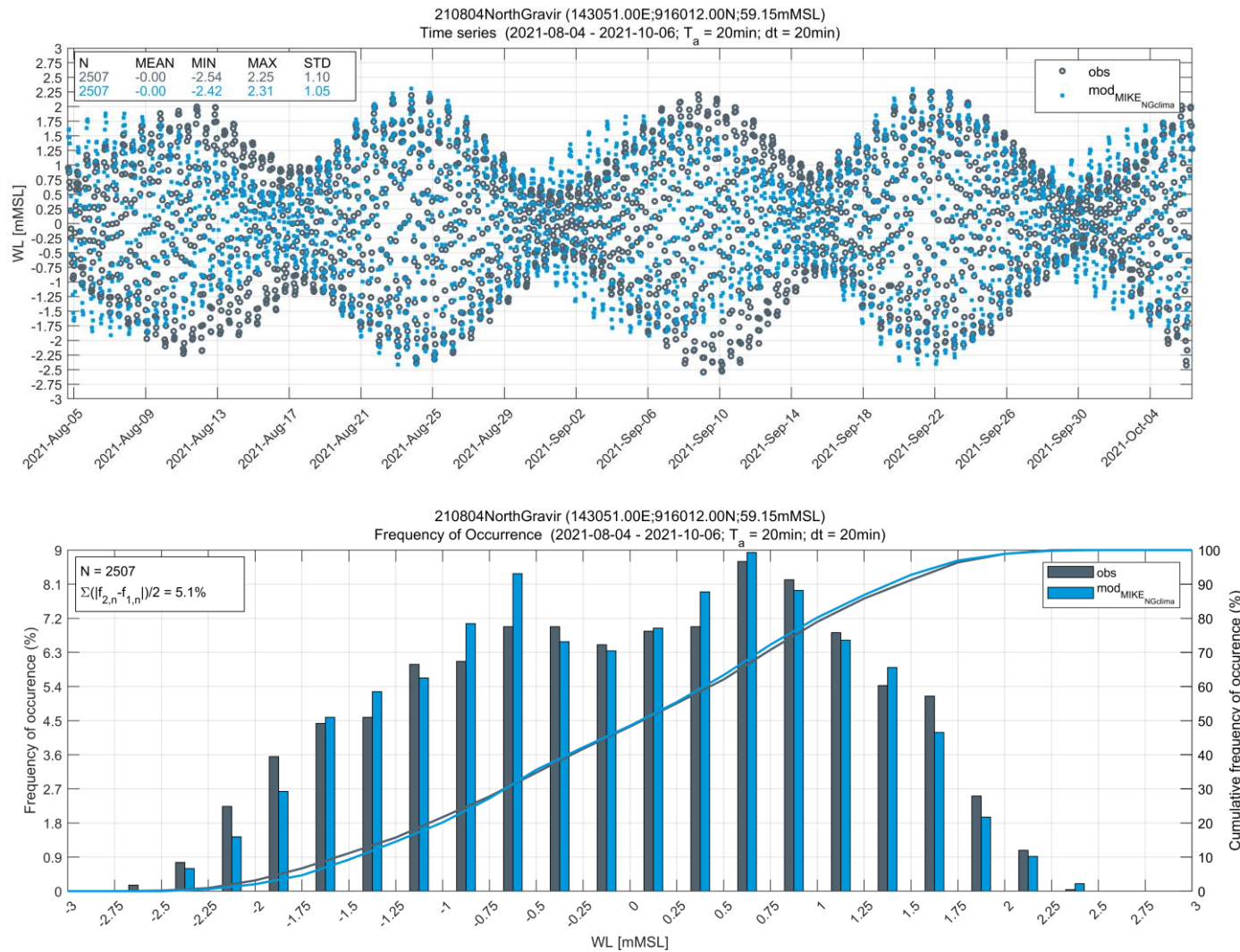


Figure 6.1 Timeseries (top panel) and frequency plot (bottom panel) of observed vs modelled water level for deployment station 210804 at North Gravir site. Modelled (climatology) timeseries are shifted to match tidal peaks for same seasonal period as in the observational record.

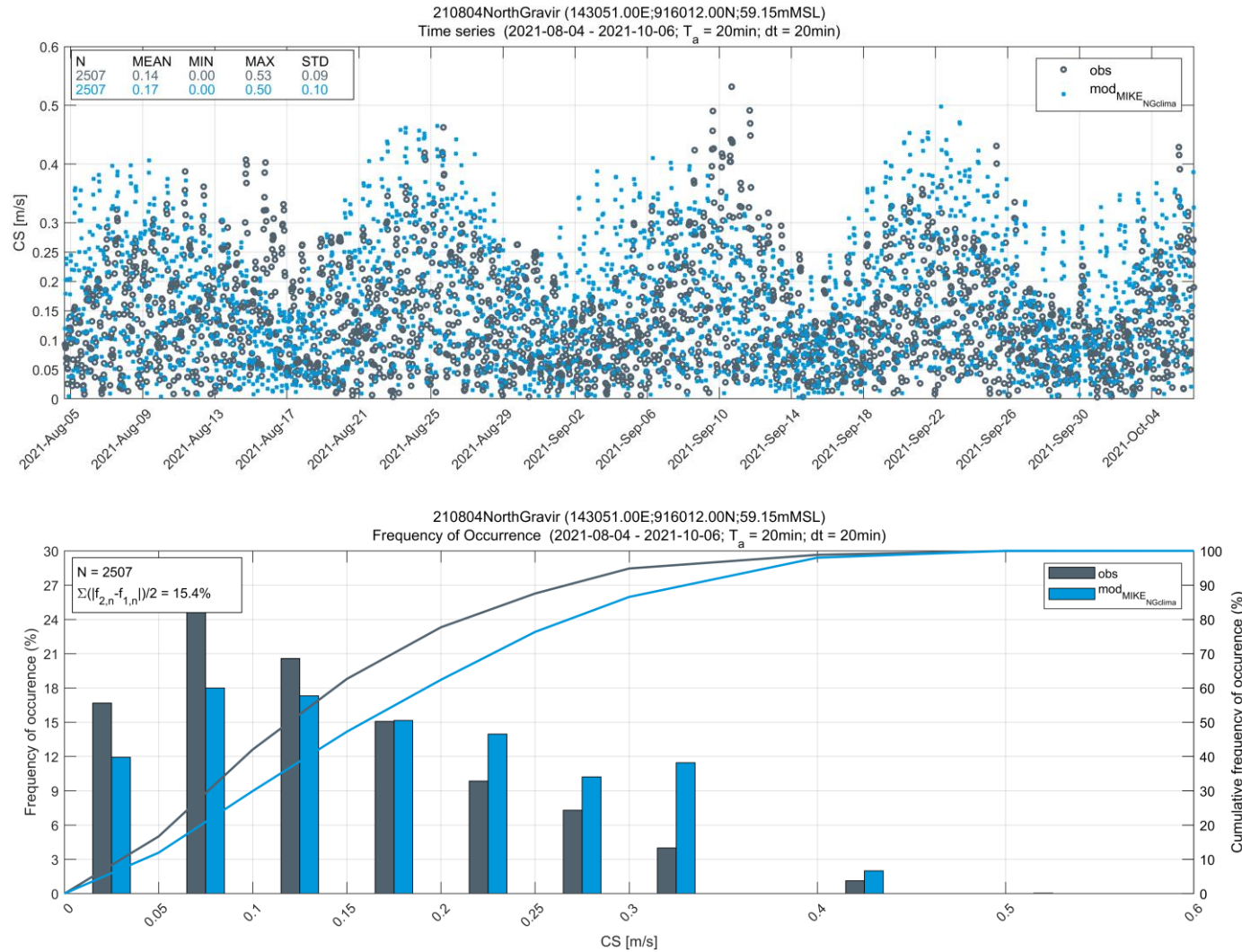


Figure 6.2 Timeseries (top panel) and frequency plot (bottom panel) of observed versus modelled (climatology) depth-averaged current speed for deployment station 210804 at North Gravir site. Modelled (climatology) timeseries are shifted to match tidal peaks for same seasonal period as in the observational record.

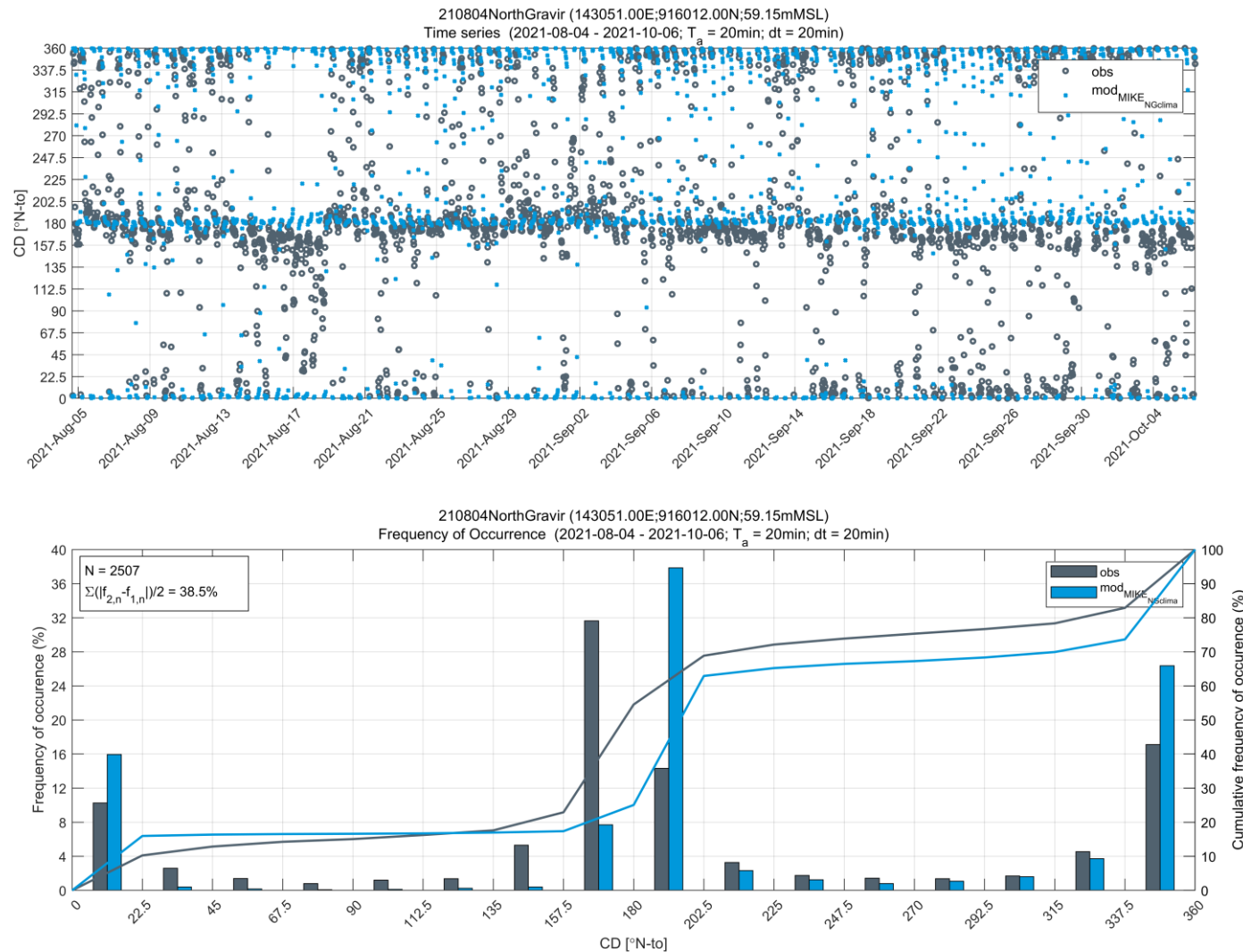
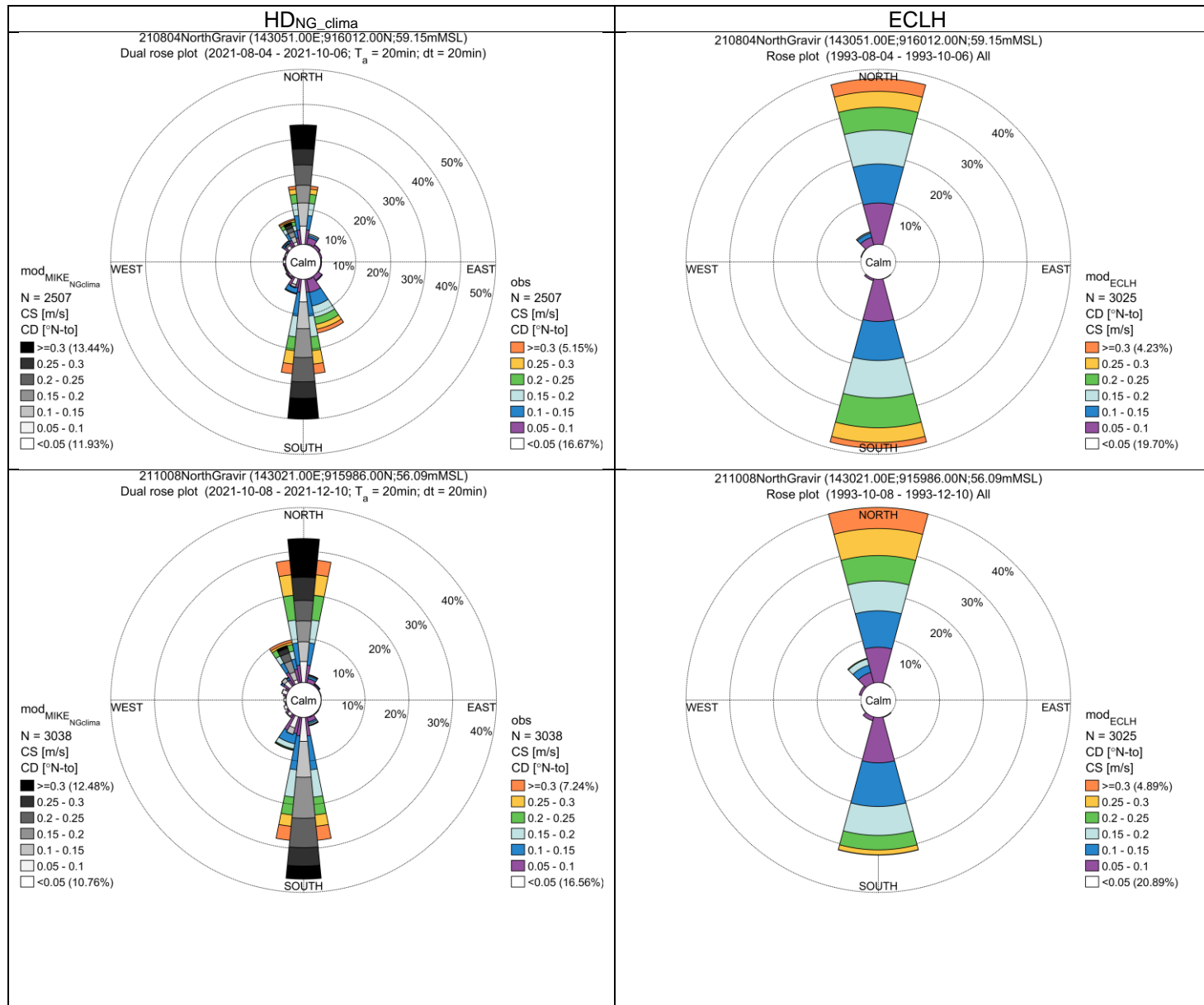


Figure 6.3 Timeseries (top panel-left) and frequency plot (bottom panel-left) and rose plot (right panel) of observed versus modelled (climatology) depth-averaged current directions for deployment station 210804 at North Gravir site. Modelled (climatology) timeseries are shifted to match tidal peaks for same seasonal period as in the observational record.



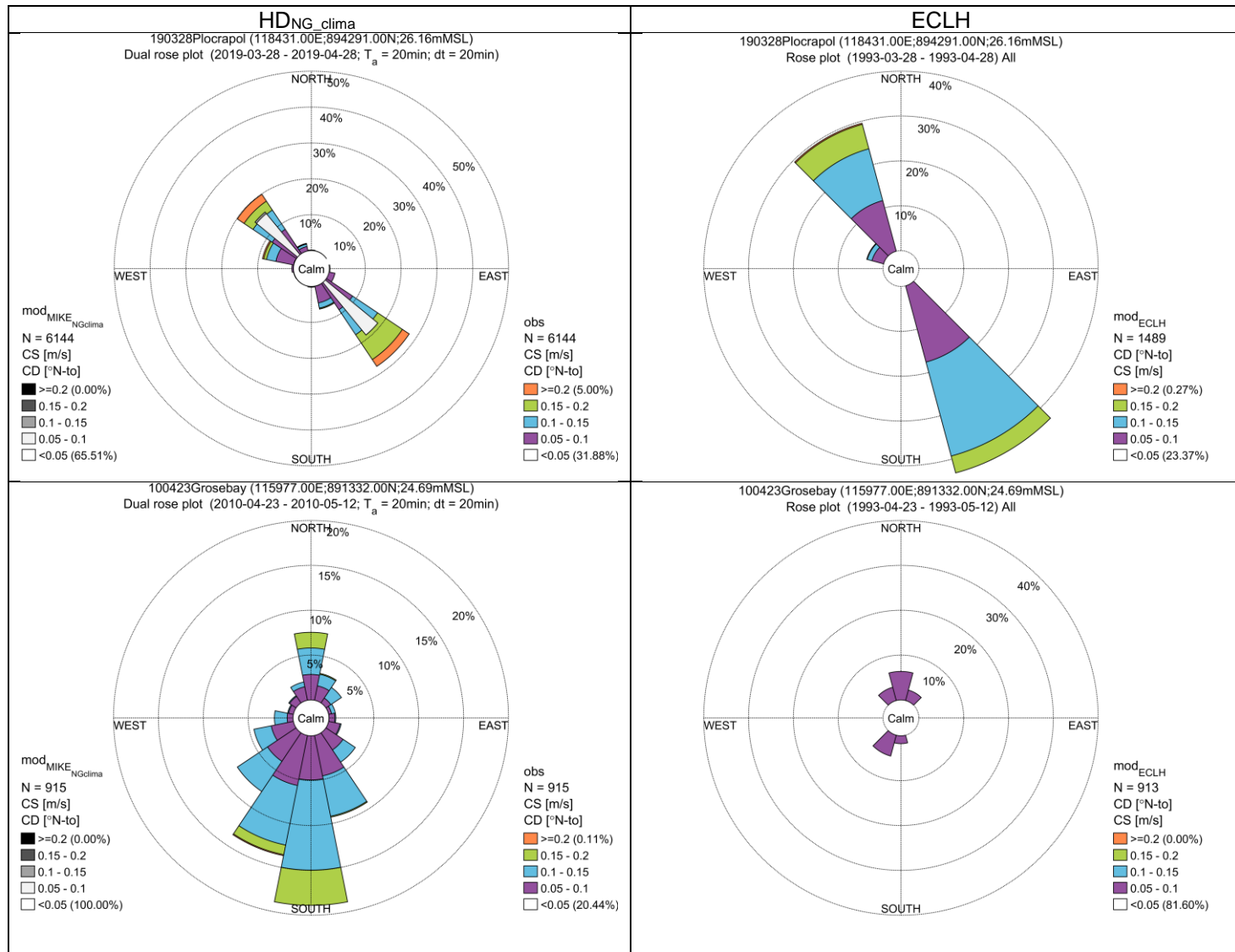


Figure 6.4 Current rose plots of observed versus HDNG_clima (left column) and ECLH (right) of depth-averaged currents at BFS's ADCP locations, see also Table 5.1. Modelled (climatology) timeseries are shifted to match tidal peaks for same seasonal period as in the observational record.

6.1.2 3D Currents

Focusing on North Gravir, the main area of interest for this hydrodynamic database, the model is replicating hydrodynamic conditions in terms of magnitude and direction of currents as depicted in the observational record¹⁷. Results are shown in the timeseries plots in Figure 6.5 and Figure 6.7 for the two North Gravir measurement campaigns at locations 210004 and 211008 respectively, and for three (3) selected vertical levels in the water column. Similarly, dual rose plots, Figure 6.6 and Figure 6.8 respectively, depict the directional distribution of currents at the same vertical levels. Results are presented near surface (~5-6 m from surface), at cage bottom (~18 m from surface) and near bed (~5 m from bottom).

The timeseries plots (see Figure 6.5 and Figure 6.7 and Table 6.2) show consistent statistics of current magnitudes for the respective vertical levels at both North Gravir stations. There is a maximum current speed of 0.5 m/s near surface level at North Gravir stations which is replicated by the model. At 211008, maximum current is about 0.09 m/s slower in the model near the surface layer though. At all other levels (i.e., cage bottom and near bed) timeseries exhibit consistent statistics.

The timeseries and dual rose plots of observed versus modelled current directions at North Gravir while on average show that the observational record is replicated, the modelled currents exhibit a stronger dominant south-northward component at all levels, see also Figure 6.6 and Figure 6.8. The same dominant direction is present in the observational record at both stations and is well captured. Still, the directional distribution of modelled currents does not fully replicate the observed variability in the respective records. Both observational records exhibit a slightly more variable current distribution especially near the bed, see Figure 6.6 and Figure 6.8.

At both other locations, Procrapol and Grosebay the model seems to be under predicting current speeds at all levels (~0.02-0.04 m/s on calculated mean velocities)¹⁸ with lower values at the Grosebay site.

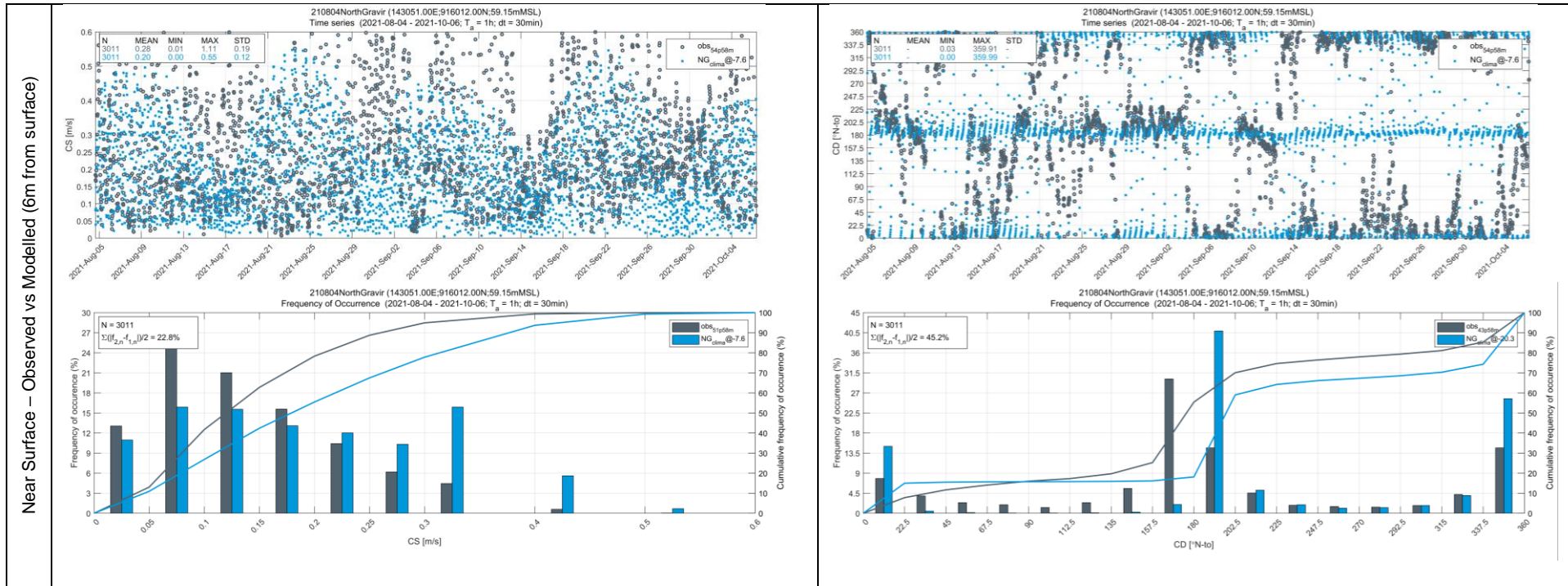
Table 6.2 summarises statistics of both the observed and modelled currents at the respective locations for all three (3) vertical levels. In Appendix C plots for all vertical levels are provided for both the observational records and the hydrodynamic database.

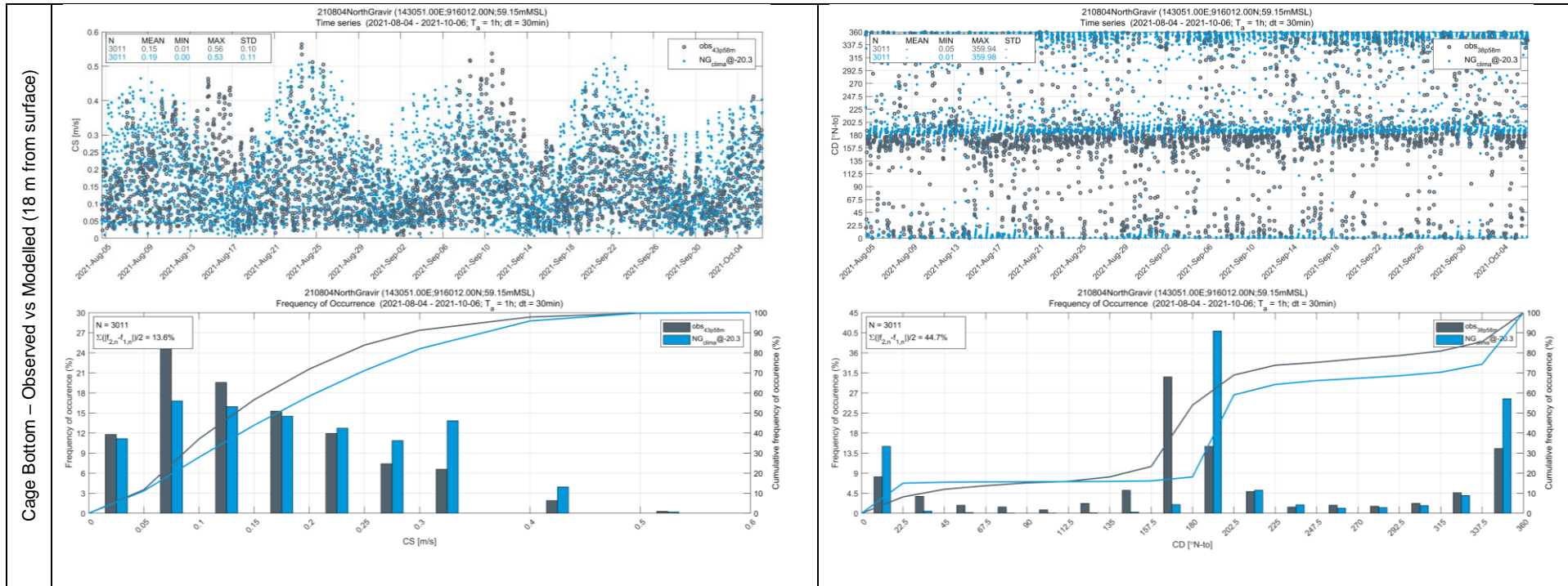
¹⁷

¹⁸ Still within limits of the 0.1 m/s SEPA regulatory modelling guidance criteria as in [10] but almost 100% as a ratio of recorded current speed.

Table 6.2 Summary of statistics for near surface, cage bottom and near bed levels for the observational versus modelled stations.

Verification – Current Speed										
Observational station	Current Speed Near Surface - Observed					Current Speed Near Surface - Modelled				
	Ndays	Mean	Min	Max	STD	Ndays	Mean	Min	Max	STD
210804_NorthGravir	42	0.14	0.01	0.53	0.09	42	0.19	0.00	0.55	0.12
211008_NorthGravir	42	0.17	0.01	0.57	0.10	42	0.18	0.00	0.48	0.11
100423_Grosebay	13	0.04	0.00	0.12	0.02	13	0.02	0.00	0.05	0.01
190328_Plocrapol	21	0.10	0.00	0.31	0.06	21	0.07	0.00	0.16	0.03
Observational station	Current Speed Cage bottom - Observed					Current Speed Cage bottom - Modelled				
	Ndays	Mean	Min	Max	STD	Ndays	Mean	Min	Max	STD
210804_NorthGravir	42	0.15	0.01	0.56	0.10	42	0.19	0.00	0.53	0.11
211008_NorthGravir	42	0.16	0.01	0.62	0.10	42	0.17	0.00	0.46	0.10
100423_Grosebay	13	0.04	0.00	0.15	0.02	13	0.02	0.00	0.04	0.01
190328_Plocrapol	21	0.09	0.01	0.32	0.06	21	0.05	0.00	0.13	0.03
Observational station	Current Speed Near bottom - Observed					Current Speed Near bottom - Modelled				
	Ndays	Mean	Min	Max	STD	Ndays	Mean	Min	Max	STD
210804_NorthGravir	42	0.14	0.01	0.39	0.08	42	0.15	0.00	0.43	0.09
211008_NorthGravir	42	0.14	0.01	0.48	0.08	42	0.15	0.00	0.40	0.08
100423_Grosebay	13	0.04	0.00	0.13	0.02	13	-	-	-	-
190328_Plocrapol	21	0.09	0.00	0.35	0.06	21	-	-	-	-





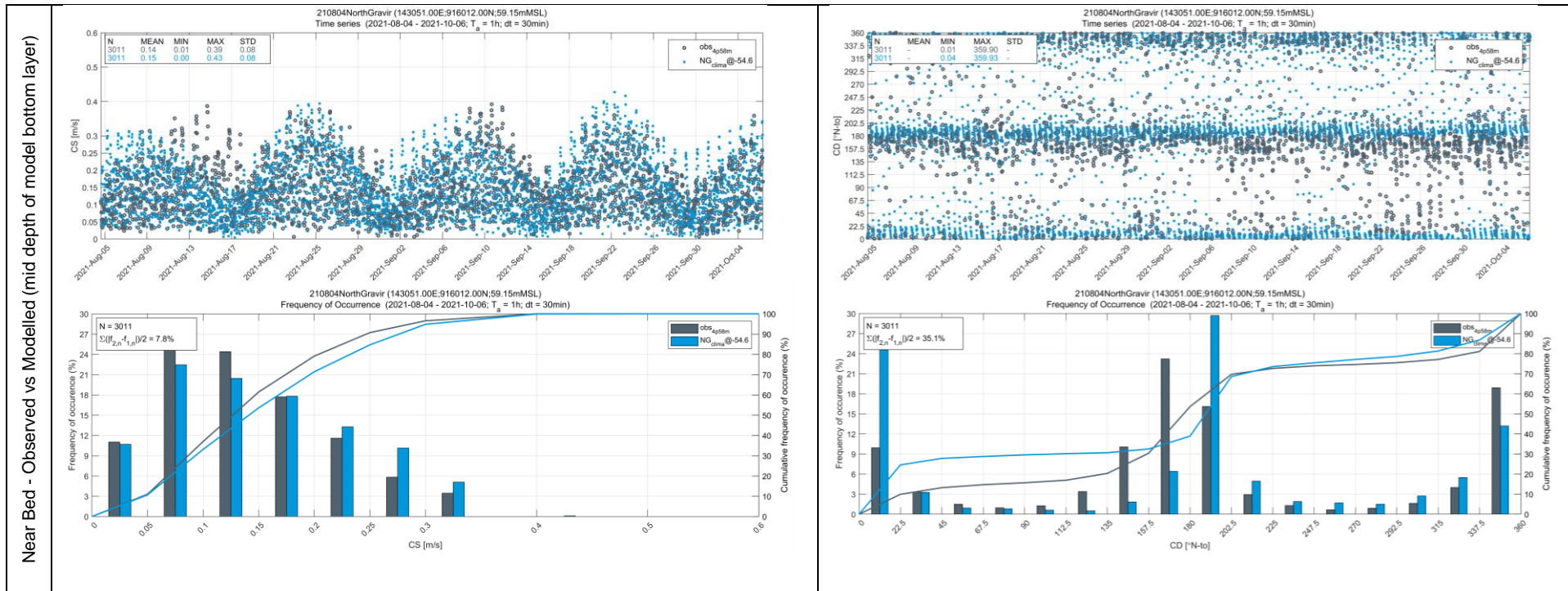


Figure 6.5 Timeseries (top) and frequency (bottom) plots of current speed (left panels) and directions (right panels) at near surface (6m from surface), cage bottom (18m from surface) and near bed (middle of bottom model layer) of observational records versus model output at the North Gravir 210804 verification site as in Table 5.1. Observational record levels are measured from the bottom. Modelled (climatology) timeseries are shifted to match tidal peaks for same seasonal period as in the observational record.

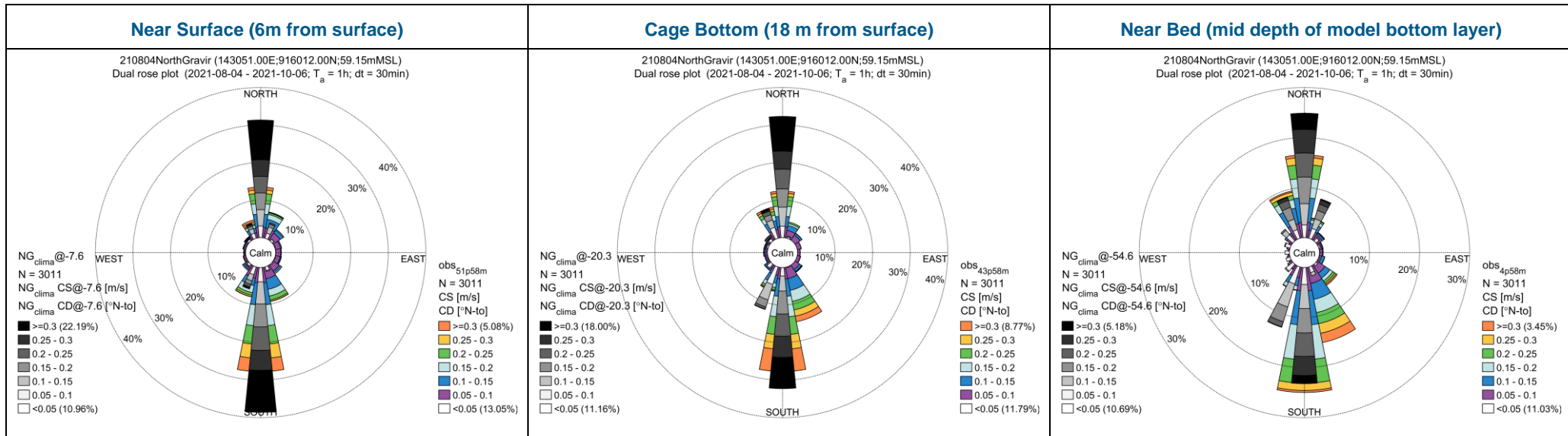
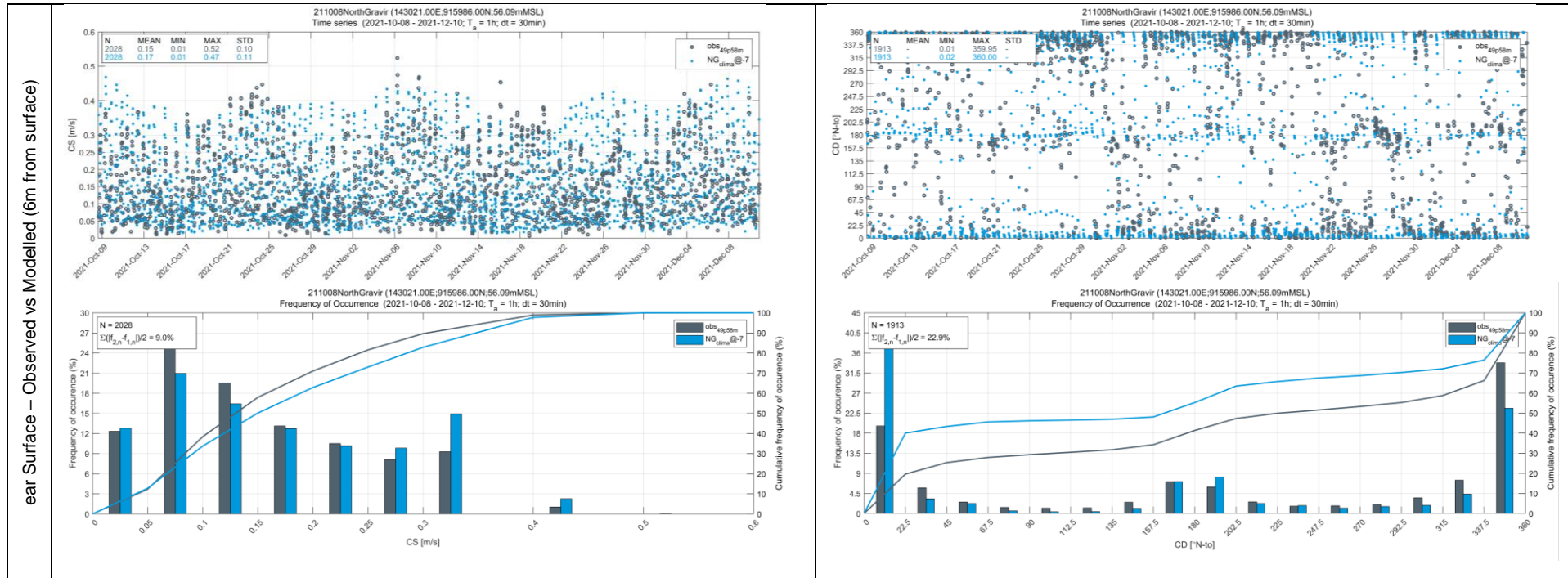
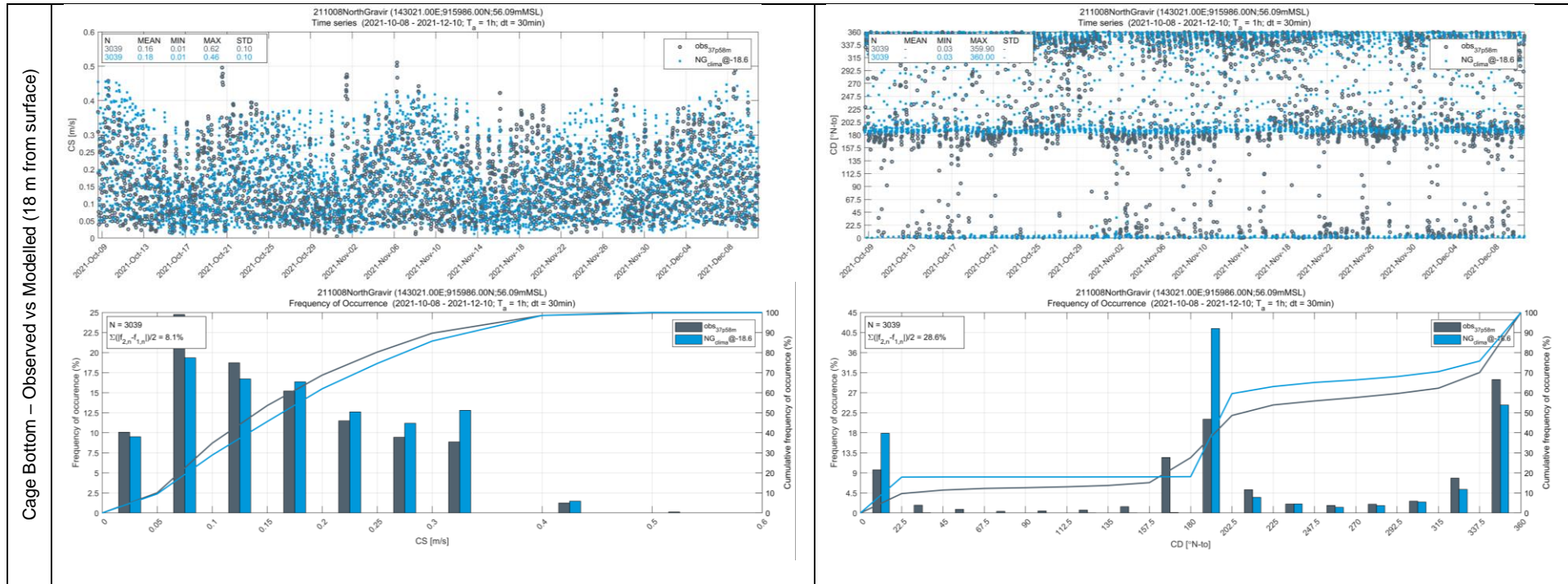


Figure 6.6 Dual rose plots of directional distribution of currents near surface (6m from surface), cage bottom (18m from surface) and near bed (middle of bottom model layer) of observed versus modelled currents at the North Gravir 210804 verification site as in Table 5.1. Observational record levels are measured from the bottom. Modelled (climatology) timeseries are shifted to match tidal peaks for same seasonal period as in the observational record.





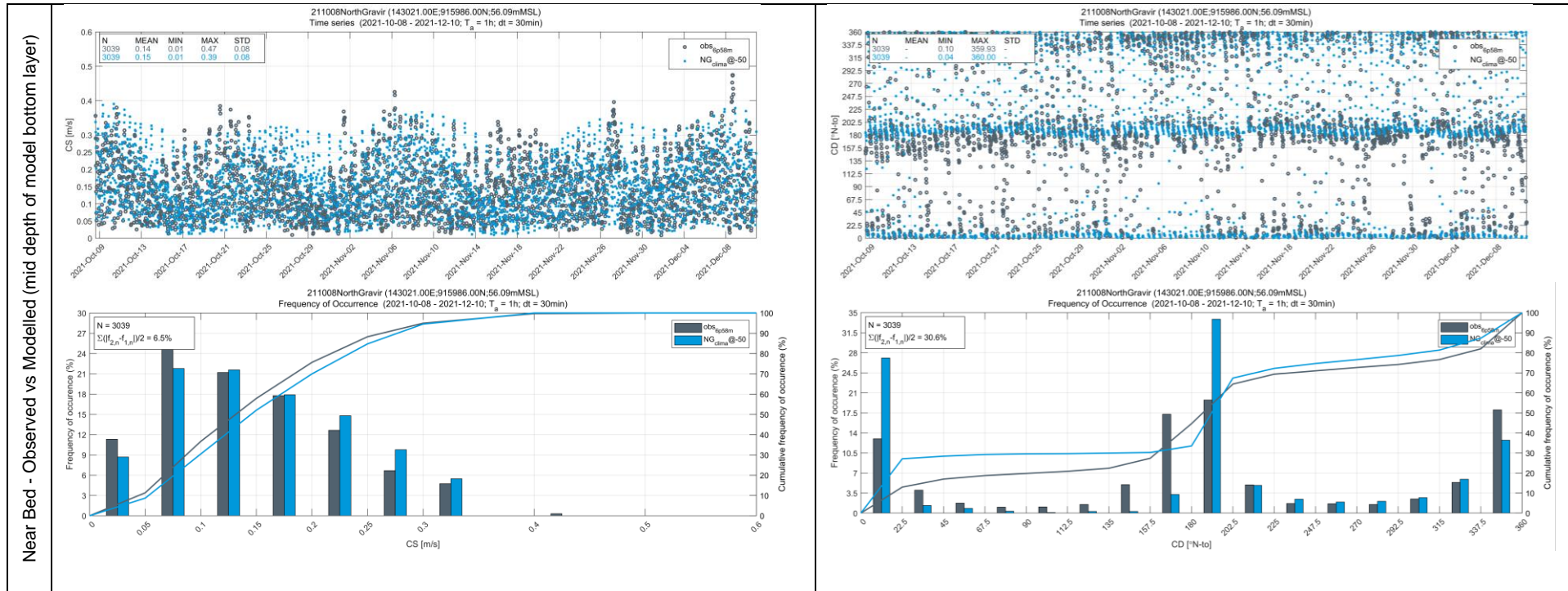


Figure 6.7 As in Figure 6.5 but for North Gravr 211008 verification site as in Table 5.1. Modelled (climatology) timeseries are shifted to match tidal peaks for same seasonal period as in the observational record.

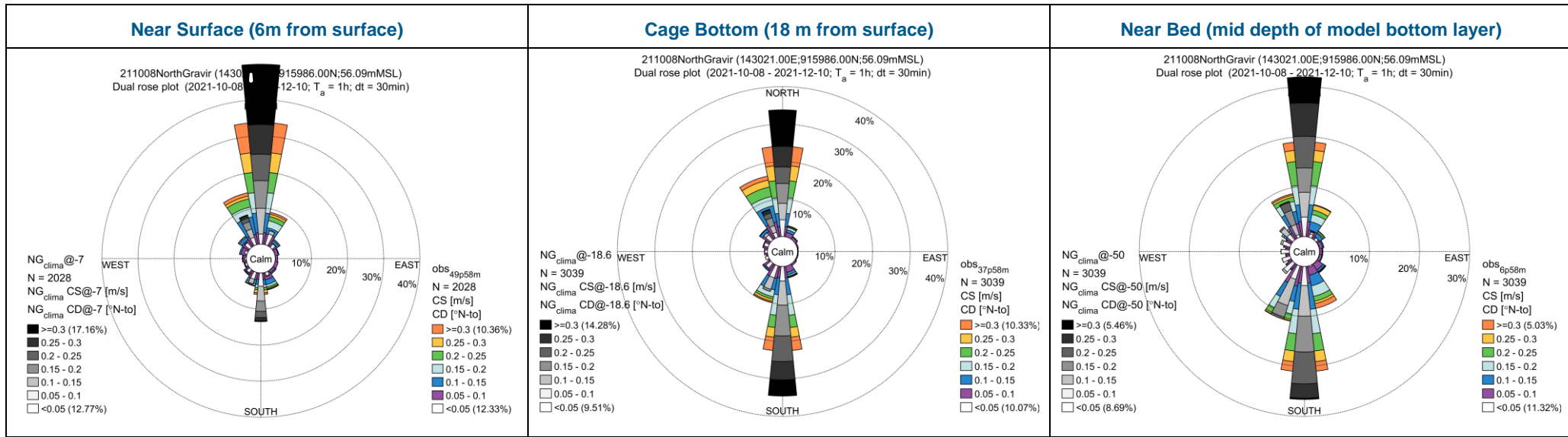


Figure 6.8 Dual rose plots of directional distribution of currents at near surface (6m from surface), cage bottom (18m from surface) and near bed (middle of bottom model layer) of observed versus modelled currents at the North Gravir 211008 verification site as in Table 5.1. Observational record levels are measured from the bottom. Modelled (climatology) timeseries are shifted to match tidal peaks for same seasonal period as in the observational record.

7 Model Results

In this section, the results of the 3D North Gravir climatological hydrodynamic model are presented. This includes a brief description of modelled hydrodynamics over the area of interest.

7.1 Model outputs

The residual circulation and statistical 50th and 90th percentiles of the depth-averaged current speed of HD_{NG_clima} are shown in Figure 7.2 (North Gravir close up - Figure 7.1), Figure 7.3 and Figure 7.4 respectively.

In general, there is a northward residual flow characterising the whole model domain, Figure 7.2, which is consistent with the assessment of the ECLH model climatology run [26].

A net northward residual flow following the steep bathymetric gradient (see also Figure 3.2) is identified just offshore of the North Gravir site which suggests sufficient capacity for dispersion of any locally introduced material/substance especially in relation to the *Burrowed Mud* PMF.

Strong currents are found where the flow is constrained around the headlands and in narrow channels driven in principle by the tidal dynamics that dominate the velocity field.

At all BFS's MPFF active sites the residual circulation hydrodynamic field is considered 'weak' (white to light blue areas Figure 7.1 - Figure 7.2) which would also suggest a reduced dispersion capacity. Specifically, for North Gravir Figure 7.1 showcases a rather weak residual circulation at the exact location of the site which is almost 'isolated' by the prominent northward circulation 'corridor' immediately to the east 'boundary' of the suggested cage location.

Maximum currents (90th percentile) are in excess of 0.5m/s in the headlands and above 0.2 m/s for most of the modelled area which indicates an energetic hydrodynamic velocity field, see Figure 7.4.

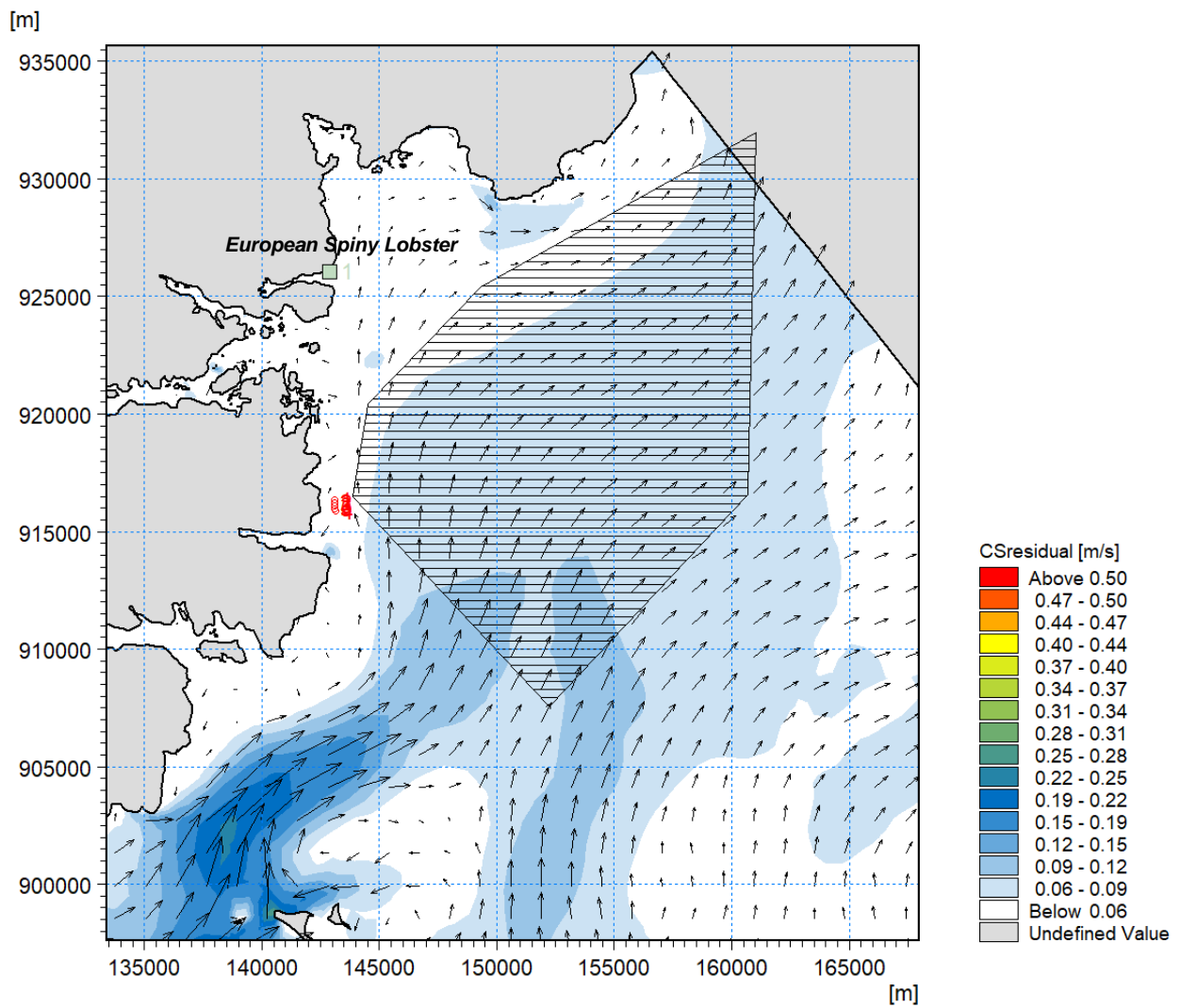


Figure 7.1 Residual circulation around North Gravr based on the hydrodynamic climatology model (HD_{NG_clima}). PMF area *European Spiny Lobster* is shown with green rectangle while *Burrowed Mud* PMF as shaded polygon. North Gravr cages' locations shown as red circles.

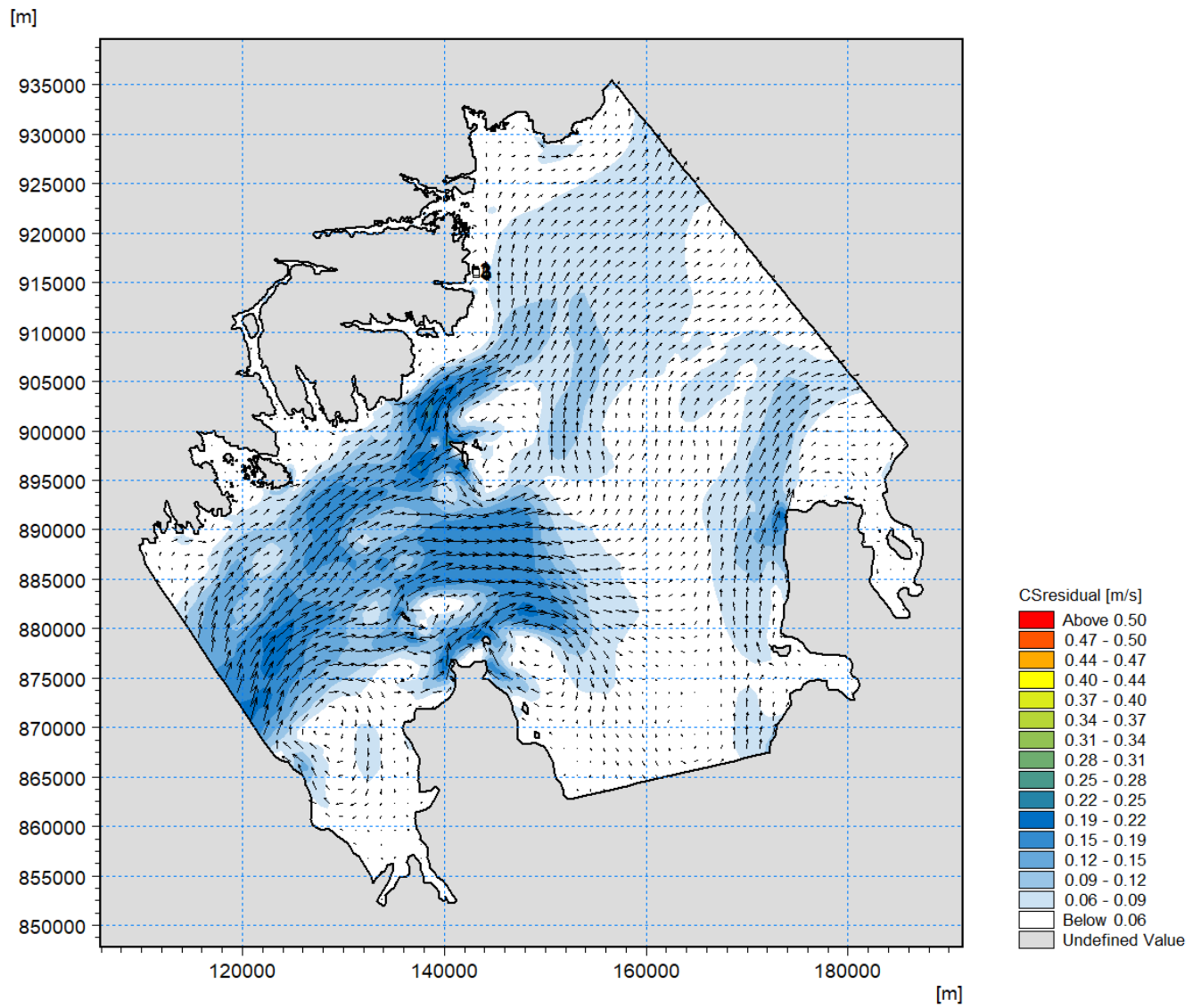


Figure 7.2 Residual circulation throughout the computational domain of the hydrodynamic climatology model (HDNG_clima).

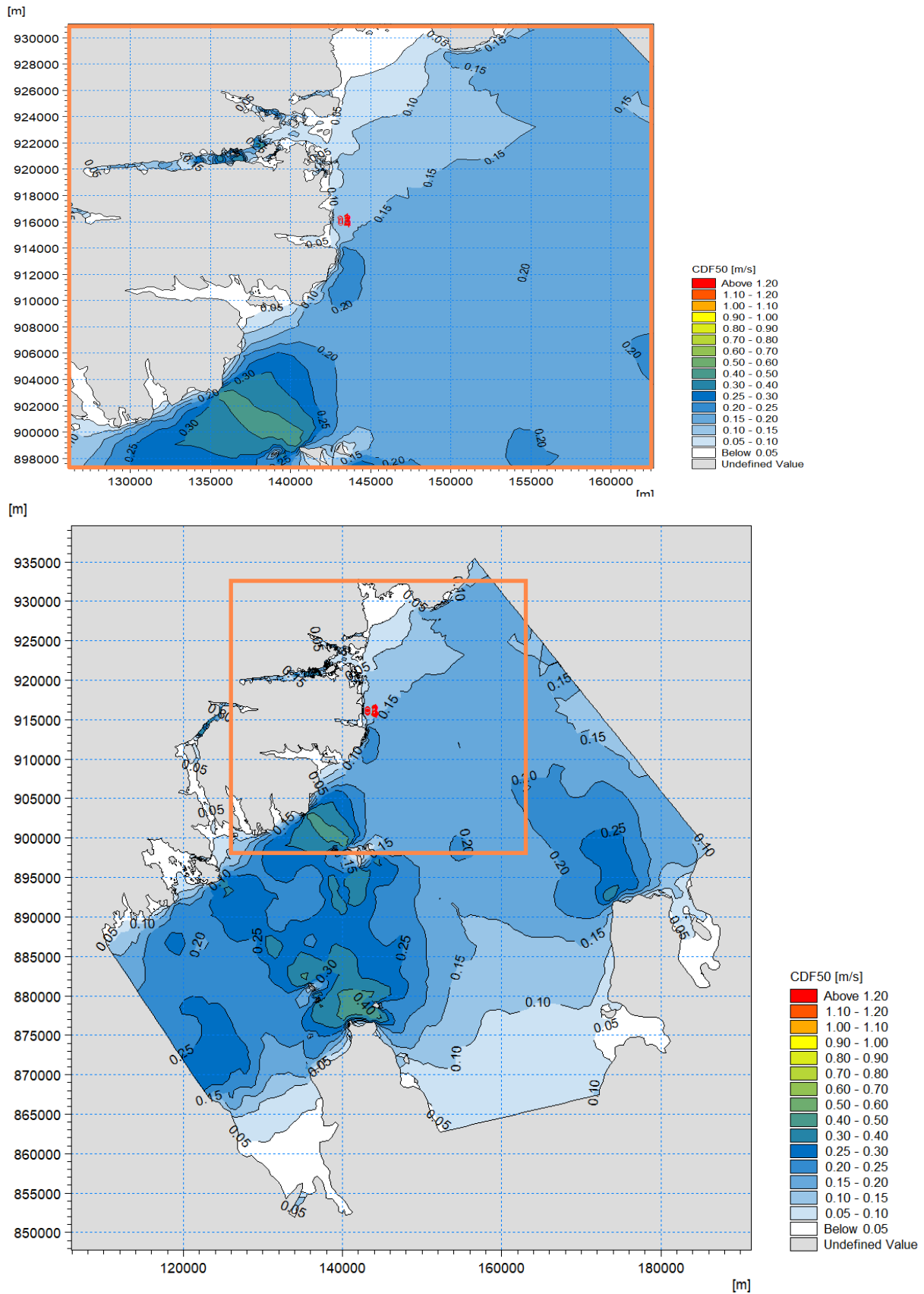


Figure 7.3 Statistical 50th percentile (based on empirical CDF) of depth-averaged current speed throughout North Gravr computational domain for the hydrodynamic climatology model (HD_{NG_clima})

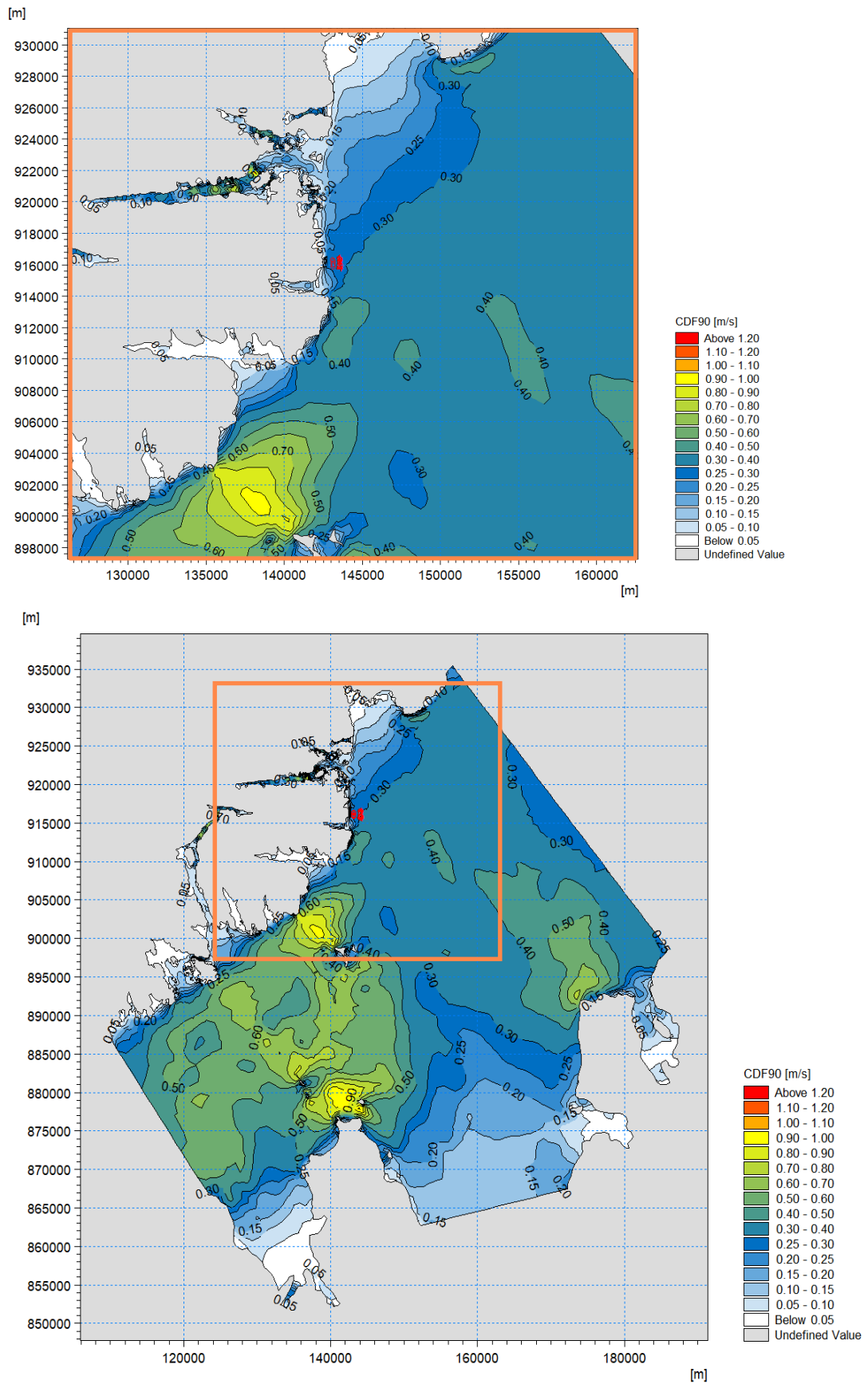


Figure 7.4 Statistical 90th percentile (based on empirical CDF) of depth-averaged current speed throughout North Gravr computational domain for the hydrodynamic climatology model (HD_{NG_clima}).

8 Summary

A 3-dimensional hydrodynamic climatology model database for the North Gravir domain has been developed to support marine pen fin fish aquaculture projects at the North Gravir, Outer Hebrides. The model database has been established using DHI's MIKE 3 FM numerical engine. The climatology version was based on the existing ECLH climatological model developed by Marine Scotland Science.

The hydrodynamic database is a regional hydrodynamic climatology with a resolution of approximately <150m at the coastline and ~30-40m at all designated BFS aquaculture sites (main areas of interest) gradually increasing to 150-200m at 1km from pen locations. The model has a refined resolution of down to 150-200m around the existing marine sensitive areas (PMFs).

The hydrodynamic climatology model database provides a basis for future modelling to support regulatory applications such as: assessing connectivity between fish farms sites located near the North Gravir site, site selection and site screening and dispersion modelling of waste solids and bath treatment medicines.

9 References

- [1] Y. Cheng and B. O. Andersen, "Improvement in global ocean tide model in shallow water regions, Poster, SV.1-68 45, OSTST," Lisbon, Oct. 18-22.
- [2] G. D. Egbert and S. Y. Erofeeva, "Efficient inverse modelling of barotropic ocean tides.," *Journal of Atmospheric and Oceanic Technology*, vol. 19, no. 2, pp. 183-204, 2002.
- [3] S. P. Neill, A. Vögler, A. Goward-Brown, S. Baston, M. J. Lewis, P. A. Gillibrand, S. Waldman and D. K. Woolf, "The wave and tidal resource of Scotland," *Renewable Energy*, vol. 114, no. Part A, pp. 3-17, 2017.
- [4] S. Government, "Scotland's Marine Atlas: Information for The National Marine Plan," 16 03 2011. [Online]. Available: <https://www.gov.scot/publications/scotlands-marine-atlas-information-national-marine-plan/pages/>. [Accessed 19 02 2021].
- [5] Marine Scotland, "OuterHebrides SMR, Marine Scotland Assessment, 2020, <https://marine.gov.scot/sma/region/outer-hebrides-smr>," Marine Scotland, 2021.
- [6] M. Office, "Nortern Scotland: climate," 10 10 2016. [Online]. Available: https://www.metoffice.gov.uk/binaries/content/assets/metofficegovuk/pdf/weather/learn-about/uk-past-events/regional-climates/northern-scotland_-climate---met-office.pdf. [Accessed 01 03 2021].
- [7] D. Cartwright, J. Huthnance, R. Spencer and J. Vassie, "On the St. Kilda shelf tidal regime," *Deep Sea Res.*, vol. 27, no. A, pp. 61-70, 1980.
- [8] Comhairle nan Eilean Siar, "Outer Hebrides Local Development Plan, Supplementary Guidance: marine Fish farming," 2012.
- [9] D. L. Codiga, "Unified Tidal Analysis and Prediction Using the UTide Matlab Functions. Technical Report 2011-01," Graduate School of Oceanography, University of Rhode Island, Narragansett, RI. 59pp, 2011.
- [10] SEPA, "Regulatory Modelling Guidance for the Aquaculture Sector, Version 1.1," Scottish Environment Protection Agency, July 2019.
- [11] DHI, "MIKE 21 & MIKE 3 Flow Model FM, Hydrodynamic and Transport Module, Scientific Documentation," 2022. [Online]. Available: https://manuals.mikepoweredbydhi.help//2022/Coast_and_Sea/MIKE3HD_Scientific_Doc.pdf. [Accessed February 2022].
- [12] DHI, "MIKE 21 & MIKE 3 Flow Model FM, Hydrodynamic and Transport Module, Scientific Documentation," 2020. [Online]. Available: https://manuals.mikepoweredbydhi.help//2021/Coast_and_Sea/MIKE3HD_Scientific_Doc.pdf. [Accessed February 2021].
- [13] Marine Scotland, "The East Coast of Lewis and Harris Model," [Online]. Available: <https://marine.gov.scot/information/east-coast-lewis-and-harris-model>. [Accessed 01 03 2022].
- [14] O. M. R. and C. L., "East Coast of Lewis and Harris Climatology 1.02," 2021.
- [15] J. Wolf, N. Yates, A. Bereton, H. Buckland, M. De Dominicis, A. Gallego and R. O'Hara Murray, "The Scottish Shelf Model. Part 1: Shelf-Wide Domain," *Scottish Marine and Freshwater Science*, vol. 7, no. 3, 2016.
- [16] M. De Dominicis, J. Wolf and R. O'Hara Murry, "Comparative Effects of Climate Change and Tidal Stream Energy Extraction in a Shelf Sea," *JGR Oceans*, vol. 123, no. 7, pp. 5041-5067, 2018.
- [17] C. Chen, H. Liu and R. C. Beardsley, "An unstructured grid, finite-volume, three-dimensional, primitive equations ocean model: Application to coastal ocean and estuaries," *Journal of Atmospheric and Oceanic Technology*, vol. 20, no. 1, pp. 159-186, 2003.
- [18] D. P. Dee, S. M. Uppala, A. J. Simmons, P. Berrisford, P. Poli and S. Kobayashi, "The ERA-Interim reanalysis: configuration and performance of the data assimilation system," *Quarterly Journal of the Royal Meteorological Society*, vol. 137, no. 656, pp. 553-597, 2011.

- [19] V. A. Bell, A. L. Kay, R. G. Jones and R. J. Moore, "Development of a high resolution grid-based river flow model for use with regional climate model output," *Hydrology and Earth System Sciences*, vol. 11, no. 1, pp. 532-549, 2007.
- [20] S. J. Cole and R. J. Moore, "Distributed hydrological modelling using weather radar in gauged and ungauged basins," *Advances in Water Resources*, vol. 32, no. 7, pp. 1107-1120, 2009.
- [21] DHI, "MIKE 21 Toolbox Global Tide Model, <https://www.mikepoweredbydhi.com/-/media/shared%20content/mike%20by%20dhi/flyers%20and%20pdf/product-documentation/mike-21-toolbox-global-tide-model.pdf>," 2022.
- [22] R. A. Flather, "A tidal model of the northwest European continental shelf," *Memories de la Societe Royale des Sciences de Liege*, vol. 6, no. 10, pp. 141-164, 1976.
- [23] DHI, "MIKE 3 Flow Model FM, Hydrodynamic and Transport Module, Scientific Documentation," 2021. [Online]. Available: https://manuals.mikepoweredbydhi.help//2021/Coast_and_Sea/MIKE_3_Flow_FM_Scientific_Doc.pdf. [Accessed 03 2021].
- [24] G. S. Carter and M. A. Merrifield, "Open boundary conditions for regional tidal simulations," *Ocean Modelling*, vol. 18, pp. 194-209, 2007.
- [25] SEPA, "Regulatory Modelling Guidance for the Aquaculture Sector," July 2019.
- [26] D. Price, C. Stuver, H. Johnson, A. Gallego and R. Murray O'Hara, "Scottish Shelf Model. Part 4: East Coast of Lewis and Harris Sub-Domain," Marine Scotland, Mar 2016.
- [27] R. J. Shucksmith, "Shetland Islands Marine Region State of the Environment Assessment," NAFC Marine Centre UHI. Report for the Shetland Islands Marine Planning Partnership. pp 172, 2017.
- [28] K. P. Edwards, R. Barciels and M. Butenschön, "Validation of the NEMO-ERSEM operational ecosystem model for the North West European Continental Shelf," *Ocean Science*, vol. 8, no. 6, pp. 983-1000, 2012.
- [29] E. J. O'Dea, A. K. Arnold, K. P. Edwards, R. Furner, P. Hyder and M. J. Martin, "An operational ocean forecast system incorporating NEMO and SST data assimilation for the tidally driven European North-West shelf," *Journal of Operational Oceanography*, vol. 5, no. 1, 2012.
- [30] R. Halliday, "Shetland Islands Wave and Tidal Resource," Natural Power for Shetland Island Council (805-NPC-SIC-004), 2001.
- [31] D. Price, C. Stuver, H. Johnson, A. Gallego and R. O'Hara Murray, "The Scottish Shelf Model. Part 3: St Magnus Bay Sub-Domain," *Scottish Marine and Freshwater Science*, vol. 7, no. 5, 2016.
- [32] M. Niazy, "Pentland Firth & Orkney Water (PFOW) Tidal Array Stronsay Firth, between Shapinsay and Stronsay," 2019.
- [33] ECMWF, *ERA5 - Reanalysis Datasets.*, European Centre for Medium-Range Weather Forecasts, 2019.
- [34] Marine Scotland Science, "Scottish Fish Farm Production Survey 2021," The Scottish Government, October 2022.
- [35] R. Pawlowicz, B. Beardsley and S. Lentz, "Classical tidal harmonic analysis including error estimates in MATLAB using T-TIDE," *Computers & Geosciences* 28, pp. 929-937, 2002.
- [36] M. G. G. Foreman, J. Y. Cherniawsky and V. A. Ballantyne, "Versatile Harmonic Tidal Analysis: Improvements and Applications.," *J. Atmos. Oceanic Tech.* 26, pp. 806-817. DOI: 10.1175/2008JTECHO1615.1171, 2009.
- [37] K. E. Leffler and D. A. Jay, "Enhancing tidal harmonic analysis: Robust (hybrid L-1/L-2) solutions," *Cont. Shelf Res.* 29, pp. 78-88. DOI: 10.1016/j.csr.2008.1004.1011, 2009.

APPENDICES

APPENDIX A

Hydrodynamic Model Database Files

A Hydrodynamic model database files

The hydrodynamic climatology models are supplied on a portable hard drive alongside this report. This includes the mesh files, offshore boundary conditions, meteorological conditions, model setup files, and the model results files. The data are provided in DHI MIKE format and can be used to generate boundary conditions for local climatology modelling or as input for scenario modelling.

Table A.1 summarises the model files provided for the HD_{NG_clima} model.

Table A.1 Hydrodynamic climatology files (HDNG_clima)

Folder	File name	File type	File size	Description
NG_final_v2_clima_ECLHplusDTU10_2min_DA_TSnudging_prod.m3fm - Result Files	area.dfsu	MIKE Zero Data Manager (.dfsu)	16.5 GB	2-Dimensional model outputs from 1-year model run (0.5-hour temporal resolution) <ul style="list-style-type: none"> • Surface elevation [mMSL] • Depth-averaged u-velocity [m/s] • Depth-averaged v-velocity [m/s] • P (power) flux [$\text{m}^3\text{s}^{-1}\text{m}^{-1}$] • Q (volume) flux [$\text{m}^3\text{s}^{-1}\text{m}^{-1}$] • Wind U-velocity@10m [m/s] • Wind V-velocity@10m [m/s] • Bed shear stresses (and x,y-components) [Nm^{-2}]
	elmnt_domain.dfsu	MIKE Zero Data Manager (.dfsu)	1.2 MB	2-Dimensional model input (single timestep) <ul style="list-style-type: none"> • Still water depth [m] • Drag coefficient • Element area [m^2]
	volume.dfsu	MIKE Zero Data Manager (.dfsu)	142 GB	3-Dimensional model outputs from 1-year model run (0.5-hour temporal resolution) <ul style="list-style-type: none"> • U-velocity [m/s] • V-velocity [m/s] • W-velocity [m/s] • Density [kg/m^3] • Temperature [degrees Celsius] • Salinity [psu] • TKE [m^2/s^2] • Dissipation of TKE [m^2/s^3] • Horizontal eddy viscosity [m^2/s] • Vertical eddy viscosity [m^2/s]

APPENDIX B

Definition of model quality indices

B Definition of model quality indices

To obtain an objective and quantitative measure of how well the model data compared to the observed data, a number of statistical parameters so-called quality indices (QI's) are calculated.

Prior to the comparisons, the model data are synchronised to the time stamps of the observations so that both time series had equal length and overlapping time stamps. For each valid observation, measured at time t , the corresponding model value is found using linear interpolation between the model time steps before and after t . Only observed values that had model values within \pm the representative sampling or averaging period of the observations are included (e.g. for 10-min observed wind speeds measured every 10 min compared to modelled values every hour, only the observed value every hour is included in the comparison).

The comparisons of the synchronised observed and modelled data are illustrated in (some of) the following figures:

- Time series plot including general statistics
- Scatter plot including quantiles, QQ-fit and QI's (dots coloured according to the density)
- Histogram of occurrence vs. magnitude or direction
- Histogram of bias vs. magnitude
- Histogram of bias vs. direction
- Dual rose plot (overlapping roses)
- Peak event plot including joint (coinciding) individual peaks

The quality indices are described below, and their definitions are listed in Table B.1. Most of the quality indices are based on the entire dataset, and hence the quality indices should be considered averaged measures and may not be representative of the accuracy during rare conditions.

The MEAN represents the mean of modelled data, while the BIAS is the mean difference between the modelled and observed data. AME is the mean of the absolute difference, and RMSE is the root mean square of the difference. The MEAN, BIAS, AME and RMSE are given as absolute values and relative to the average of the observed data in percent in the scatter plot.

The scatter index (SI) is a non-dimensional measure of the difference calculated as the unbiased root-mean-square difference relative to the mean absolute value of the observations. In open water, an SI below 0.2 is usually considered a small difference (excellent agreement) for significant wave heights. In confined areas or during calm conditions, where mean significant wave heights are generally lower, a slightly higher SI may be acceptable (the definition of SI implies that it is negatively biased (lower) for time series with high mean values compared to time series with lower mean values (and same scatter/spreading), although it is normalised).

EV is the explained variation and measures the proportion [0 - 1] to which the model accounts for the variation (dispersion) of the observations.

The correlation coefficient (CC) is a non-dimensional measure reflecting the degree to which the variation of the first variable is reflected linearly in the variation of the second variable. A value close to 0 indicates very limited or no (linear) correlation between the two datasets, while a value close to 1 indicates a very high or perfect correlation. Typically, a CC above 0.9 is considered a high correlation (good agreement) for wave heights. It is noted that CC is 1 (or -1) for any two fully linearly correlated variables, even

if they are not 1:1. However, the slope and intercept of the linear relation may be different from 1 and 0, respectively, despite CC of 1 (or -1).

The Q-Q line slope and intercept are found from a linear fit to the data quantiles in a least-square sense. The lower and uppermost quantiles are not included on the fit. A regression line slope different from 1 may indicate a trend in the difference.

The peak ratio (PR) is the average of the N_{peak} highest model values divided by the average of the N_{peak} highest observations. The peaks are found individually for each dataset through the Peak-Over-Threshold (POT) method applying an average annual number of exceedance of 4 and an inter-event time of 36 hours. A general underestimation of the modelled peak events results in PR below 1, while an overestimation results in a PR above 1.

An example of a peak plot is shown in Figure B.1. 'X' represents the observed peaks (x-axis), while 'Y' represents the modelled peaks (y-axis), based on the POT methodology, both represented by circles ('o') in the plot. The joint (coinciding) peaks, defined as any X and Y peaks within ± 36 hours¹⁹ of each other (i.e. less than or equal to the number of individual peaks), are represented by crosses ('x'). Hence, the joint peaks ('x') overlap with the individual peaks ('o') only if they occur at the same time exactly. Otherwise, the joint peaks ('x') represent an additional point in the plot, which may be associated with the observed and modelled individual peaks ('o') by searching in the respective X and Y-axis directions, see example with red lines in Figure B.1. It is seen that the 'X' peaks are often underneath the 1:1 line, while the 'Y' peaks are often above the 1:1 line.

¹⁹ 36 hours is chosen arbitrarily as representative of an average storm duration. Often the observed and modelled storm peaks are within 1-2 hours of each other.

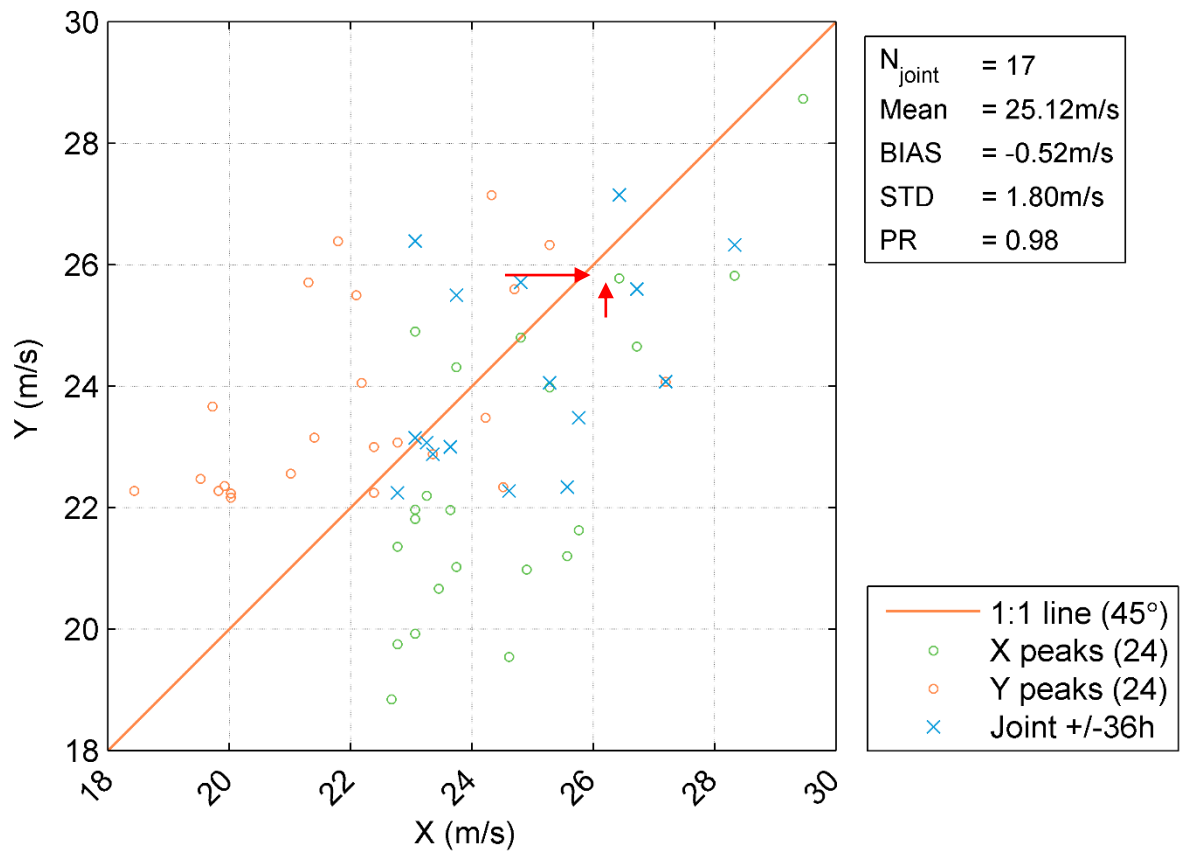


Figure B.1 Example of peak event plot (wind speed).

Table B.1 Definition of model quality indices (X = Observation, Y = Model).

Abbreviation	Description	Definition
N	Number of data (synchronised)	–
MEAN	Mean of Y data, Mean of X data	$\frac{1}{N} \sum_{i=1}^N Y_i \equiv \bar{Y}, \frac{1}{N} \sum_{i=1}^N X_i \equiv \bar{X}$
STD	Standard deviation of Y data Standard deviation of X data	$\sqrt{\frac{1}{N-1} \sum_{i=1}^N (Y - \bar{Y})^2}, \sqrt{\frac{1}{N-1} \sum_{i=1}^N (X - \bar{X})^2}$
BIAS	Mean difference	$\frac{1}{N} \sum_{i=1}^N (Y - X)_i = \bar{Y} - \bar{X}$
AME	Absolute mean error	$\frac{1}{N} \sum_{i=1}^N (Y - X)_i$
RMSE	Root mean square error	$\sqrt{\frac{1}{N} \sum_{i=1}^N (Y - X)_i^2}$
SI	Scatter index (unbiased)	$\frac{\sqrt{\frac{1}{N} \sum_{i=1}^N (Y - X - \text{BIAS})_i^2}}{\frac{1}{N} \sum_{i=1}^N X_i }$
EV	Explained variance	$\frac{\sum_{i=1}^N (X_i - \bar{X})^2 - \sum_{i=1}^N [(X_i - \bar{X}) - (Y_i - \bar{Y})]^2}{\sum_{i=1}^N (X_i - \bar{X})^2}$
CC	Correlation coefficient	$\frac{\sum_{i=1}^N (X_i - \bar{X})(Y_i - \bar{Y})}{\sqrt{\sum_{i=1}^N (X_i - \bar{X})^2 \sum_{i=1}^N (Y_i - \bar{Y})^2}}$
QQ	Quantile-Quantile (line slope and intercept)	Linear least square fit to quantiles
PR	Peak ratio (of N_{peak} highest events)	$\text{PR} = i = 1N_{\text{peak}} Y_i \sum_{i=1}^{N_{\text{peak}}} X_i$

APPENDIX C

Digital container of calibration/validation plots

C Digital container of calibration/validation plots